NKS-503
ISBN 978-87-7893-601-1

Source Term and Timing Uncertainty in Severe accidents
NKS-STATUS Phase 3 report

Sergey Galushin[1],
Govatsa Acharya[2], Dmitry Grischenko[2], Pavel Kudinov[2]
Sara Ojalehto[3], Tuomo Sevón[3], Ilona Lindholm[3]
Patrick Isaksson[4]
Naeem Ul-Syed[5]

[1] Vysus Sweden AB
[2] KTH Royal Institute of Technology
[3] VTT Technical Research Centre of Finland Ltd
[4] SSM Swedish Radiation Safety Authority
[5] DSA Norwegian Radiation and Nuclear Safety Authority

September 2025

Abstract

The overall goal of the NKS-STATUS project is to advance knowledge on the uncertainty in the magnitude of fission product release during potential severe accidents in Nordic Boiling Water Reactors (BWRs). The work aims to provide insights into the effect of various types of uncertainty on the source term predictions.
This 4th phase of the NKS-STATUS project builds on previous work by focusing on fission product behavior inside the containment, with particular attention to remobilization, mitigative actions, and probabilistic evaluation of uncertainty.
Results obtained for the SBO scenario leading to filtered containment venting showed a limited contribution of cesium remobilization to total release, with dominant sensitivity to aerosol shape factors (GAMMA, CHI). The role of independent containment spray systems was also assessed in this scenario. Sprays slightly reduced cesium release to the environment, primarily affecting the initial release phases, but had minimal influence on remobilization.
In LOCA scenarios, significant remobilization of Cs and I_2 deposited in the reactor pressure vessel and containment was observed, with the mode of debris ejection (IDEJ) identified as the main driver of uncertainty. The project further examined vessel lower head failure and debris ejection, identifying conditions under which steam explosion loads increase containment failure probabilities. Debris ejection conditions were shown to significantly influence the probability of containment failure due to ex-vessel steam explosions. A statistical approach using TEXAS-V demonstrated that non-reinforced hatch doors are highly vulnerable, with failure probabilities exceeding 80% in some scenarios. Updated empirical CDFs for Cs and I_2 releases show variability depending on containment failure timing; later failures generally result in lower releases due to increased deposition and scrubbing.
Probabilistic evaluation of uncertainty analysis results for fission product release in filtered containment venting scenarios initiated by LOCA (RC7B) indicates that despite significant phenomenological uncertainties, the overall impact on unacceptable release frequency remains limited, with containment bypass sequences and Interfacing System LOCAs (IS-LOCAs) scenarios continuing to dominate the risk profile.

Key words

Severe accident, uncertainty quantification, MELCOR, Nordic BWR, fission products, source term

NKS-503
ISBN 978-87-7893-601-1
Electronic report, September 2025

NKS Secretariat
P.O. Box 49
DK - 4000 Roskilde, Denmark
Phone +45 4677 4041
www.nks.org
e-mail nks@nks.org

Source Term and Timing Uncertainty in Severe accidents

Final Report from the NKS-R STATUS activity
(Contract: AFT/NKS-R(24)133/1)

Sergey Galushin[1]

Govatsa Acharya[2], Dmitry Grischenko[2], Pavel Kudinov[2]

Sara Ojalehto[3], Tuomo Sevón[3], Ilona Lindholm[3]

Patrick Isaksson[4]

Naeem Ul-Syed[5]

[1] Vysus Sweden AB

[2] KTH Royal Institute of Technology

[3] VTT Technical Research Centre of Finland Ltd

[4] SSM Swedish Radiation Safety Authority

[5] DSA Norwegian Radiation and Nuclear Safety Authority

NKS conveys its gratitude to all organizations and persons who by means of financial support or contributions in kind have made the work presented in this report possible.

Table of contents

1. Introduction

Analyzing and estimating risks is an integral part of both the industrial use and the public debate on nuclear power. At the same time, global climate change is increasing the demand for low-carbon sources of electricity, and the nuclear industry strives to maintain and expand its share of global energy production. With these observations in mind, it is reasonable to expect that the need for technological advances and reduction of uncertainties in both financial and radiological risks related to nuclear power will be as big as ever in the coming decades.

An important part of the risk profile of nuclear power relates to so-called severe accidents – i.e., events leading to a partly or fully damaged (melted) reactor core. State-of-the-art assessments of radiological risks related to such events rely on estimations of two fundamental quantities: their frequency and their consequence. As simple as these notions may seem, their quantification depends heavily on input data as well as on scope and complexity of the mathematical modelling used.

In so-called level 2 probabilistic safety assessments (L2 PSA), the main frequency estimate of interest is the large release frequency (LRF), or sometimes the large early release frequency (LERF). Assessing these frequencies based on summation over a large number of possible event sequences implies, among other things, that radioactive releases (the source term) need to be calculated for a set of representative scenario classes and compared to a predefined threshold to classify them as large or not large. These assessments are typically performed with integral plant response codes, such as ASTEC, MAAP or MELCOR, and are in themselves subject to uncertainty, both regarding the accident scenarios (aleatory uncertainty) and in the modelling of phenomena (epistemic uncertainty). Aleatory uncertainty arises from the natural variability of stochastic processes and cannot be reduced beyond this level, while epistemic uncertainty relates to our knowledge of systems, processes or parameters and can therefore be reduced by gathering more knowledge.

Typically, the source term evaluation is performed for a limited set of accident scenarios, using point estimate values of epistemic uncertain parameters in the code used. Furthermore, such analyses typically do not consider the effect of epistemic uncertainty on interactions between physical phenomena or processes and transient accident scenarios, i.e., when different samples on the epistemic uncertainty range can significantly affect the course of the accident progression.

For some accident sequences, the standard practice, for the sake of conservatism, is to define the source term as everything escaping the containment. This creates a situation where a potentially very diverse family of realistic scenarios is represented by a set of assumed sequences that may contribute substantially to the LRF in a typical PSA L2. In this case, the uncertainty lies in the level of applied conservatism.

In both cases described above, source term uncertainty presents a challenge for any attempt to develop, use or increase the level of detail in L2 PSA results and merits targeted research solely on the basis of this.

Within the field of nuclear emergency preparedness towards severe accidents, the main goal is ultimately to be able to perform relevant and efficient actions to protect the public. The International Atomic Energy Agency (IAEA) states on the one hand that decisions on these actions should be based on observations of plant conditions, and on the other hand that decisions or protective actions should not be delayed by attempts to perform detailed source term estimates [1,2]. It is acknowledged that performing source term assessments with integral plant response codes is sufficiently complicated outside of accident conditions, which

creates a need for simpler and faster tools for assessment of plant condition and source term estimation. One such tool is the Rapid Source Term Prediction (RASTEP) methodology, developed by Vysus Group. This method relies on a database of pre-calculated source term scenarios together with a probabilistic Bayesian Belief Network (BBN) model. The tool has the ability to take observed plant conditions and rescale results from L1-L2 PSA using conditional probabilities, logical relations and expert judgements. The output is a complete list of scenarios ranked by likelihoods, which is continuously updated with any new observations. In this way, current plant conditions can always be mapped to a representative class of scenarios. A problem arises if a RASTEP model (or any approach based on pre-calculated source terms) is used with overly conservative or uncertain data. Within emergency preparedness planning, source term uncertainties therefore also come with an operational aspect, directly impacting decisions taken in a stressful situation.

Within this project, the analysis of severe accident progression and fission products release to the environment are performed using MELCOR. MELCOR is a fully integrated, engineering-level computer code that models the progression of severe accidents in light water reactor nuclear power plants. A broad spectrum of severe accident phenomena in both boiling and pressurized water reactors is treated in MELCOR in a unified framework. These include thermal-hydraulic response in the reactor coolant system, reactor cavity, containment, and confinement buildings; core heat-up, degradation, and relocation; core-concrete attack; hydrogen production, transport, and combustion; fission product release and transport behavior. Current uses of MELCOR include estimation of severe accident source terms and their sensitivities and uncertainties in a variety of applications [6,7].

It is our hope that this project will be able to shine some light on all of the above-mentioned aspects of the source term uncertainty, limited to Nordic Boiling Water Reactors (BWR).

2. Project scope and goals

The overall goal of the project is to generate a body of knowledge regarding the uncertainty in the magnitude of fission products release in the event of a potential severe accident in Nordic nuclear power plants. The work aims to provide insights into the effect of various types of uncertainty on the source term predictions. The results will be useful for both probabilistic and deterministic safety assessments, as well as for emergency response applications.

Within the first phase of the project (see [23]) the participating organizations performed the analysis of the safety design of Swedish and Finnish Nordic BWRs and respective MELCOR modelling, review of the PSA L2 for a typical Nordic BWR design and identification of risk significant accident sequences, as well as the state-of-the-art review of the modelling of severe accident phenomena and identification of possible sources of uncertainty in severe accident progression and the source term.

In the second phase of the project (see [50]) the participating organizations focused on evaluating methods and tools to perform sensitivity and uncertainty analyses. Using these methods and tools, they identified the main contributors to the uncertainty in the source term released to the environment and quantified the source term uncertainty due to the most influential MELCOR code modeling parameters. In these analyses, the uncertain modeling parameters involved the modeling of core degradation and relocation, fission product release from fuel, debris behavior in the core region and vessel lower head, vessel lower head failure, fission product behavior in the RCS and the containment, as well as modeling of the filter trapping, containment sprays, and pool scrubbing.

In the third phase of the project (see [67]) the participating organizations focused on the analysis of containment bypass sequences. Particular attention was given to scenarios involving failed isolation of main steam valves and release paths through the turbine system and condenser. Additional work included sensitivity and uncertainty analyses, specifically, the impact of release paths in cases of containment failure due to ex-vessel phenomena; evaluation of mitigative actions in filtered containment venting scenarios; and the development and implementation of a refined model for the filtered containment venting system using improved thermohydraulic nodalization of the MVSS FILTRA system and the SPARC-90 pool scrubbing model in MELCOR..

The current (fourth) phase of the NKS-STATUS project aims to address issues identified in previous phases. The focus has been placed on the analysis of fission product remobilization within the containment, including the effect of mitigative actions such as the late activation of an independent spray system and manual containment depressurization. Additional analyses target the impact of the mode of debris ejection from the reactor vessel on steam explosion loads and source term, as well as the probabilistic evaluation of uncertainty analysis results for filtered containment venting scenarios initiated by a large-break LOCA.

The expected outcome of this phase is to provide important insights into the influence of MELCOR code modelling uncertainties on accident progression, fission products behavior inside the containment and radioactive release to the environment, particularly in scenarios involving filtered containment venting or containment failure. Furthermore, the project aims to improve the understanding of the impact of potential mitigative actions on the fission products behavior inside the containment and the source term released to the environment.

3. Background on Nordic Boiling Water Reactors

Designed by ASEA/ABB Atom, a total of 10 BWRs have been commissioned in Sweden and Finland since the first unit, Oskarshamn 1, was brought online in 1972. Two of the original design families, BWR69 and BWR75, are in operation today, distributed as four units in Sweden and two units in Finland, all with planned lifetimes extending to around 2040.

Over time, these reactors have evolved in partly different directions. The configurations of the sister reactors Forsmark 1/2 as well as Olkiluoto 1/2 are still more or less identical within the sites, while the differences between the sites are more marked.

3.1. Safety design

The Nordic Boiling Water Reactor (NBWR) will hereby be used as a common name for ~3300 MW_{th} BWRs designed by ASEA/ABB Atom. A summary of main technical data for the currently operational NBWRs is given in [3].

Table 3-1. Main technical data for operating NBWRs, some numbers rounded.

	O3/F3 (BWR75)	**F1/2 (BWR69)**	**OL1/2 (BWR69)**
Thermal power [MW]	3900/3300	3000/3250	2500
Reactor operating pressure [MPa]	7.0	7.0	7.0
Number of fuel elements [-]	700	676	500
Number of control rods [-]	169	161	121
Gas volume in containment [m^3]	8300/8500	6800	7600
Capacity of system [kg/s]:			
Containment drywell spray	300	360	250
Containment wetwell spray	400	N/A	120
Containment design pressure [MPa]	0.6	0.5	0.5
Containment operating pressure [MPa]	<0.1	<0.1	<0.1
Filtered containment venting pressure setpoint [MPa]	0.5	0.57	0.2/0.5-0.6*
Unfiltered containment venting pressure setpoint [MPa]	0.65		
Containment rupture pressure [MPa]	~1	~1	~1

*For wetwell venting in OL1/2, the drywell pressure needs to exceed the defined overpressure that depends on drywell gas temperature (total pressure 0.5-0.6 MPa). The drywell venting takes place if the water level in the wetwell is too high to allow venting from there, and the drywell pressure is higher than 0.2 MPa.

The safety design of the NBWRs is described further in the following.

The reactor pressure vessel (RPV) consists of carbon steel clad by stainless steel on the inside. The reactor containment is of the pressure suppression (PS) type with vertical blowdown pipes, and its outer cylindrical shell is made of pre-stressed concrete. It is sealed at the top by a large steel cupola which sits at the bottom of the reactor service pool. The containment also functions as a radiological shield to the environment. During normal operation, the

containment gas volume is filled with nitrogen to prevent ignition of hydrogen if generated during a severe accident.

Details on the NBWR safety systems relevant for severe accident progression (and source term) are provided below:

- Hydraulic control rod insertion: The hydraulic actuating power shut-off system gives full insertion of all control rods within a few seconds after initiation. Should this system fail, an electromechanic system inserts the rods within a few minutes. If this also fails, boric acid can be added to the reactor vessel via a dedicated injection system.
- Pressure control and relief system: This system has several operating modes and can operate with battery backup only:
    - TA Function: The spring-operated part of the overpressure protection system will open valves stepwise, starting at slightly above 7 MPa to release steam and protect the RPV from catastrophic failure. After a properly controlled pressure transient, the system will continue to control the pressure to around 7 MPa.
    - TB Function (ADS): Activation of TB initiates steam discharge into the wetwell (WW) on setpoint 1 m below top of active fuel (TAF). The pressure is reduced to a level sufficient for water injection by the emergency core cooling system (ECCS) or the independent core cooling system. The TB function is at the same time leading to coolant being lost from the primary system quite rapidly, which leads to core uncover.
- Emergency core cooling system (ECCS): This is an AC power driven, low-pressure coolant injection system comprised of four independent trains, which can pump water to the reactor from the suppression pool. The system has activation setpoints on water level 2 m above TAF and low reactor pressure. Actual water injection will not occur unless the pressure difference between WW and downcomer (DC) is less than 1.25 MPa and the injection capacity is, in general, dependent on this pressure difference.
- Independent core cooling system: This is, in the Swedish configuration, an AC power driven injection system comprised of one independent train with one or several separate water sources as well as a dedicated diesel generator. In the Finnish configuration, this is a separate steam turbine driven injection system, taking suction from water storage tanks in the system for distribution of demineralized water.
- Auxiliary feedwater system (AFW): This is an AC power driven high-pressure coolant injection system comprised of four independent trains, which provides water to the reactor from the wetwell or from a separate storage tank into the downcomer. The system activation logics includes several different setpoints. Water injection is more or less independent of reactor pressure.
- Drywell flooding system: Flooding of drywell from the wetwell is initiated to provide cooling of melt fragmentation and debris in case of melt release from the reactor pressure vessel. The system is typically actuated on downcomer water level 2 m below the TAF for more than 10 minutes, or 30 minutes after containment isolation, depending on plant.
- Non-filtered containment venting system: This is a pressure relief directly to the ambient atmosphere designed for LOCA events with failing PS function. It is

activated by the opening of a rupture disc at around 0.65 MPa containment pressure. The line is automatically closed by a shut-off valve 20 minutes after containment isolation signal. It should be noted that this containment isolation signal is triggered individually by any of the typical conditions that are indicative of a serious event e.g. low reactor water level, high containment temperature, high containment pressure or triggered TB function.

- Filtered containment venting system: In the Swedish configuration, this is achieved from the upper drywell to the atmosphere via a multi-venturi scrubbing system situated in a separate building, equipped with a dedicated stack. Venting is activated by a rupture disc opening around 0.55 MPa containment pressure. In parallel with this rupture disc, two valves for manual depressurization are also installed for cases where additional capacity is required, e.g. when manual operation of the filtered venting is an option due to for instance favorable weather conditions.

  In the Finnish configuration, filtered venting can be done both from the wetwell and drywell to the atmosphere via a SAM-scrubber placed inside the reactor building. Wetwell venting is possible if the water level is below 14.5 m. The drywell pressure needs to exceed the defined overpressure that depends on drywell gas temperature. At a drywell temperature of 293 K, the threshold overpressure is 0.5 MPa.
  The drywell venting through a rupture disk takes place if the water level in the wetwell has been higher than 14.5 m for longer than a specified time (which precludes possibility of venting from wetwell) and the drywell pressure is higher than 0.2 MPa.

- Suppression pool: The suppression pool, located in the wetwell, is an inherently passive system designed to limit the containment pressure by use of the so-called PS function; Steam leaking or blown out from the primary system to the drywell will be pushed through blowdown pipes ending in the wetwell pool where the steam is condensed. Vacuum valves in large pipes between wetwell and lower drywell ensure that the wetwell pressure will not be higher than that of the drywell.
- Residual heat removal and containment spray system (RHR and CSS): This is an AC power driven system, comprised of four independent trains with heat exchangers, all recirculating water from the suppression pool. All four loops are connected to feed spray nozzles located in the containment. The safety functions of the system are to reduce the containment pressure by condensing steam in case of a LOCA, to remove heat from the suppression pool through a series of heat exchangers and to provide scrubbing of airborne fission products from the containment atmosphere in case of core damage.
- Independent containment heat removal and spray system: This is an EOP/SAMG spray system in the upper drywell (UDW) that takes water from an independent external water source. It can be used to reduce pressure in the containment as well as to provide scrubbing of airborne fission products. Water level control is provided in order to not damage the containment.

3.2. MELCOR models

3.2.1. Swedish MELCOR modelling of NBWR

The MELCOR model of NBWR used in this project is the further development of the input deck originally developed for the analysis of accidents in power uprated plants [4], mainly

maintained by KTH. In this model, the core is represented by five non-uniform radial rings and eight axial levels. The 6th ring represents the downcomer region (Figure 3-1).

The reactor pressure vessel (Figure 3-2) and the containment (Figure 3-3) are represented by 27 control volumes (CV), connected with 45 flow paths (FL) and 73 heat structures (HS). The vessel is represented by 6 rings and 19 axial levels, with the first 10 axial levels representing the lower plenum; the 11th axial level represents the core support plate; levels 12 and 19 represent the core inlet and outlet regions and structures; and levels 13-18 represent the active core region. Lower head penetrations for 66 instrumentation guide tubes (IGTs) are distributed between rings 1-5 proportionally to the cross-sectional area of these rings. Containment leakage is modelled from the drywell directly to the environment.

The containment is subdivided into control volumes for upper and lower drywell, wetwell, blowdown pipes and overflow pipes from lower drywell to wetwell.

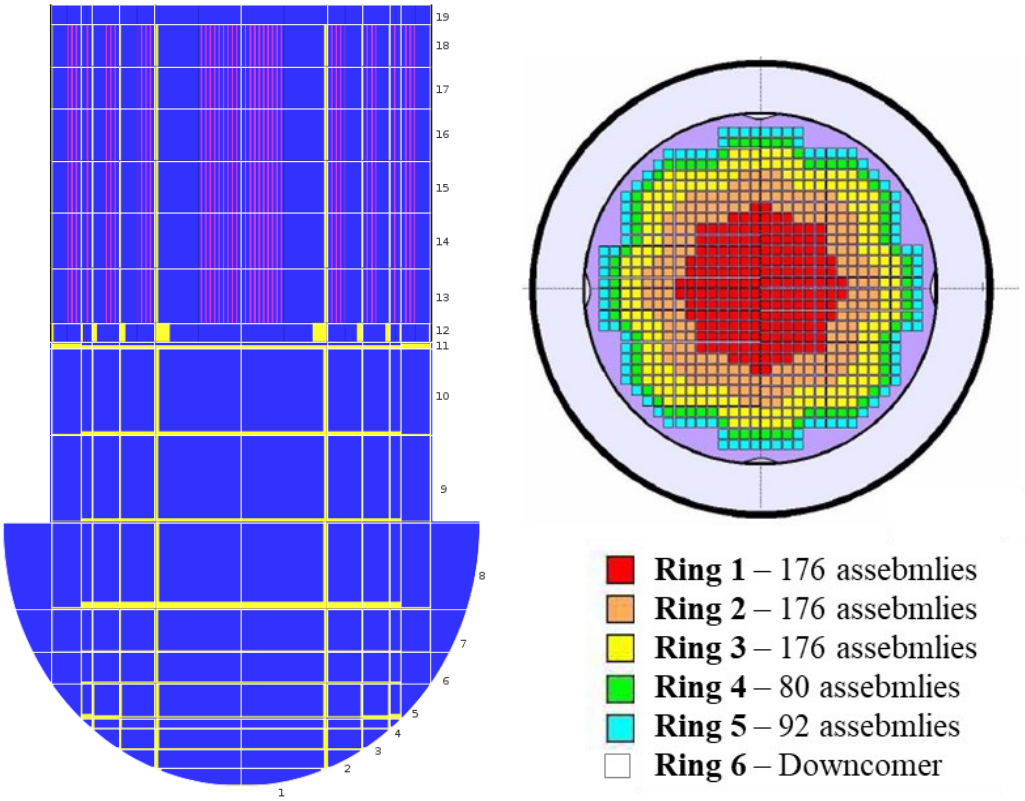

Figure 3-1. Swedish NBWR model COR nodalization.

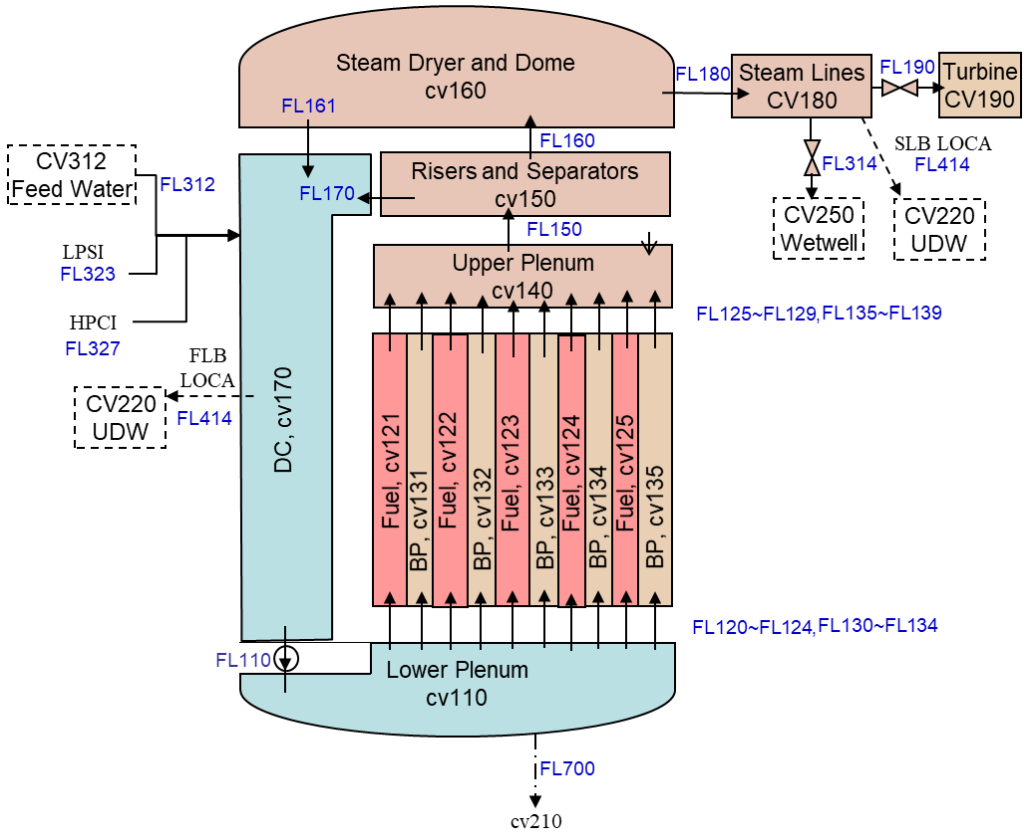

Figure 3-2. Swedish NBWR model CVH nodalization of the core.

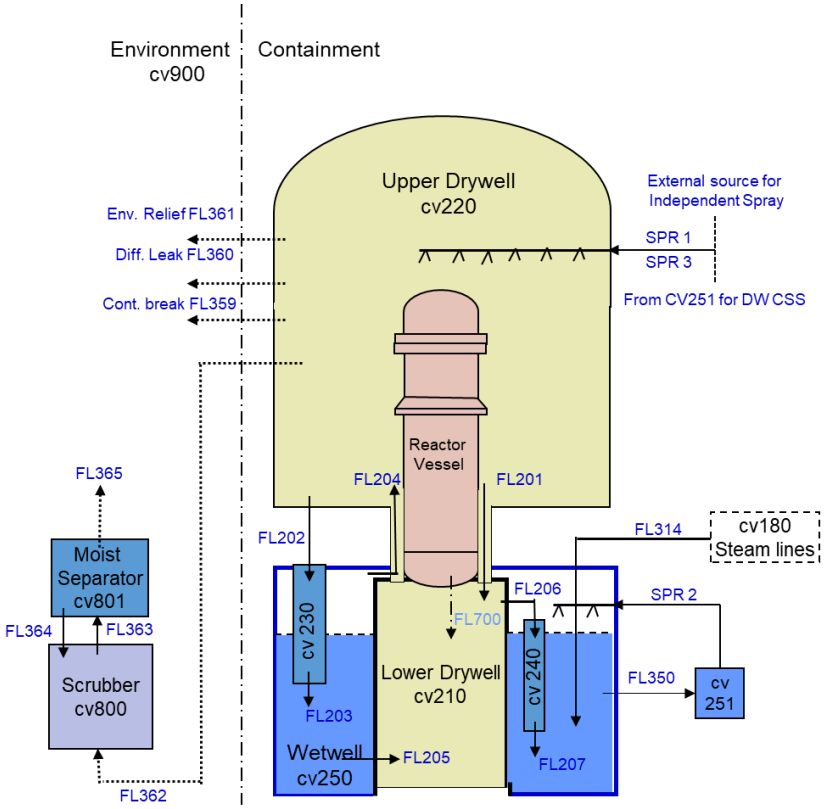

Figure 3-3. Swedish NBWR model containment nodalization.

The following safety systems are implemented in the model:

- Hydraulic control rod insertion
  - The effect of this system is modeled in MELCOR by fission power decrease (during 3.5 s) according to a tabular function at time zero.
- Pressure control and relief system
  - Both TA and TB valves as well as pipelines are implemented as a single flow path (FL314) from the steamlines to the wetwell, controlled by a set of control and tabular functions. SPARC pool scrubbing model is activated at the pool discharge end of the 314-pipes.
- Emergency core cooling system
  - All 4 trains are modeled by a single flow path (FL323) to the downcomer, with the number of trains and flow managed by a set of control functions. Flow rate vs. back pressure is controlled by a tabular function. The wetwell is used as water source for the system in the model and the injection is stopped on high suppression pool temperature.
- Auxiliary feedwater system.
  - All 4 trains are modeled by a single flow path (FL171) to the downcomer, with the number of trains and flow managed by a set of control functions. It is assumed that the system injects water with constant flow rate of 26 kg/s regardless of the pressure difference between DW and WW. The wetwell is used as water source for the system in the model and the injection is stopped on high suppression pool temperature.
- Drywell flooding system.
  - The system is implemented as a single flow path (FL205) from the wetwell to the lower drywell; the valves are controlled by a set of control functions. Together with the drywell flooding system an overflow pipe is modelled connecting the lower drywell and the wetwell to prevent lower drywell overfilling.
- Drywell blowdown pipes
  - A total of 24 drywell blowdown pipes are modelled from the drywell floor to the suppression pool. The diameter of the pipes is about 60 cm. The SPARC pool scrubbing model is activated at wetwell discharge at the end of the blowdown pipe. The blowdown pipes are purposed for the LOCA situations, when rapid and large steam release is able to clear the water in the pipes, and steam is driven into the suppression pool for condensation.
- Vacuum breakers
  - Vacuum breakers are modelled as a single flow path (FL204) that connects wetwell gas space with upper drywell to prevent wetwell pressure exceeding the drywell pressure.
- Non-filtered containment venting system.
  - Implemented as a single flow path (FL361) from the upper drywell to the environment, the rupture disk and shut-off valves are modelled as a set of control functions.

- Filtered containment venting system.
    - Implemented by a set of flow paths and control volumes (c.f. Figure 3-3). The rupture disk and valves are controlled by a set of control functions. The actual filtering of substances containing radionuclides is modelled by simple filter factors based on system requirements.
- Residual heat removal and containment spray system.
    - Currently modelled as two sprays (SPR2 in the wetwell and SPR3 in the drywell). The wetwell spray (SPR2) represents up to 4 trains of the containment spray system with 100 kg/s per train, with a possibility to reroute up to 3 spray trains to the upper drywell. Control volume CV251 represents the heat exchangers in the residual heat removal system and used as a water (and temperature) source by the containment spray system and enthalpy source for the residual heat removal system.
- Independent containment spray system
    - Implemented as a single train system with flow path (SPR1) ending in the upper drywell. The capacity is 100 kg/s assuming a constant water source temperature at 293.15 K.

The MELCOR model does not include the newly implemented independent core cooling system. As the aim is to study source terms of severe accidents, i.e. cases where all core cooling fails, this is judged to be acceptable.

The MELCOR model is not built to treat cases with failing hydraulic control rod insertion, as sequences with failing reactor shutdown also require the electromechanical insertion and the boron injection to fail, thereby rendering this core damage mode a very small contributor in the PSA.

Note that steam lines, condenser and turbine plant are not modelled, as is also the case for the reactor building and its ventilation system. This implies that containment rupture or bypass cases will be conservative in terms of the source term, as any retention and delay in the turbine system or building structures will not be taken into account.

In the last few years, KTH has developed and demonstrated a systematic approach to quantification of uncertainty in severe accident scenarios and phenomena based on the Risk Oriented Accident Analysis Methodology framework (ROAAM+). The approach combines the most recent development in the areas of sensitivity analysis, uncertainty quantification and surrogate modeling approaches. In the previous ROAAM+ work the focus was on the quantification of uncertainty in containment failure probability. The next step in the ROAAM+ development is application to quantification of uncertainty in the source term.

3.2.2. Finnish MELCOR modelling of NBWR

VTT's MELCOR model of Olkiluoto 1&2 was developed for code version 1.8.2 in 1994. The model has been updated several times when new code versions have been taken into use. The latest update was made in 2017 by Magnus Strandberg who converted the model to MELCOR 2.1 with funding from the SAFIR2018 research program [5]. Systematic checking of the input deck or comparisons to current plant configuration have not been made for at least 19 years. The model is somewhat outdated because it does not follow current best modelling practices, and plant modifications are not included in the model.

The core nodalization is presented in Figure 3-4 (left). The core is modelled with five uniform radial rings; the sixth ring represents the downcomer region. The first three axial levels represent the lower plenum; the fourth axial level represents the core support plate; levels 5–14 represent the active core region; and level 15 represents the core outlet region.

The reactor thermal-hydraulic nodalization is presented in Figure 3-4 (right). There are 7 control volumes and 10 flow paths, plus one flow path from the core to the bypass that is opened upon failure of the channel boxes. The steam lines are not modelled as a separate volume. Instead, the steam to the safety relief valves is taken directly from the downcomer volume. The instrument guide tube penetrations in the lower head were added to the model during the current project.

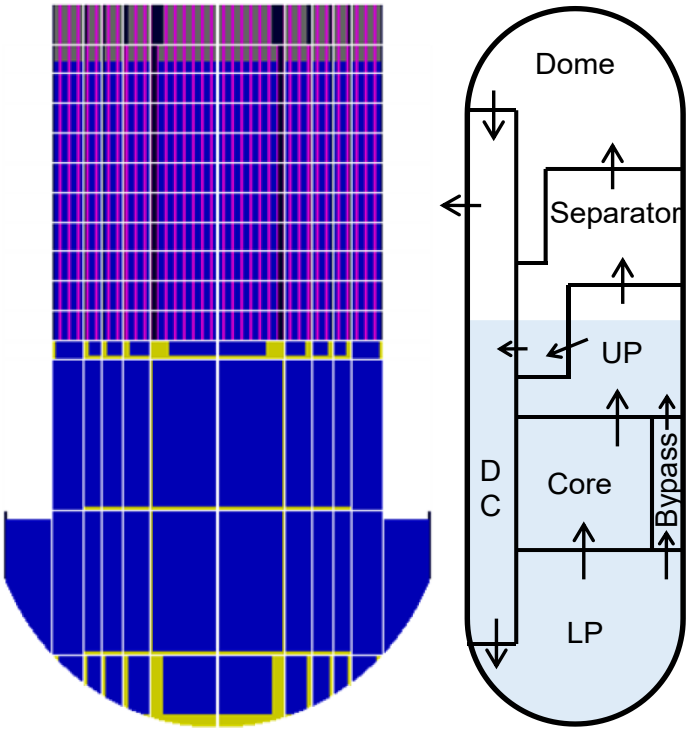

Figure 3-4. Finnish NBWR core model COR (left) and CVH (right) nodalization.

The containment is modelled with four control volumes, see Figure 3-5. The biological shield volume represents the space between the RPV and the concrete wall around it. The RPV lower head is interfaced with the biological shield volume. In addition, the model has six volumes representing rooms in the reactor building and a time-independent volume representing the environment. The control volumes of the reactor building represent major potential leakage routes from the containment to the reactor building and were purposed for hydrogen spreading and combustion analyses. The reactor building model is not purposed to model the entire complex RB configuration. Containment leakage is modelled from the drywell to the reactor building.

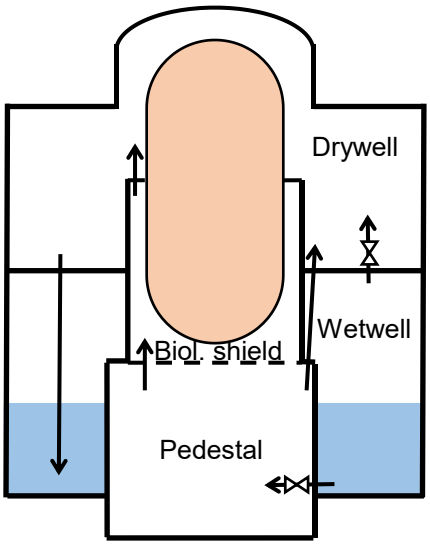

Figure 3-5. Finnish NBWR model containment nodalization.

The following systems are implemented in the Finnish NBWR MELCOR model:

- Hydraulic control rod insertion
  - Reactor scram is assumed to take place at time zero.
- Containment isolation
  - Closure of the main steam isolation valves (system 311) is activated by I-isolation or at a predefined time.
- Reactor main recirculation,
  - Modelled as a coast-down curve during the first 9.1 s of the calculation
- Pressure control and relief system
  - Relief valves controlled by downcomer pressure are modelled to discharge from the RPV downcomer to the suppression pool in the wetwell as four different groups: Group 1 opens when the downcomer pressure exceeds 8 MPa and closes when the pressure decreases below 7.4 MPa. The second group opens at 7.4 MPa and close at 7.1 MPa, the third group of valves opens at 8.5 MPa and closes at 7.6 MPa and the fourth group is open at pressure higher than 7.0 MPa and otherwise closed. The vertical discharge lines are submerged 4.5 meters in the suppression pool. SPARC pool scrubbing model is activated at the pool discharge end of the 314-pipes.
  - Automatic depressurization system of the reactor (314-ADS)

    Automatic depressurization is initiated on any of the following three signals:

    1) automatic TB signal

    2) manual TB signal

    3) on L4 signal lasting for the delay of 906 s.

    The automatic TB signal is generated if L4 signal is obtained and drywell pressure simultaneously exceeds 95 kPa and the drywell pressure increases faster than 130 Pa/s. The valve opening generates a delay of 15 s. The ADS blowdown takes place from the downcomer to the suppression pool at water

submergence of 4.5 m. SPARC model is activated at the pool discharge end of the 314 pipes by input parameter.

- Emergency core cooling system
  - The system 323 injects water to the Upper Plenum (UP node) and takes suction from the suppression pool. The injection starts when L4 signal is obtained (downcomer water level goes below 28.25 m (0.5 meters above TAF)) and the 323 pumps run until the water level in the downcomer reaches 32.25 m (= 4.5 meters above TAF). There are four (4) pumps with each having the capacity ranging from a maximum of 115 kg/s to zero at respective downcomer counter pressure range from 0.1 MPa to 1.0 MPa. The initiation of 323 injection to core spray requires also that suppression pool heat removal recirculation mode (system 322) is first locked-off.
- Auxiliary feedwater system
  - System 327 injects coolant to downcomer (50%) and to upper plenum via core spray spargers (50%). The system incorporates four (4) piston-driven pumps that produce constant water flow rate of 25 kg/s per pump independently of counter-pressure up to the pressure 2.0 MPa. The signals L2 and L3 are received when the collapsed water level in the downcomer becomes less than 2.9 m and less than 1.8 m above the top of active fuel (TAF), respectively (i.e. DC water height is less than 30.65 m and 29.55 m). Two 327 pumps start to inject water to downcomer when L2 signal is reached and a 10-s pump delay has elapsed. The DC injection continues until the collapsed water height in the DC reaches 4.0 meters above TAF. The 327 injection with two pumps through core spray spargers initiates from L3 signal with a 10-s pump delay and continues until the DC collapsed level reaches 4.5 meters above TAF.
- Failure of reactor lower head
  - A flow path from the reactor lower plenum to the pedestal is opened when MELCOR calculates lower head failure. The flow area is determined by MELCOR.
- Vacuum breaker between wetwell and drywell
  - Vacuum breakers are modelled as valves between the wetwell and the drywell near the ceiling of the wetwell. The vacuum breakers are purposed to relief wetwell pressure in situations where non-condensable gases accumulate in the wetwell thus diminishing steam suppression in the wetwell pool. The valves open when the pressure in 10 kPa higher in the wetwell than in the drywell. After pressure balancing to the level 1000 Pa the valves are fully closed.
- Drywell-wetwell leak
  - A small leakage between the wetwell and drywell is modelled, the leak area is assumed to increase with drywell pressure being at least 0.01 m2 at drywell pressure higher than 0.5 MPa.
- Drywell blowdown pipes
  - A total of 16 drywell blowdown pipes are modelled from the drywell floor to the suppression pool with a submergence depth of 6.5 m. The diameter of the pipes is about 60 cm. The SPARC pool scrubbing model is activated at wetwell discharge at the end of the blowdown pipe. The 316 pipes are purposed for the LOCA

situations, when rapid and large steam release is able to clear the water in the pipes, and steam is driven into the suppression pool for condensation.

- Containment heat removal and spray system
  - Drywell spray starts on I-isolation signal or by manual activation of the operator. The 322 system is also used for wetwell pool cooling in recirculation mode. A heat exchanger aligned in the 322 recirculation loop removes 172 kJ/K/kg from the pool water with flow capacity of 45 kg/s. The cut-off pool temperature for recirculation cooling is 291 K. Manual starting of spray requires that the water level in the drywell is lower than 2.5 m. The drywell spray flow rate is 60 kg/s.
  - The 322 spray can also be aligned to sprinkle wetwell airspace. The flow rate is then 30 kg/s. The initiation signal is I-isolation or manual start.
- Drywell flooding.
  - Assumed within 30 minutes in a station blackout situation.
- Filtered containment venting system
  - Wetwell venting is possible if the water level is below 14.5 m. The vent line elevation in the wetwell is 17.5 m. The drywell pressure needs to exceed the defined overpressure (to ambient pressure) that depends on drywell gas temperature in the following way: at a drywell temperature of 293 K, the threshold overpressure is 0.5 MPa and at 453 K the threshold is 0.4 MPa. The actual filtering of substances containing radionuclides is modelled by simple filter factors based on system requirements.
  - The drywell venting through a rupture disk takes place if the water level in the wetwell has been higher than 14.5 m for longer than a specified time (which precludes possibility of venting from wetwell) and the drywell pressure is higher than 0.2 MPa.
- Reactor building blow-off panel
  - opening at a pressure difference of 2.5 kPa to the environment.

4. Methods and Tools for Uncertainty Analysis with MELCOR code

4.1. Methods used for sensitivity and uncertainty analysis

4.1.1. Sensitivity analysis

The sources of uncertainty in analysis of severe accident progression are numerous and it is impractical to address all of them quantitatively. Experience in performing uncertainty studies of severe accident phenomena (e.g. [15,16,17,18]) suggests that the effects of uncertainties from some sources are larger and more dominant than the effects of uncertainties from other sources. In an integral sense, then, the aggregate uncertainty in main figures of merit (FOMs) can be estimated by selecting the dominant sources of uncertainty and treating them in detail. The dominant sources of uncertainty should be identified by sensitivity analysis.

A review of global sensitivity analysis methods (see [12] for more details) presents a brief summary on a great variety of different sensitivity analysis methods. Figure 4-1 provides a synthesis of SA methods presented in the paper.

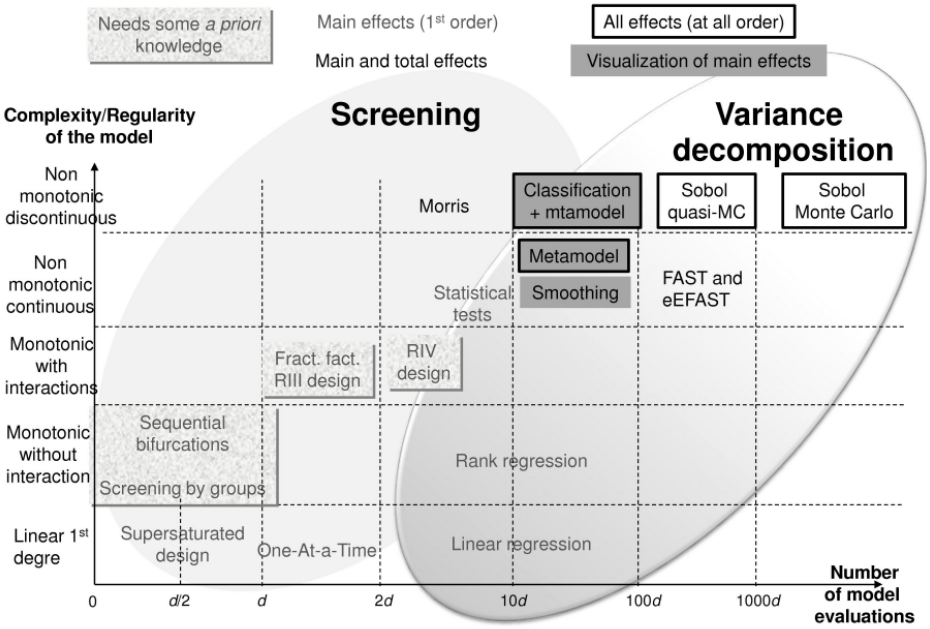

Figure 4-1. SA methods graphical synthesis [12].

Based on the review, the Morris method has been selected as an appropriate tool to perform sensitivity analysis. The Morris method is a screening method that can be applied to models with non-monotonic and discontinuous behavior. Furthermore, based on [8,12] the Morris method should give reasonable results given relatively low computational effort (from approximately *2d* to *10d* model evaluations, where *d* is the number of uncertain parameters).

4.1.1.1. Morris method for sensitivity analysis

The Morris method [9] is a global sensitivity analysis method. The Morris method performs analysis of the model outputs along different trajectories in the input space where parameters are varied "one-factor-at-a-time" (OAT) and the effect of changing every parameter is evaluated through elementary effects - $d_i(x^j)$ calculated by:

$$d_i(x^j) = \frac{[f(x^{i+1}) - f(x^i)]}{\Delta} \quad (1)$$

where $f(x)$ – is the model function, x^j – j-th input vector, Δ - variation step, which is linked to the number of levels (p) as follows:

$$\Delta = \frac{p}{2(p-1)} \tag{2}$$

The number of levels - p and number of elementary effects – r, are defined by a user. The large values of p will require large number of r to be calculated to have reasonable coverage on input domain. Based on [8] the recommended choice for the number of elementary effects is $r = 10$ (or at least $r \geq 4$), and the number of levels should be equal to $p = 4$.

When r – elementary effects are calculated for each input parameter, two sensitivity measures are used:

$$\mu_i = \sum_{i=1}^{r} \frac{|d_i|}{r}; \sigma_i = \sqrt{\sum_{i=1}^{r} (d_i - \mu)^2 / r} \tag{3}$$

where the values of μ_i , substantially different from zero, indicate significant overall influence of i^{th} input; and large values of σ_i indicate possible interactions with other input parameters and non-linear behaviour of the output with respect to the input.

The number of model evaluations to be performed is calculated by

$$N = r * (k + 1) \tag{4}$$

where k is the number of input factors and r is the number of elementary effects.

The Morris method for SA is available in the Dakota package [10]. A pyDakota coupling interface for Morris SA has been developed and implemented in pyMELCOR simulation platform (see section 4.1.3). It performs processing of the user input and generation of the sampling set, as well as processing of the results and generation of sensitivity analysis results.

4.1.1.2. One-way ANOVA

One-way ANOVA can be used to perform analysis of variance in the data set produced by Morris method for SA. The levels p and variation step Δ divide the space of the model input parameters into the subsets where each parameter has an unique fixed value. The variance within each subset can be analyzed whether the subsets means are equal (null hypothesis).

The F-statistic can be used to judge the effect/importance of the parameter in question, i.e., as F-value is defined as variation between sample means vs. variation within the samples, large F>>1 values can indicate that the parameter has significant effect on the results.

4.1.2. Uncertainty analysis

Uncertainty quantification (UQ) is the process of determining the effect of input uncertainties on model responses. These input uncertainties may be characterized as either aleatory uncertainties, which are irreducible variabilities inherent in nature, or epistemic uncertainties, which are reducible uncertainties resulting from a lack of knowledge. Since sufficient data is generally available for aleatory uncertainties, probabilistic methods are commonly used for computing response distribution statistics based on input probability distribution specifications. Conversely, for epistemic uncertainties, data is generally sparse, making the use of probability theory questionable and often leading to non-probabilistic methods based on e.g., interval specifications (Dempster-Shafer evidence theory) [10].

The objective of evidence theory is to model the effects of epistemic uncertainties. Epistemic uncertainty refers to the situation where one does not know enough to specify a probability distribution on a variable. Sometimes epistemic uncertainty is referred to as subjective, reducible, or lack of knowledge uncertainty. In Dempster-Shafer theory of evidence, the uncertain input variables are modelled as sets of intervals. The user assigns a basic probability assignment (BPA) to each interval, indicating how likely it is that the uncertain input falls within the interval. The intervals may be overlapping, contiguous, or have gaps. The intervals and their associated BPAs are then propagated through the simulation to obtain cumulative distribution functions on belief and plausibility. Belief is the lower bound on a probability estimate that is consistent with the evidence, and plausibility is the upper bound on a probability estimate that is consistent with the evidence [10,14].

Alternatively, ROAAM+ methods can be employed, which make use of the second order probabilities [13]. The ROAAM+ framework for Nordic BWR employs the concept of second-order probability in quantification of the conditional containment failure probability. The need for the second-order probabilities comes from the realization of the nature of epistemic uncertainties in prediction of failure probability (i.e., partial probabilistic knowledge). Epistemic uncertain parameters in ROAAM+ framework is separated into two groups, depending on the degree of knowledge:

- Model deterministic parameters – complete probabilistic knowledge (i.e., range and probability distribution).
- Model intangible parameters – incomplete or no probabilistic knowledge, one can only speculate regarding the possible range.

Based on ROAAM+ formulation, since probabilities are designed to handle uncertainty, it would be logical to consider representing uncertain probabilities with probabilities. Thus, in order to assess the importance of the missing information about the distributions of intangible parameters the distributions itself are considered as uncertain (i.e., parameters that characterize distributions, as in hierarchical Bayesian models).

4.1.2.1. Sampling-based uncertainty propagation

An analysis outcome of a model will have an uncertainty structure that derives from the uncertainty structure of the model input parameters. For uncertainty propagation through a model, it is important that the sampling set of model input parameters provides an adequate coverage of the space of these parameters. Adequate coverage of the uncertainty space of model input parameters depends on various factors, such as the number of samples, selected probability distributions as well as the choice of sampling approach.

4.1.2.2. Number of samples

Wilks' non-parametric method for setting tolerance limits is one of the common choices to determine tolerance limits with some confidence level for input parameters with unknown distributions in computational applications in the nuclear industry. The advantage of Wilks' method is the required sample size is independent of the number of input parameters and all input parameters can be sampled simultaneously.

Table 4-1 provides the minimum sample size N required to obtain various tolerance/confidence upper bounds (one sided) and intervals (two-sided) for ranks from 1 to 10. It shows that larger sample sizes N are required to increase the tolerance and the confidence. In addition, higher rank order statistics require an increase in the number of samples [19].

Table 4-1. Minimum sample size required for tolerance/confidence Wilks tolerance limits and bounds. Results are shown for four common tolerance/confidence combinations for ranks from 1 to 10 [19].

r	95%/95%		95%/99%		99%/95%		99%/99%	
	Bound	**Interval**	**Bound**	**Interval**	**Bound**	**Interval**	**Bound**	**Interval**
1	59	93	90	130	299	473	459	662
2	93	153	130	198	473	773	662	1001
3	124	208	165	259	628	1049	838	1307
4	153	260	198	316	773	1312	1001	1596
5	181	311	229	371	913	1568	1157	1874
6	208	361	259	425	1049	1818	1307	2144
7	234	410	288	478	1182	2064	1453	2409
8	260	458	316	529	1312	2306	1596	2669
9	286	506	344	580	1441	2546	1736	2925
10	311	554	371	631	1568	2784	1874	3179

Higher rank Wilks' estimates correspond to using more centrally located order statistics to estimate the desired tolerance limit. These estimates require larger sample sizes but estimate the same tolerance with approximately equal confidence [19].

4.1.2.3. Random and LHS Sampling

Random sampling is a part of the sampling technique in which each sample has an equal probability of being chosen.

A sample chosen randomly is meant to be an unbiased representation of the total population. Latin hypercube sampling (LHS) is a statistical method for generating a near-random sample of parameter values from a multidimensional distribution. When sampling a function of N variables, the range of each variable is divided into M equally probable intervals. M sample points are then placed to satisfy the Latin hypercube requirements; this forces the number of divisions, M, to be equal for each variable. This sampling scheme does not require more samples for more dimensions (variables); this independence is one of the main advantages of this sampling scheme. Another advantage is that random samples can be taken one at a time, remembering which samples were taken so far.

Both random and LHS sampling techniques are available in the Dakota[1] package [10]. A pyDakota interface for random and LHS sampling in Dakota has been developed. It performs user input processing (parameters, ranges and distributions) and generation of the sampling set. Currently, the interface supports truncated normal, truncated lognormal, uniform, loguniform, triangular, exponential, beta, gamma and Weibull distributions, as well as discrete real and integer sets with predefined probabilities. Furthermore, the sampling accounts for correlations among the variables, which can be defined by a user-supplied correlation matrix.

[1] Dakota is an open-source Multilevel Parallel Object-Oriented Framework for Design Optimization, Parameter Estimation, Uncertainty Quantification, and Sensitivity Analysis developed by SNL.

4.1.2.4. Importance sampling

Importance sampling is a method that allows one to estimate statistical quantities such as failure probabilities in a way that is more efficient than Monte Carlo sampling. The core idea in importance sampling is that one generates samples that are preferentially placed in important regions of the space (e.g. in or near the failure region or user-defined region of interest), then appropriately weights the samples to obtain an unbiased estimate of the failure probability [10].

Importance sampling technique can be applied when performing post-processing of the uncertainty analysis results, to assess the effect of missing information regarding probability distributions of intangible parameters (see section 4.1.2).

4.1.3. MELCOR simulation platform

A simulation platform (pyMELCOR) has been developed in Python to perform sensitivity and uncertainty analysis with MELCOR code.

Based on the user input, the pyDakota interface generates an input file for sensitivity/uncertainty analysis using Dakota [10]. The simulation driver (pyMELCOR) generates a set of MELCOR input decks and performs parallel execution of the MELCOR code. In case of code convergence issues and crashes, pyMELCOR performs adaptive refinement of the maximum time step and restarting in case of crashed simulations. The plot data (FOMs and other MELCOR code plot variables defined by the user) is extracted using the pyPTF extraction script, written in Python based on the MELCOR plot file format described in [11]. The extracted data is stored in the MELCOR database of solutions, while FOMs are analyzed in the Dakota package [10].

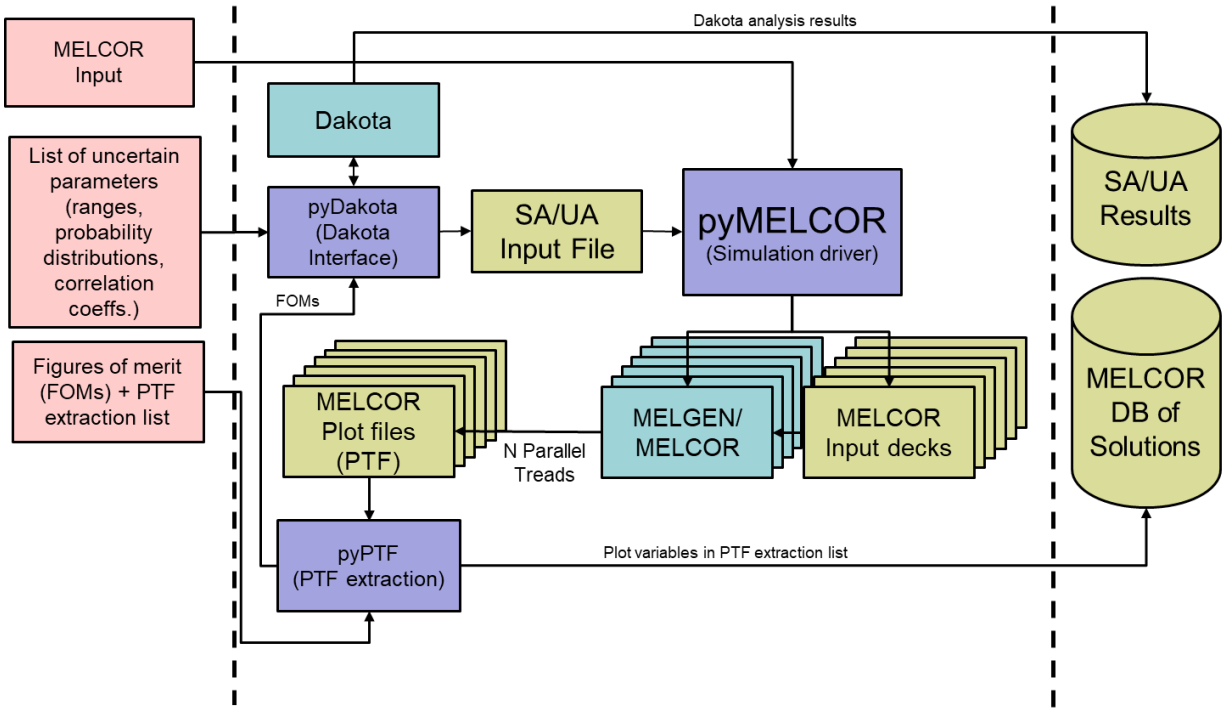

Figure 4-2. pyMELCOR simulation platform.

4.2. Methods used for sensitivity and uncertainty analysis by VTT

VTT's method of choice for both the sensitivity and uncertainty analyses was Dakota SNAP plug-in, which was used to sample the model parameters and to post-process majority of the results.

SNAP (Symbolic Nuclear Analysis Package) is an analysis tool developed by ISL (Information Systems Laboratories), and it consists of multiple integrated analysis code applications such as MELCOR, CONTAIN, and TRACE. It enables the creation and editing of model inputs, as well as setting up job streams and running the models and the other codes. SNAP also provides a robust visualization of the models [37].

Dakota (Design Analysis Kit for Optimization and Terascale Applications) toolkit has been developed by Sandia National Laboratories (SNL) for optimization and uncertainty quantification [38]. The SNAP plug-in for Dakota enables the addition of the uncertainty step in the job stream in SNAP. The main tasks of the uncertainty step are parameter sampling according to the user-input data (sampling method, target probability and confidence levels, bounds of the parameter values, probability distributions) of which Dakota calculates the adequate number of samples using the Wilks method mentioned in chapter 4.1.2.2, and post-processing of the results into a report form.

Using Dakota with SNAP is not necessarily straightforward. One well-known issue with the plug-in is that if even one of the generated MELCOR input files fails during the MELGEN step, no Dakota uncertainty report is generated at the end of the simulation run. Crashes during the MELCOR step might not prevent Dakota from generating the report, but they may produce incomplete results, which will affect the final results of the sensitivity and uncertainty studies. Moreover, even though the SNAP plug-in for Dakota uses the actual Dakota code, the features within SNAP are rather limited. For example, there seems not to be an intuitive way to use other sensitivity analysis methods such as the Morris method.

To combat these issues, Python directed job streams were set up in SNAP. With Python, it is possible to extend the definition of the failed cases to cover the crashed cases as well and to utilize SNAP's "replacement samples" feature, which allows the resampling and rerunning of the failed cases. To use other sensitivity methods, it should be possible to run Dakota with Python. However, that was unsuccessful, so SALib Python library was used instead to perform the Morris sensitivity analysis.

For SNAPs default sensitivity analysis method, Dakota calculates multiple correlation coefficients that can be used in assessing the sensitivity of the model against the input parameters. The first one is called simple correlation coefficient in Dakota, but it is also known as Pearson correlation coefficient. It measures the linear correlation between two datasets, in this case between the parameter and the FOM. Pearson correlation between variables x and y can be calculated with [38].

$$Corr(x,y) = \frac{\sum_i (x_i - \bar{x})(y_i - \bar{y})}{\sqrt{\sum_i (x_i - \bar{x})^2 \sum_i (y_i - \bar{y})^2}} \quad (5)$$

The second coefficient is called partial correlation coefficient. In addition to the linear correlation between two variables, it also considers the effect of the other parameters. Both coefficients also have a rank form. The rank form of Pearson correlation coefficient is called simple rank correlation coefficient in Dakota and Spearman correlation coefficient elsewhere.

The difference between the original correlation and rank correlation is that instead of actual values, rank correlation coefficients are calculated from the ranks of the datasets. This way, the effect of possible outliers in datasets can be minimized.

5. Results

5.1. Investigation of Cs/I_2 Remobilization Sources in Finnish NBWR

In order to study the sources of Cs/I_2 remobilization and the most influential parameters, an uncertainty analysis performed during the 2nd phase of the NKS-STATUS project was repeated. Like in the previous phases of the project, VTT's Olkiluoto 1 and 2 BWR MELCOR model was used, and the studied scenario was a station blackout (SBO) with filtered containment venting. Some improvements and modifications were made to the MELCOR model. The simulation time was extended to 30 hours according to the preliminary analyses. In order to reduce the occurrence of crashes, the timestep control was optimized by studying the old results and decreasing the maximum timestep accordingly. The aerosol resuspension model was not enabled in the previous models, so it was enabled for this work. Moreover, the solid debris ejection model (IDEJ) was selected for the separate effect analysis.

5.1.1. Preliminary sensitivity and uncertainty analyses

Sensitivity and uncertainty analyses were performed simultaneously using SNAP's Dakota plug-in. No separate sensitivity studies such Morris analysis were done this time. The analyses were run twice – with the solid debris ejection model switched on (IDEJ0) and off (IDEJ1).

In order to save computational resources, only one figure of merit, the fraction of cesium release to the environment, was selected. According to the Wilks' formula mentioned in earlier chapters, with 95% confidence and probability levels this resulted in 59 model evaluations. Even though the timestep optimization reduced the number of code crashes significantly, some still occurred. The crashed model runs were resampled and recalculated.

The selection of input parameters was reassessed, the focus being on the parameters thought to be affecting mainly aerosol behavior. A total of 26 input parameters were studied, and most of the value ranges were taken from the first phase of the STATUS project. The distribution of the parameters was set to uniform. The parameters are listed in Table 5-1.

Table 5-1. Parameters used in the first sensitivity and uncertainty analysis.

N	Parameter	Default value	Range	Unit
1	HDBH2O	100	[200, 2000]	W/m2-K
2	TPFAIL	1273	[1273, 1600]	K
3	CHI	1	[1.0, 3.0]	-
4	GAMMA	1	[1.0, 3.0]	-
5	FSLIP	1.257	[1.1, 1.3]	-
6	STICK	1	[0.5, 1]	-
7	RHONOM	1000	[1000, 4900]	kg/m^3
8	TURBDS	1.E-3	[7.5E-4, 1.25E-3]	m^2/s^3
9	TKGOP	0.05	[0.006, 0.06]	-
10	FTHERM	2.25	[1.75, 2.75]	-
11	DELDIF	1.0E-5	[1e-6, 1e-4]	m
12	SC7111I1	4.982	[4.2347, 5.7293]	Å

N	Parameter	Default value	Range	Unit
13	SC7111I2	550	[467.50, 632.50]	K
14	SC7111CS1	3.617	[3.0745,4.1595]	Å
15	SC7111CS2	97	[82.450,111.550]	K
16	SC7170CS	3.95	[3.3575, 4.5425]	kg/kg H2O
17	SC7170CSI3	0.44	[0.374, 0.5060]	kg/kg H2O
18	SC7170CSI4	2.25	[1.9125, 2.5875]	kg/kg H2O
19	SC715111	3.45	[2.9325, 3.9675]	-
20	SC71521	0.007	[5.E-3, 8.E-3]	m
21	SC71531	7.876	[6.6946, 9.0574]	cm/s
22	SC71551	1.79182	[1.5230, 2.0606]	-
23	SC71555	1.13893	[0.9681, 1.3098]	-
24	SC71542	3.011E-3	[2.5593E-03, 3.4626E-03]	l-s/cm2
25	SC71568	-2.321E-3	[-2.6691e-03, -1.9728e-03]	-
26	DECAYH	1	[0.96 – 1.04]	-

The sensitivity of the parameters was studied by observing the sensitivity correlations. The correlations between the Cs release and the input parameters are presented in Figure 5-1 and Figure 5-2 below.

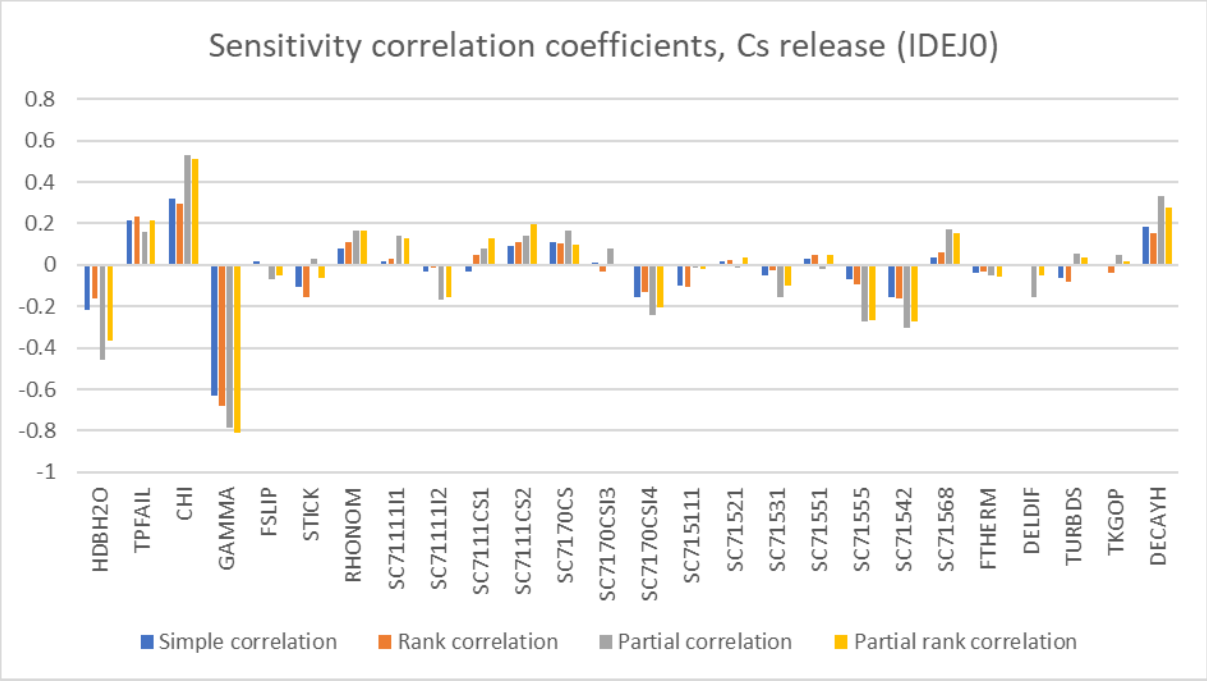

Figure 5-1. The sensitivity correlation coefficients, Cs release fraction (IDEJ0).

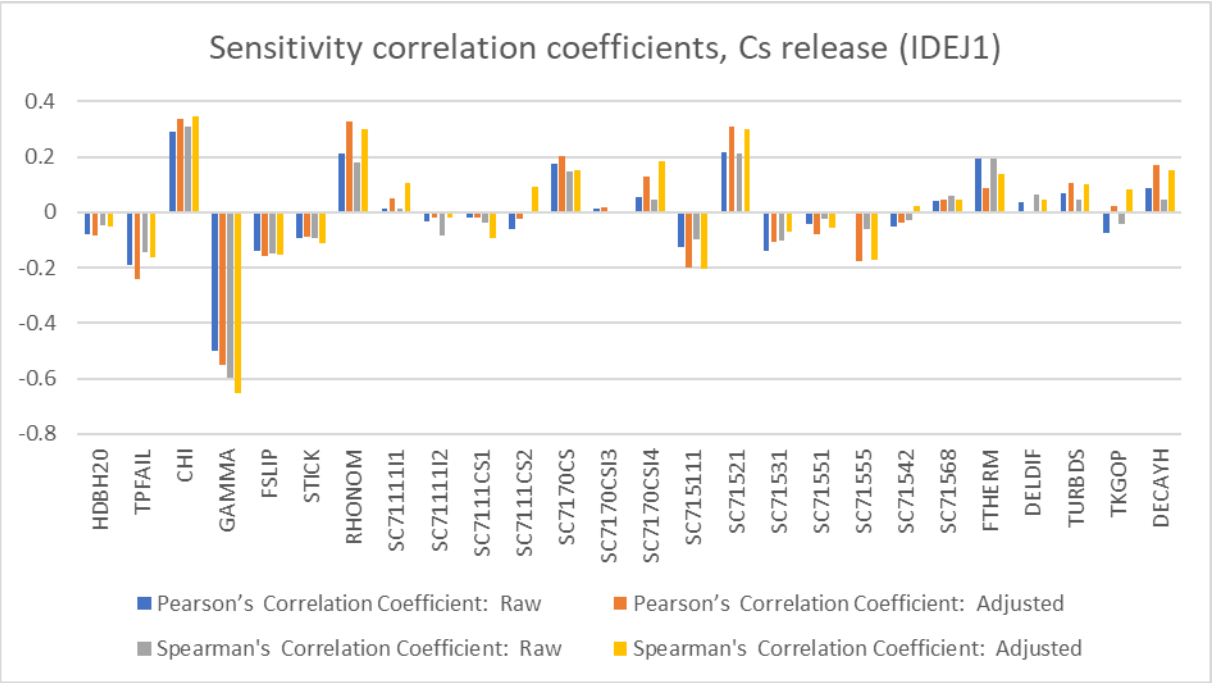

Figure 5-2. The sensitivity correlation coefficients, Cs release fraction (IDEJ1).

According to the sensitivity correlation coefficients, it seems that in both cases the most influential parameters are GAMMA and CHI, i.e. aerosol agglomeration factor and aerosol dynamic shape factor. In the case of IDEJ0, HDBH2O (heat transfer coefficient from debris to water) seems to have slightly increased partial correlation. In the case of IDEJ1, RHONOM (nominal aerosol density) and SC71521 (initial bubble diameter correlation coefficient in pool scrubbing model) have also slightly elevated partial correlations.

Cesium release as a function of time is shown in the horsetail plots in Figure 5-3 and Figure 5-4 below. In both figures it can be seen that the cesium release steadies out after 8 hours but starts increasing again after 15 to 20 hours. The increase, however, is very slight and its effect on the total release of cesium could be considered almost negligible.

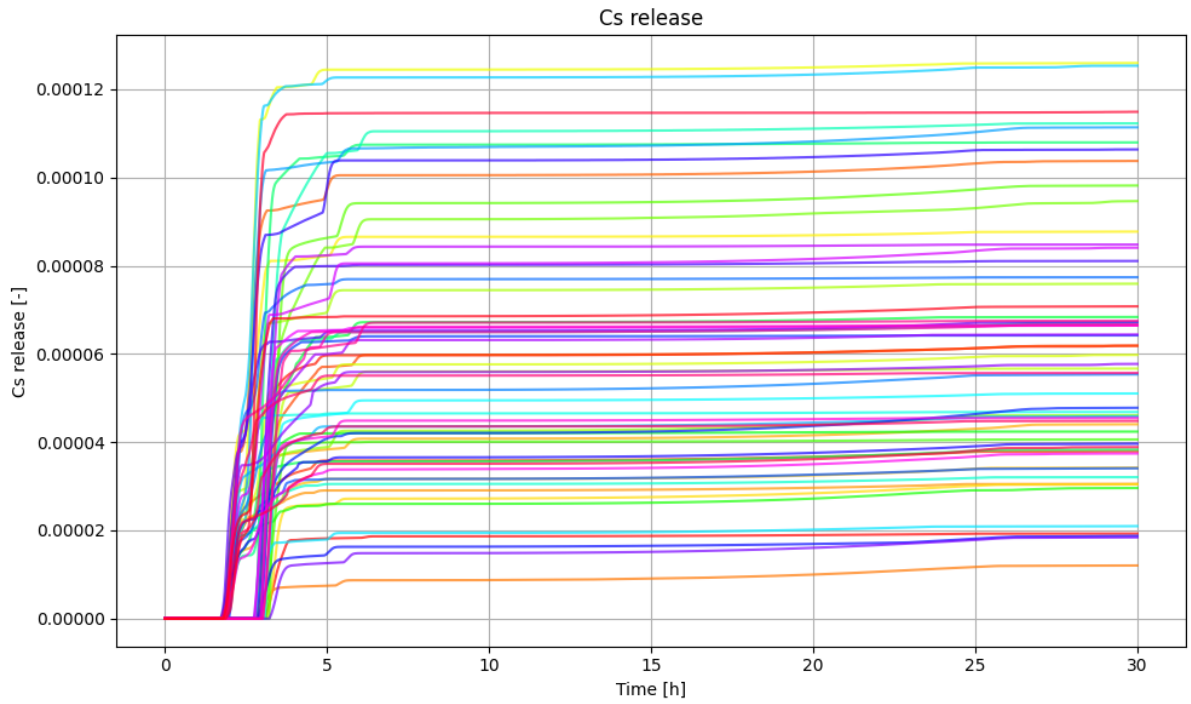

Figure 5-3. Horsetail plot of the Cs release fraction [-] in IDEJ0 case.

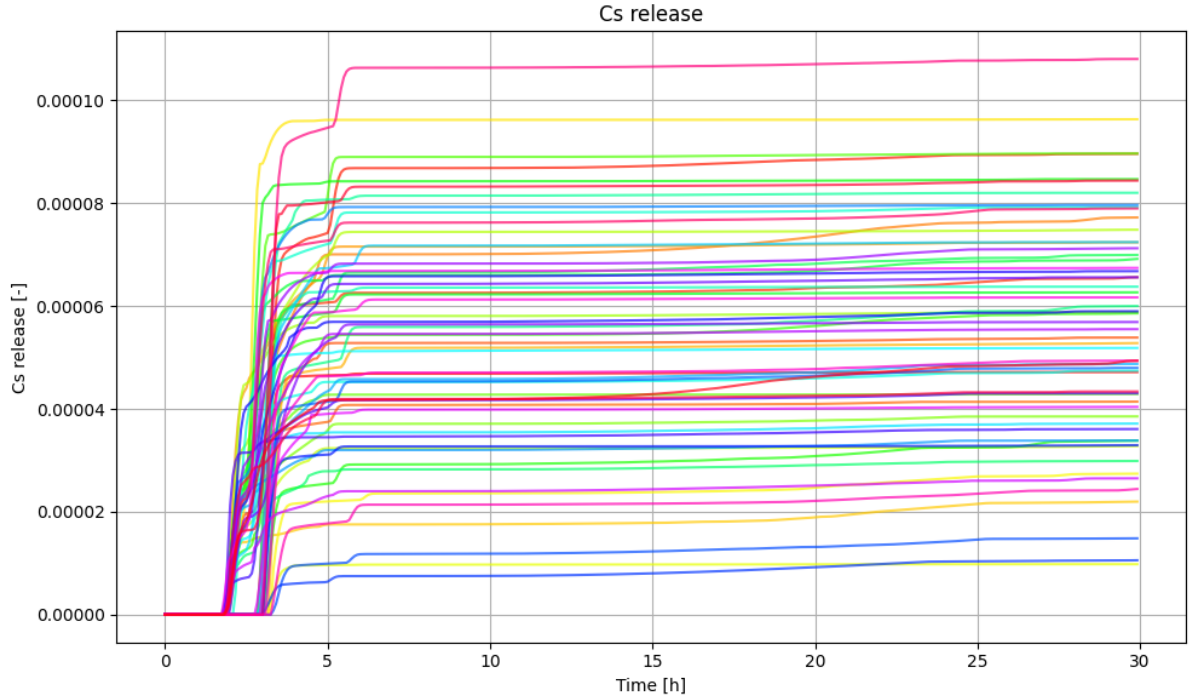

Figure 5-4. Horsetail plot of the Cs release fraction [-] in IDEJ1 case.

The key data values for Cs release are presented in Table 5-2 below.

Table 5-2. Cs release fraction [-]. Minimum, maximum, mean, median and standard deviation in both uncertainty cases.

	Cs release fraction [-] IDEJ0	**Cs release fraction [-] IDEJ1**
Min	1.20E-05	9.81E-06
Max	1.26E-04	1.23E-04

	Cs release fraction [-] IDEJ0	Cs release fraction [-] IDEJ1
Mean	6.05E-05	5.60E-05
Median	5.86E-05	5.39E-05
Standard deviation	2.83E-05	2.27E-05

Distributions of Cs release fraction [-] in both cases are presented in the histograms found in Figure 5-5 and Figure 5-6 below.

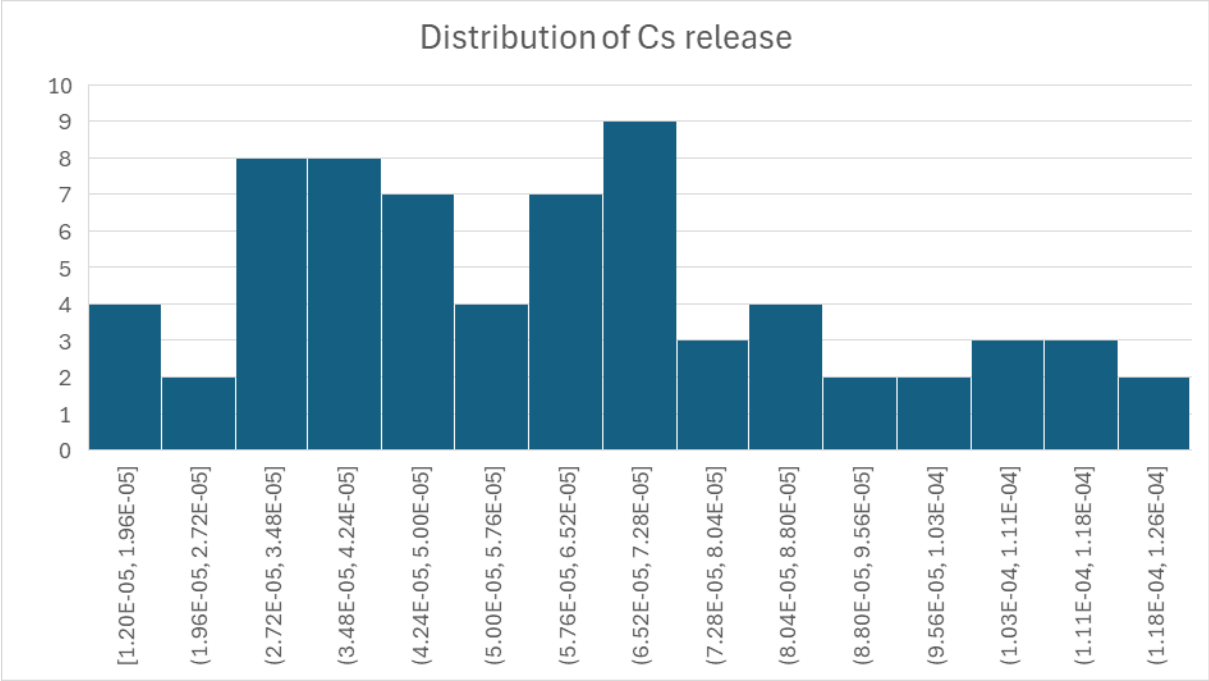

Figure 5-5. Histogram of Cs release [-] (N samples vs. binned values) (IDEJ0).

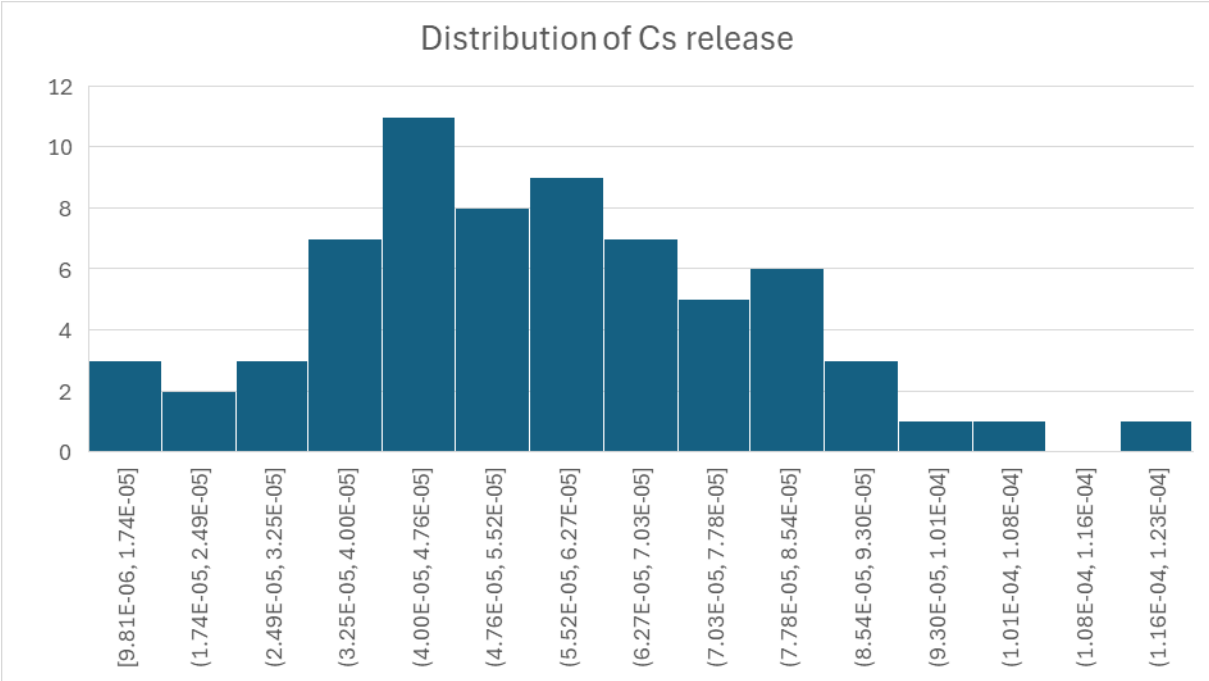

Figure 5-6. Histogram of Cs release [-] (N samples vs. binned values) (IDEJ1)

In both cases, the distribution of cesium is somewhat close to the normal distribution – but especially in the case of IDEJ1 the normal distribution is more pronounced. In the case of IDEJ0 the distribution is somewhat broader, and it might be affected by the uniform distribution of the input parameters. According to these results, IDEJ0 might also result in slightly higher cesium releases.

5.1.2. Identifying the main sources of Cs/I2 remobilization

The sources of remobilization were identified by examining the fission product deposits on the heat structures, and fission product masses in control volume pools and atmosphere. This was done by analyzing both the sensitivity/uncertainty analysis results and picking random model runs for further studies.

Figure 5-7 and Figure 5-8 present the total mass of the radioactive species deposited on all heat structures (MELCOR plot variable RN1-TMDTR) in each IDEJ case. The decreasing curves towards the ends of the simulations suggest that some resuspension may occur after 10-15 hours. However, the plot variable TMDTR does not reveal the estimated masses of each FP, and thus further studies are needed.

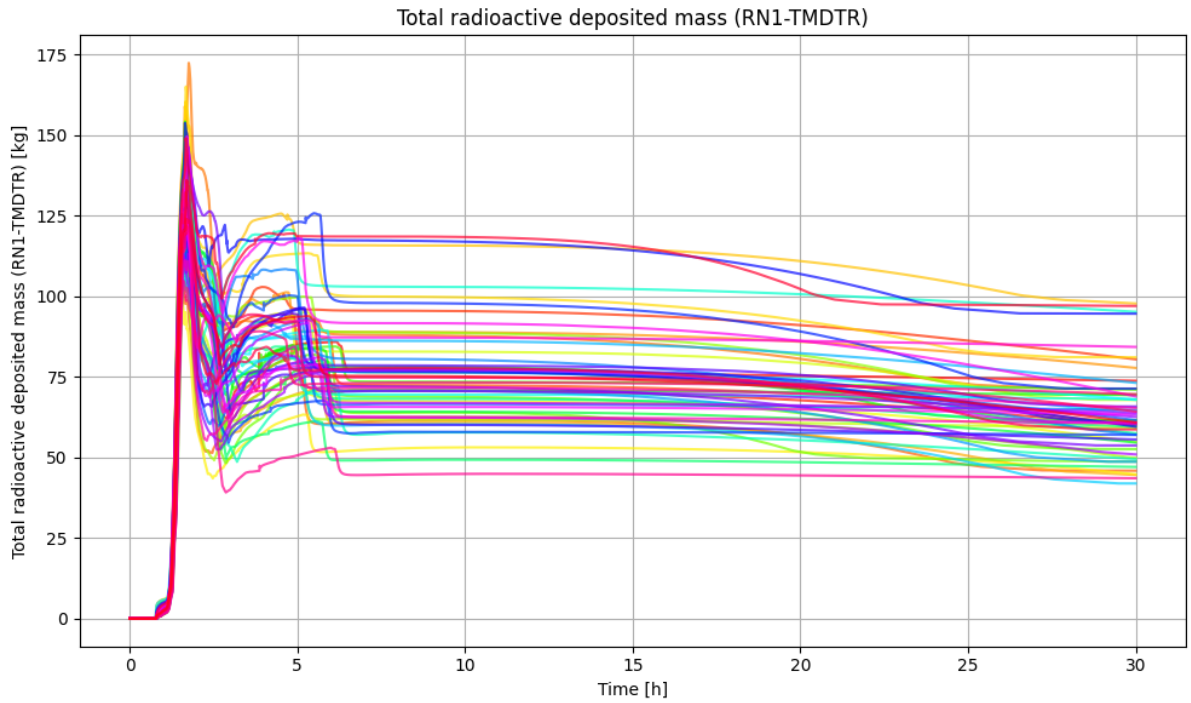

Figure 5-7. The total mass of deposited aerosols[kg] on all heat structures (IDEJ0).

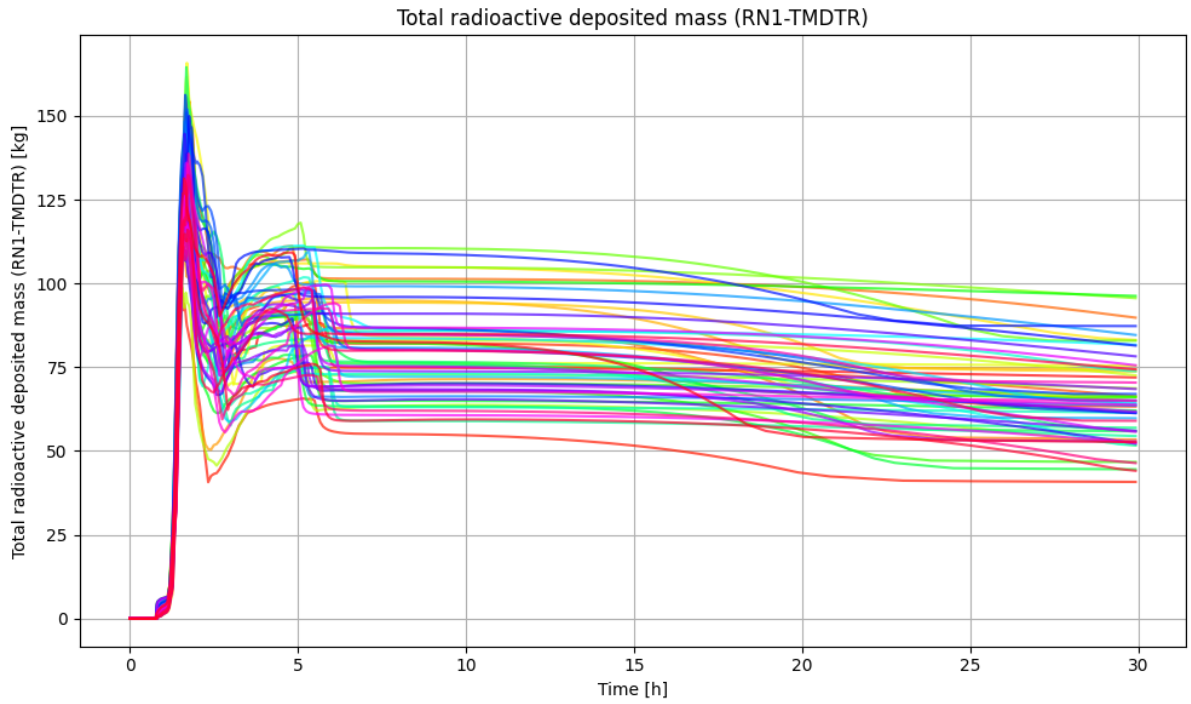

Figure 5-8. The total mass of deposited aerosols [kg] on all heat structures (IDEJ1).

Key values for the change in RN1-TMDTR between 10 and 30 hours are shown in the Table 5-3 below. The data shows that disabling the solid debris ejection model might increase resuspension. However, the change in FP masses between the two IDEJ cases is generally quite small – only a few kilograms.

Table 5-3. Key values for the change in RN1-TMDTR [kg] between 10 and 30 hours in both IDEJ cases.

	RN1-TMDTR [kg] IDEJ0	**RN1-TMDTR [kg] IDEJ1**
Min	0.94	0.82
Max	26.42	33.03
Mean	11.31	13.39
Median	11.29	14.06
Standard deviation	6.75	7.14

By studying the deposit masses in different control volumes and heat structures further, it is revealed that a significant amount of the deposited mass belongs to cesium. Deposits consisting of other species such as uranium oxide were also observed, but here focus is on cesium, iodine and CsI. The total masses of deposited cesium, iodine and CsI in a random case from the IDEJ0 SA/UA analyses are presented in Figure 5-9. It can be seen that the shape of the cesium curve follows quite closely the curve representing the total deposited mass. This suggests that most of the resuspended FP is also cesium. Similar behavior was observed in other randomly picked model evaluations as well.

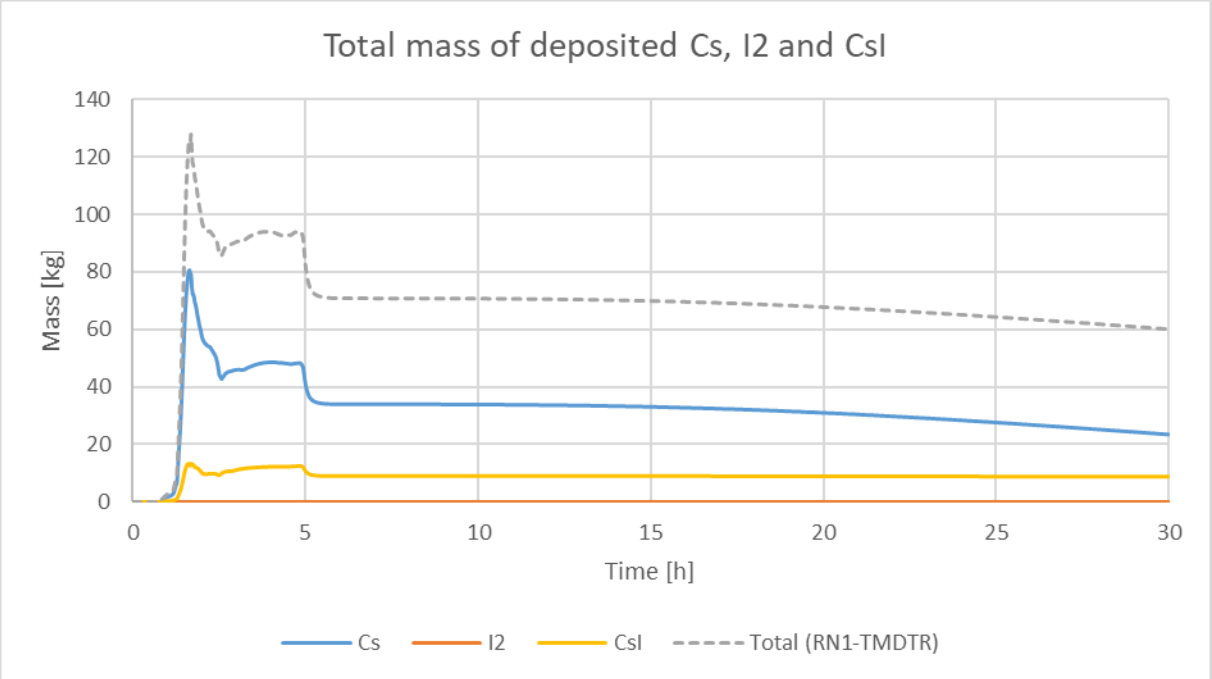

Figure 5-9. Deposited cesium, iodine and CsI masses [kg] in the whole system, along with the total mass of deposited radioactive species [kg] taken from an example case calculated during the SA/UA.

Further investigations show that most of the radioactive cesium is deposited on heat structures of the inner walls of the annulus region of the RPV, i.e. downcomer. Depositions also occur on the heat structures of the other control volumes, but only in the downcomer notable changes in the mass of the deposited FP can be observed.

Aerosols could also be trapped in pools. The investigation showed that most of the radioactive aerosols could be found first in the wet well pool, from where they are then relocated to the lower drywell due to the flooding of it. Most of this aerosol mass belonged to cesium. The portion of iodine and CsI of the total aerosol mass was quite negligible – the masses of iodine and CsI were from a few grams to a few kilograms respectively. Moreover, no significant relocation of aerosols from the pool to the atmosphere was observed during the 30h.

The masses of cesium in the liquid phase in the wet well and the lower drywell in a randomly picked model run (IDEJ0) are presented in Figure 5-10.

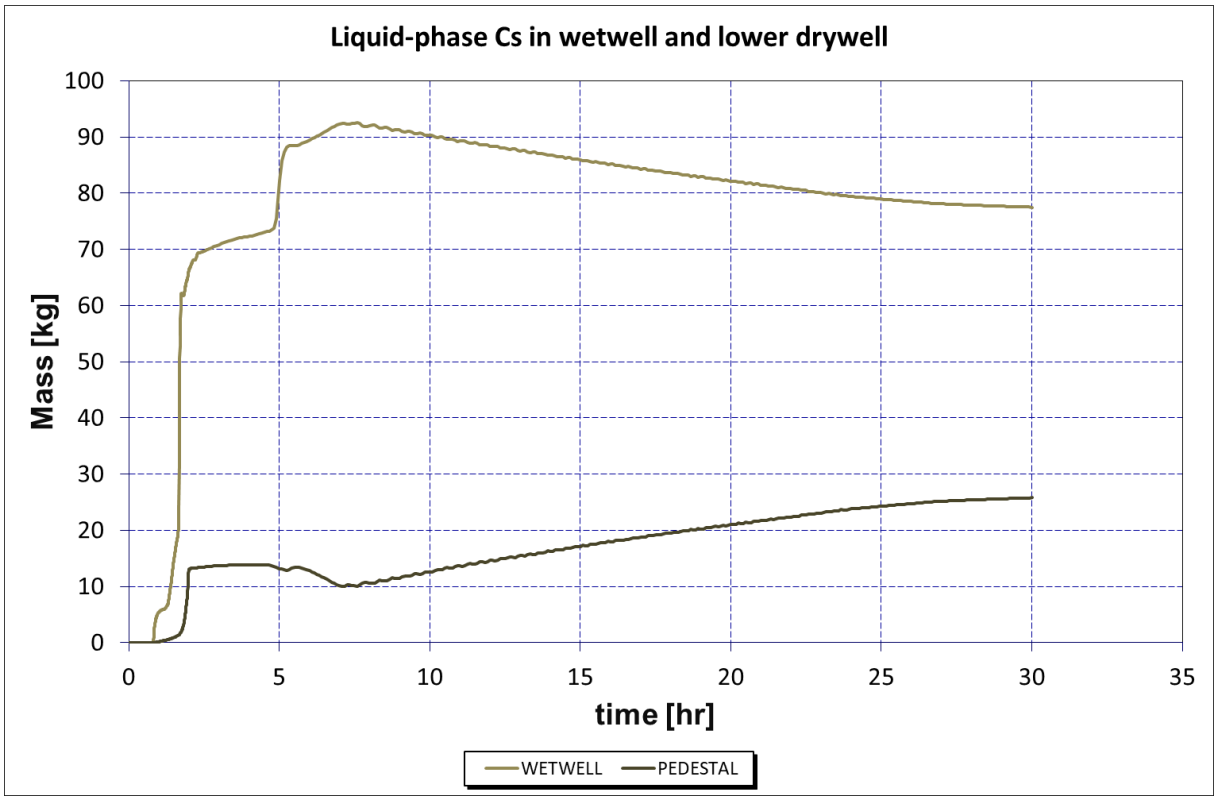

Figure 5-10. Cs mass [kg] in the wet well and the lower drywell pools.

Overall, the amount of FP remobilization in these calculations was observed to be quite small and not really significant compared to the main releases. The slight increases in Cs releases towards the ends of the 30-hour simulations, do not contribute much towards the overall release to the environment. To demonstrate this, the change in Cs release between 10 and 30 hours was calculated for each model run, and the results were further used to calculate some key values such as minimums, maximums and averages. These values are listed in Table 5-4.

Table 5-4. Key values for the change in Cs release fraction [-] between 10 and 30 hours.

	Cs release fraction [-] IDEJ0	**Cs release fraction [-] IDEJ1**
Min	2.22E-07	8.50E-08
Max	5.72E-06	7.46E-06
Mean	1.94E-06	1.78E-06
Median	1.80E-06	1.26E-06
Standard deviation	1.28E-06	1.59E-06

Considering that the order of magnitude of Cs releases in the most cases was around 10^{-5}, it can be seen that the change in the release between 10 and 30 hours is only tenth of the main Cs release.

5.1.3. Further sensitivity studies

In order to find possible correlation between the input parameters and the aerosol remobilization, robust sensitivity studies were performed afterwards. Figure 5-11 and Figure 5-12 present the sensitivity correlation coefficients between the change in Cs release between 10 and 30 hours and the input parameters.

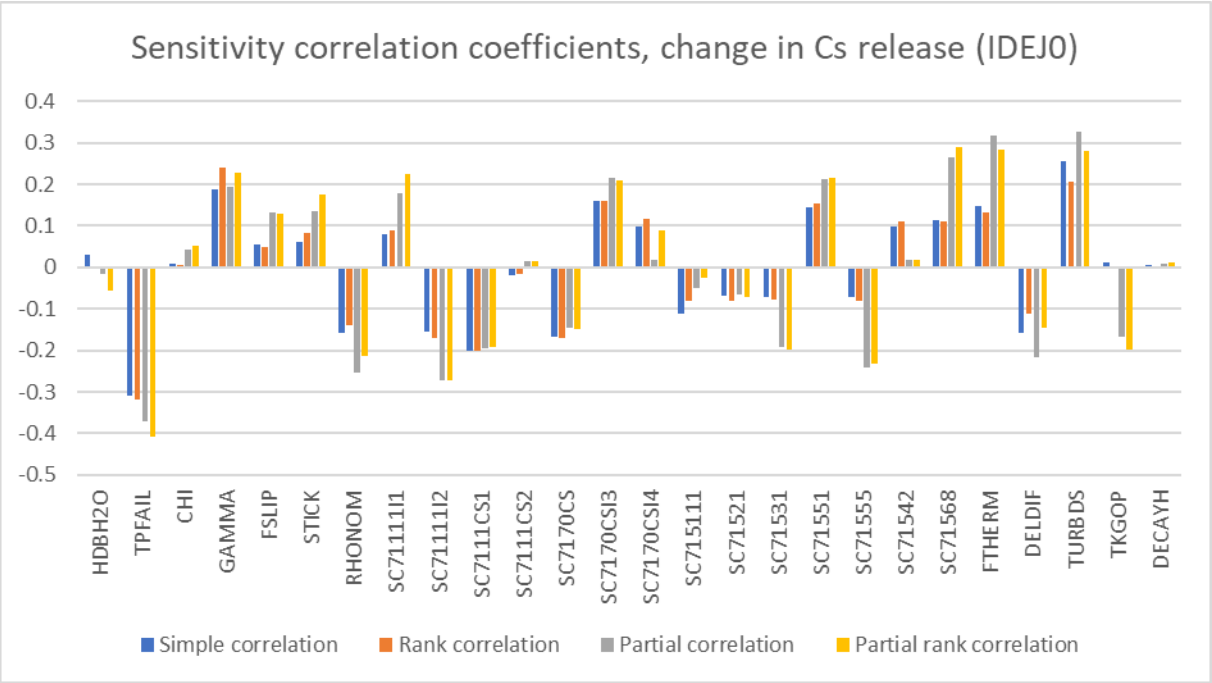

Figure 5-11. Sensitivity correlation coefficients for change in Cs release between 10 and 30 hours (IDEJ0).

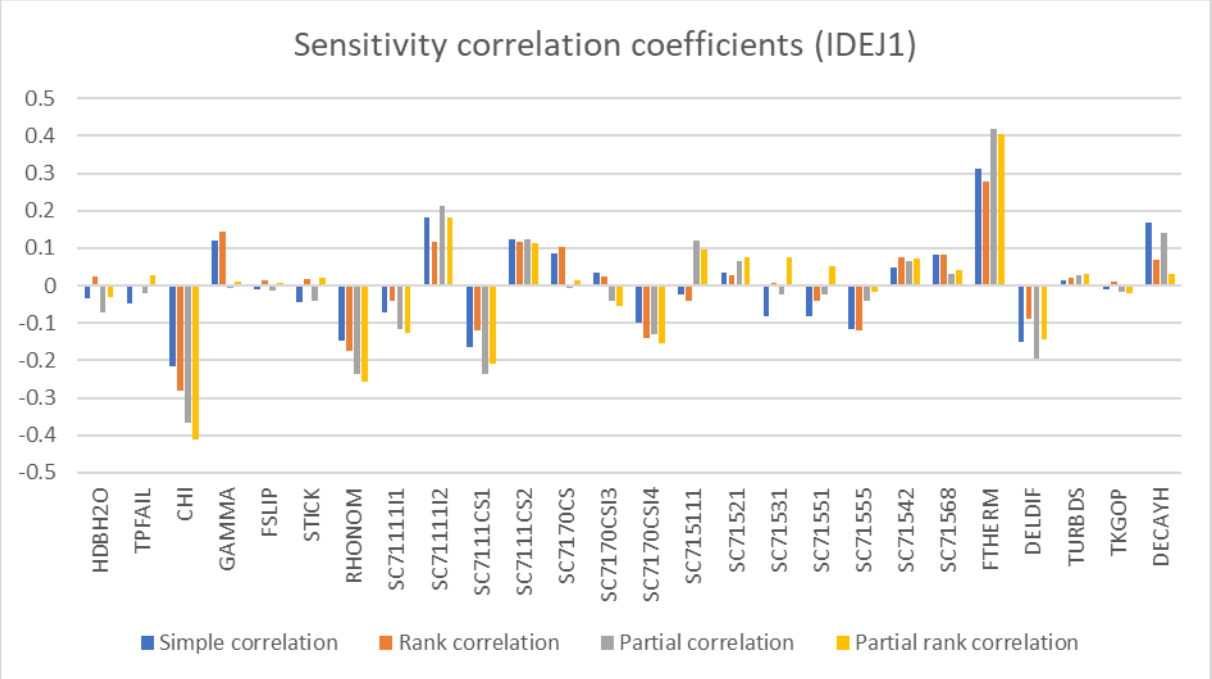

Figure 5-12. Sensitivity correlation coefficients for change in Cs release between 10 and 30 hours (IDEJ1).

The sensitivity coefficients suggest that for IDEJ0, the most influential parameters might be TPFAIL (vessel failure temperature), SC71568 (Multiplicative constant in a temperature correction correlation), FTHERM (thermal accommodation coefficient) and TURBDS (turbulence dissipation ratio), and for IDEJ1 these might be CHI (aerosol dynamic shape factor) and FTHERM.

5.2. Analysis of the Effect Independent Containment Spray System on Fission Product Remobilization in Finnish NBWR

VTT studied the potential effect of an independent containment spray system on fission product remobilization. The model and accident scenario stayed the same as in the baseline

case (Section 5.1), with the addition of the independent spray system. The analyses performed here are quite similar to the ones performed during the third phase of the STATUS project [67], although, as mentioned earlier, some model modifications and improvements have been made. Only IDEJ0 case was run here.

The spray system is set up so that it starts after some user-defined time after the vessel break. The delay between the breach and the start of the spray system is selected as one of the input parameters

5.2.1. Preliminary sensitivity and uncertainty analyses

The model used in the baseline case (Section 5.1) was used again to perform sensitivity and uncertainty analyses with the spray system enabled. Input parameters were changed so that some of the most non-influential parameters were dropped. Additionally, parameters for spray droplet size (DIAMO) and spray start delay (SPRDELAY) were added to the analysis. The parameters are listed in Table 5-5. The explanations of each parameter not mentioned here can be found from NKS STATUS Phase 1 report [23].

Table 5-5. Parameters used in the sensitivity and uncertainty analysis.

N	Parameter	Default value	Range	Unit
1	HDBH2O	100	[200, 2000]	W/m2-K
2	TPFAIL	1273	[1273, 1600]	K
3	CHI	1	[1.0, 3.0]	-
4	GAMMA	1	[1.0, 3.0]	-
5	FSLIP	1.257	[1.1, 1.3]	-
6	STICK	1	[0.5, 1]	-
7	RHONOM	1000	[1000, 4900]	kg/m3
8	TURBDS	1.00E-03	[7.5E-4, 1.25E-3]	m2/s3
9	TKGOP	0.05	[0.006, 0.06]	-
10	FTHERM	2.25	[1.75, 2.75]	-
11	DELDIF	1.00E-05	[1e-6, 1e-4]	m
12	DIAMO	1.00E-03	[0.0001, 0.002]	m
13	SC7170CS	3.95	[3.3575, 4.5425]	kg/kg H2O
14	SC7170CSI3	0.44	[0.374, 0.5060]	kg/kg H2O
15	SC7170CSI4	2.25	[1.9125, 2.5875]	kg/kg H2O
16	SC715111	3.45	[2.9325, 3.9675]	-
17	SC71521	0.007	[5.E-3, 8.E-3]	m
18	SC71531	7.876	[6.6946, 9.0574]	cm/s
19	SC71551	1.79182	[1.5230, 2.0606]	-
20	SC71555	1.13893	[0.9681, 1.3098]	-

N	Parameter	Default value	Range	Unit
21	SC71542	3.01E-03	[2.5593E-03, 3.4626E-03]	l-s/cm2
22	SC71568	-2.32E-03	[-2.6691e-03, -1.9728e-03]	-
23	DECAYH	1	[0.96 – 1.04]	-
24	SPRDELAY	0	[1.0, 3000.0]	s

The sensitivity of the parameters was studied by observing the sensitivity correlations between the parameters and Cs release. The correlations are presented in Figure 5-13 below.

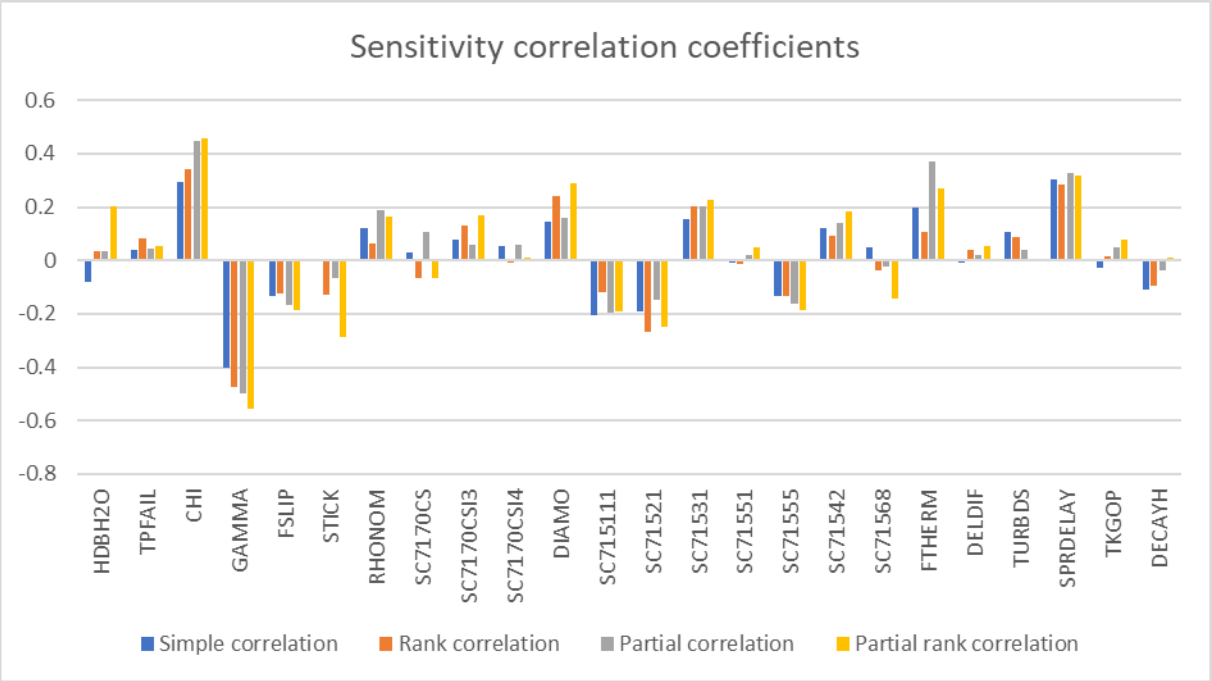

Figure 5-13. The sensitivity correlation coefficients for Cs release to the environment [-], containment sprays enabled.

The results from the sensitivity analysis suggest that the most influential parameters might be CHI and GAMMA, which is on the line with the previous analyses. Additionally, some increased significance can be seen on SPRDELAY and FTHERM.

Cesium releases in all model evaluations are shown in Figure 5-14. Key values such as minimum, maximum and average are presented in Table 5-6.

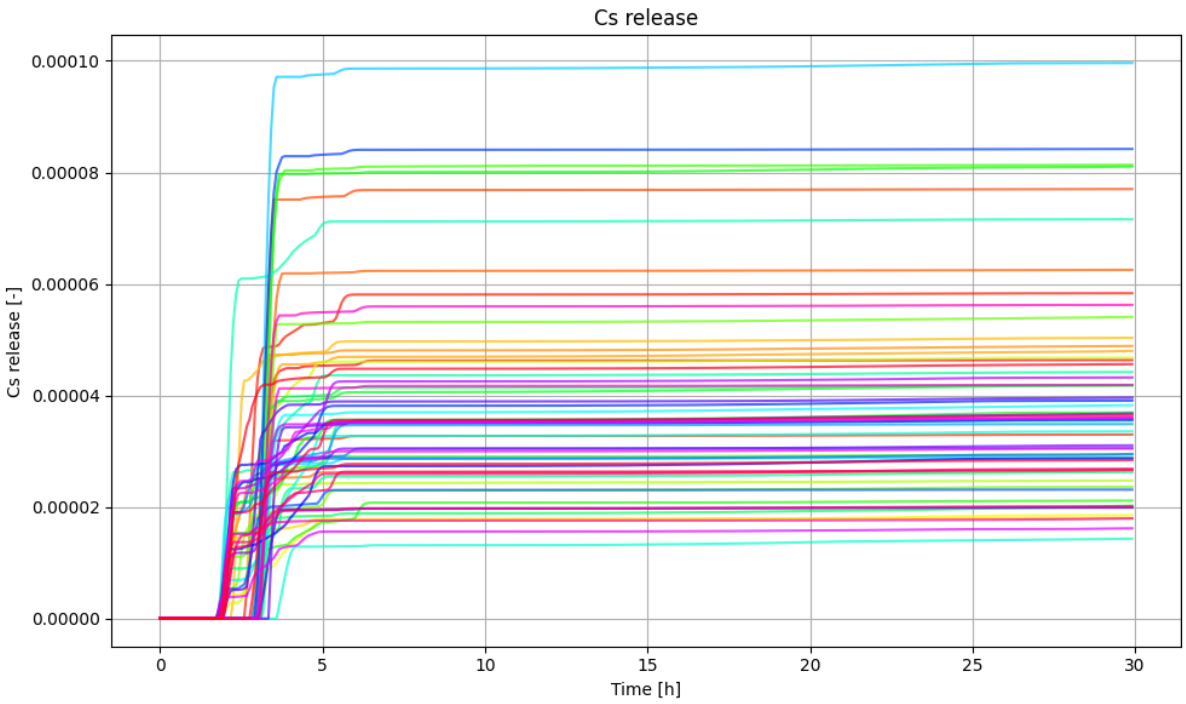

Figure 5-14. Cs release to the environment [-], spray systems enabled.

Table 5-6. Minimum, maximum, mean, median and standard deviation of total Cs release to the environment [-] in the case with spray systems enabled, compared with the data from the previous analyses without the spray system.

	SPRAY (IDEJ0)	**NO SPRAY (IDEJ0)**	**NO SPRAY (IDEJ1)**
Min	1.43E-05	1.20E-05	9.81E-06
Max	9.96E-05	1.26E-04	1.23E-04
Mean	3.93E-05	6.05E-05	5.60E-05
Median	3.60E-05	5.86E-05	5.39E-05
Standard deviation	1.83E-05	2.83E-05	2.27E-05

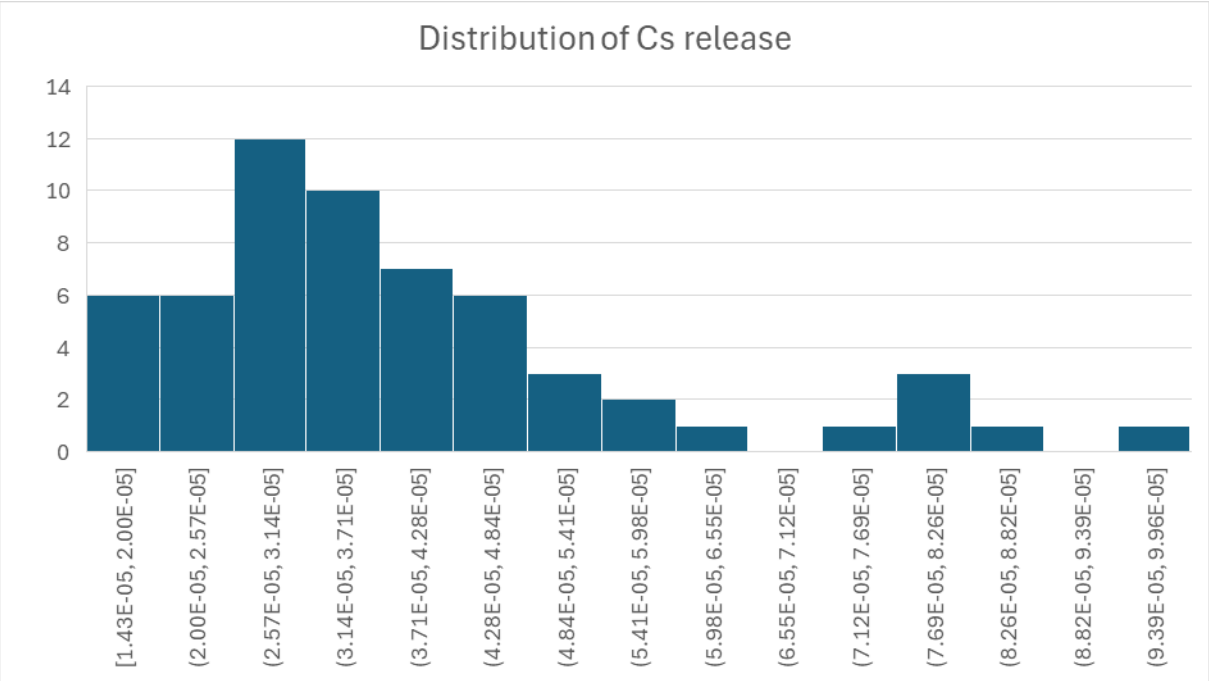

Figure 5-15. Distribution of Cs release fraction [-] (N samples vs. binned values)

The results seem to suggest that enabling the spray system results in lower Cs releases and in a narrower distribution of the release. Another notable difference is that in the horsetail plot of Figure 5-14, the increase of Cs release towards the end of simulation is barely noticeable. In order to check whether increase occurs, the difference in Cs release between 10 and 30 hours was calculated. The minimums, maximums, averages etc. are gathered to Table 5-7 along with the corresponding values from the baseline analyses (Section 5.1),

Table 5-7. Key values for the change in Cs release fraction [-] to the environment between 10 and 30 hours.

	NO SPRAY (IDEJ0)	**NO SPRAY (IDEJ1)**	**SPRAY (IDEJ0)**
Min	2.22E-07	8.50E-08	6.60E-08
Max	5.72E-06	7.46E-06	1.39E-06
Mean	1.94E-06	1.78E-06	5.95E-07
Median	1.80E-06	1.26E-06	5.72E-07
Standard deviation	1.28E-06	1.59E-06	3.62E-07

According to the data, it can be confirmed that some cesium is released between 10 and 30 hours. The order of the magnitude of the Cs release matches the IDEJ0 case from the results presented in Section 5.1. However, the increase in the release is quite insignificant compared to the initial Cs release.

5.2.2. Fission product remobilization

The fission product remobilization was studied as in the baseline scenarios (Section 5.1). Figure 5-16 presents the total mass of the deposited radioactive species in all simulated cases. Like in the previous analyses, some decrease in the deposited masses towards the end of the simulations can be observed.

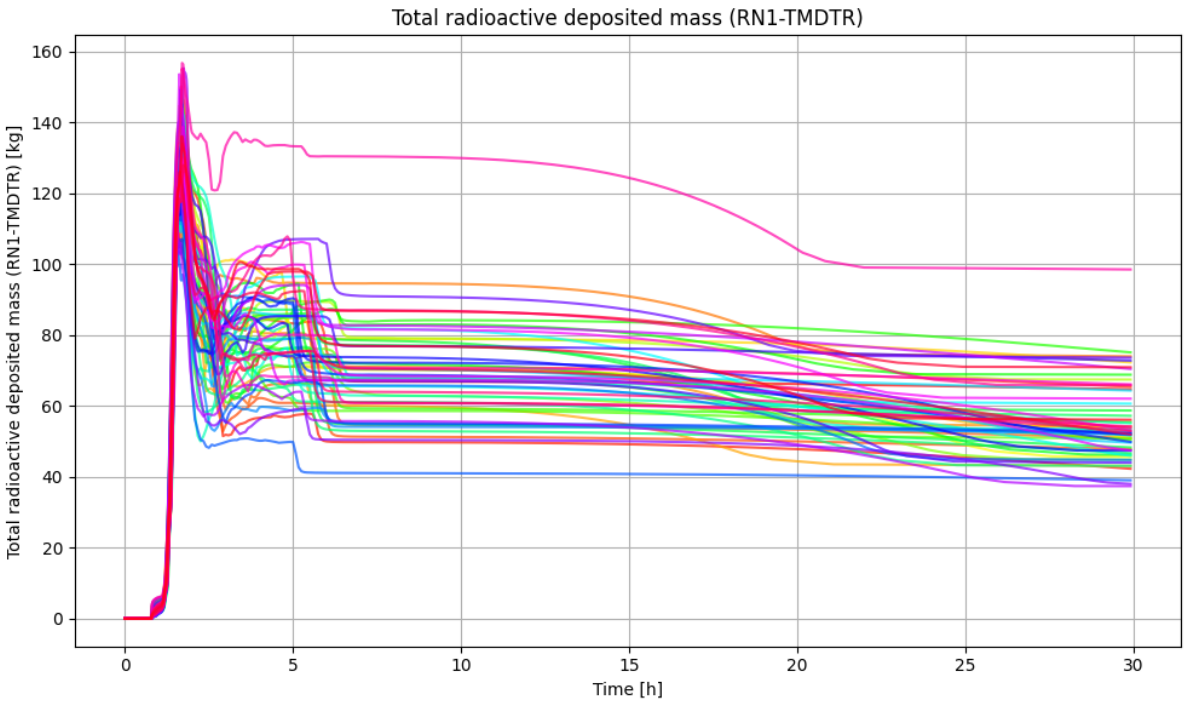

Figure 5-16. The total mass of aerosols [kg] deposited on all heat structures.

In order to better visualize the change in the deposited masses, the change in the masses between 10 and 30 hours was calculated and further analyzed. Some key values such as minimum, maximum and average values were calculated and listed in Table 5-8 along the data from the baseline analyses (Section 5.1) for comparison purposes.

Table 5-8. Key values for the change in total deposited aerosol mass [kg] between 10 and 30 hours.

	SPRAY (IDEJ0)	**NO SPRAY (IDEJ0)**	**NO SPRAY (IDEJ1)**
Min	1.81	0.94	0.82
Max	31.50	26.42	33.03
Mean	13.63	11.31	13.39
Median	15.72	11.29	14.06
Standard deviation	7.37	6.75	7.14

The data suggests that using the spray system might increase the loss of deposits in the system, which might mean resuspension of the deposited FPs.

5.2.3. Further sensitivity studies

In order to find possible correlation between the input parameters and the aerosol remobilization, robust sensitivity studies were performed afterwards. Figure 5-17 present the sensitivity correlation coefficients between the change in deposited FP masses between 10 and 30 hours and the input parameters. Since most of the changes in the masses of the deposited FP was traced back to the changes in Cs deposits, it could be assumed that the results shown here hold true for cesium deposits and resuspension as well.

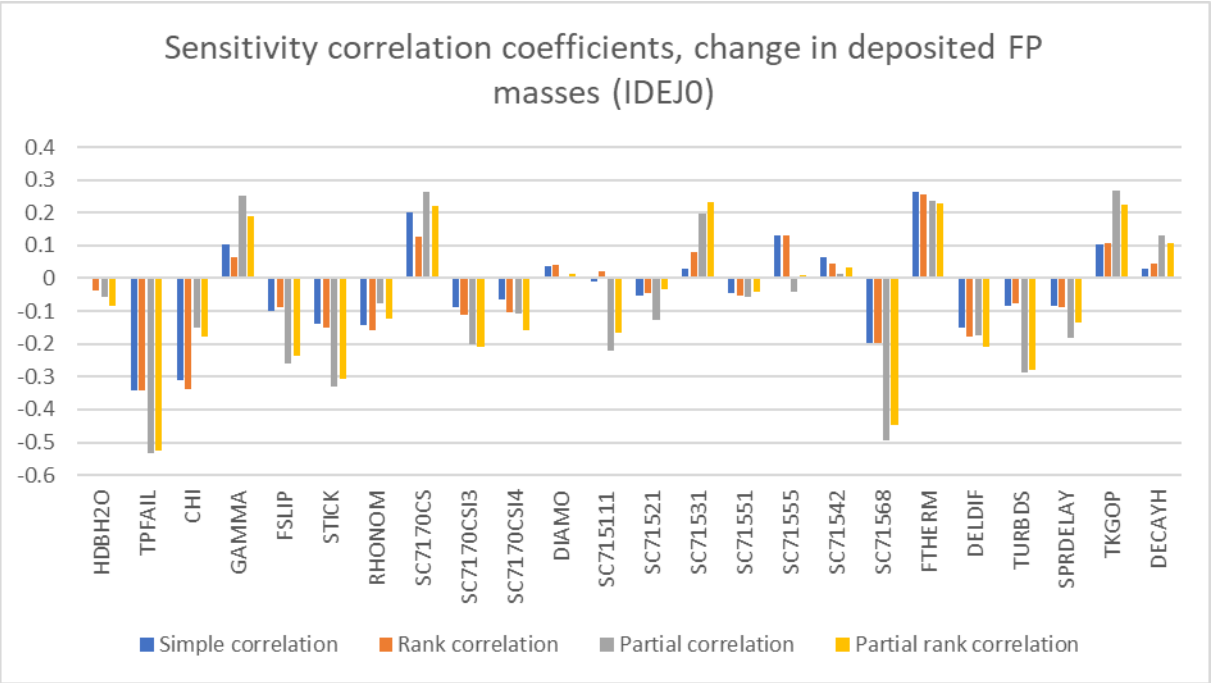

Figure 5-17. Sensitivity correlation coefficient, change in deposited FP masses (IDEJ0).

The correlation coefficients suggest that the most influential parameters regarding the FP resuspension might be TPFAIL and SC71568.

5.3. Analysis of Fission Products Remobilization in Nordic BWR

During the previous phases of the project KTH analyzed the release of fission products, in particular Cesium and Iodine, to the environment. Sensitivity studies were conducted to identify important MELCOR parameters for the source term release. Other fractions of the fission products that were within the containment (CNT) or the reactor pressure vessel (RPV) as depositions on the heat structures or the pool were not studied in detail. Here we present the results of cesium and iodine deposited in the RPV and the CNT (excluding the wetwell).

As was done previously, the accident scenarios considered here are RC4A and RC4B, unmitigated accidents initiated by LOCA and SBO respectively, with containment failure due to ex-vessel phenomena (FCI like steam explosions)/basemat melt through. These are denoted as LOCA-IDEJ0, LOCA-IDEJ1, SBO-IDEJ0 and SBO-IDEJ1, where IDEJ is the debris ejection switch in MELCOR that represents if molten debris is ejected with solid debris (IDEJ0) or without solid debris (IDEJ1). All simulations are run for 72h. Any instance of crashed simulation is rerun with time refinement. In total 400 simulations were run for LOCA and 380 for SBO, varying the 19 parameters important for LOCA and 18 parameters important for SBO.

5.3.1. Fission Products Deposited in RPV

Figure 5-18 and Figure 5-19 below shows the mass fraction of deposited cesium and iodine inside the RPV. CS includes cesium from RN Class 2 (CsOH), Class 16 (CsI) and Class 17 (CsM), while I2 includes iodine from RN Class 4 (I) and Class 16 (CsI). In the figures, red line shows the mean of all the simulations and pink line corresponds to the case that releases the earliest FPs to the environment. The maximum amount of deposited fraction as seen in the figures reach a maximum at ~0.3h in the case of LOCA and at ~1.5h in the case of SBO. Subsequently as the core degrades further, and initial deposits dry out from the structures inside the RPV, and transferred to the CNT, the deposited fraction reduces. Small differences are

observed between IDEJ0 and IDEJ1 cases, mainly as in IDEJ1, some solid debris remain in the lower plenum even after LHF failure.

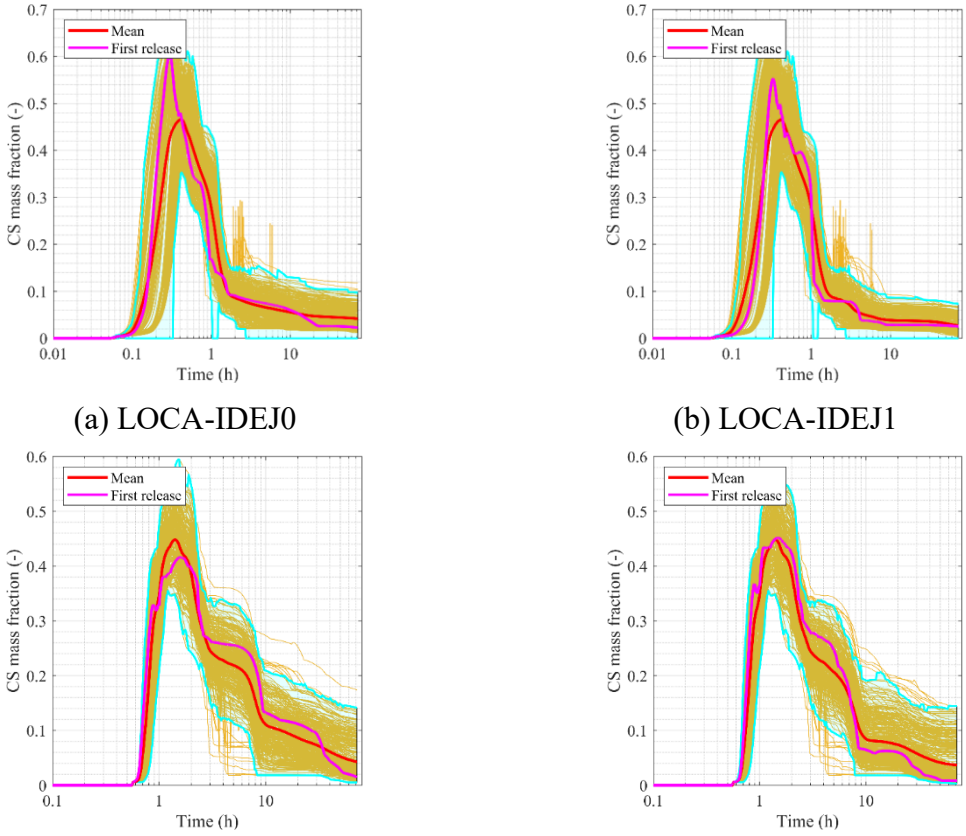

(a) LOCA-IDEJ0 (b) LOCA-IDEJ1

(c) SBO-IDEJ0 (d) SBO-IDEJ1

Figure 5-18. CS mass fraction [-] deposited in the RPV for 4 SA scenarios.

Figure 5-20 and Figure 5-21 presents the time evolution of Morris sensitivity indices: modified mean μ^* and standard deviation σ for deposited CS and I2 mass fractions respectively. For better reading and removing large fluctuations the results presented are averaged and smoothed. From the perspective of significance, during LOCA and before LHF, SC710641 which is the activation energy in the diffusion correlation, SC3210 which is the decay heat multiplier, and GAMMA which is the agglomeration shape factor are the most important parameters. These directly affect the release of the CS from the fuel matrix and consequently the deposited fraction inside the RPV. Similarly for SBO, the same parameters hold importance for CS deposition. Post RPV failure, for SBO-IDEJ1 for a brief period, GAMMA becomes the most important, likely driven by large amounts of agglomeration within the RPV and the CNT. Once the large aerosols settle, GAMMA becomes less influential. And in the case of SBO-IDEJ1, in addition to SC710641, SC7111I2 also becomes significant. SC7111I2 is the vapour diffusivity constant (characteristic energy of interaction between the molecules divided by the Boltzmann constant) for the fission product vapours in the bulk gas (I2).

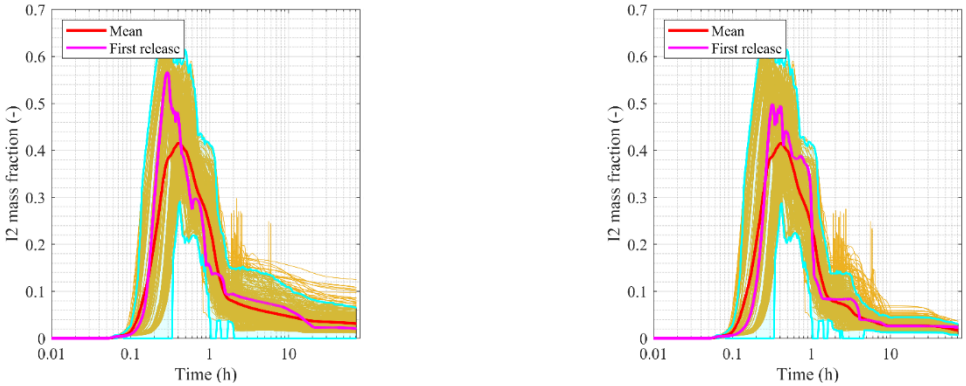

(a) LOCA-IDEJ0 (b) LOCA-IDEJ1

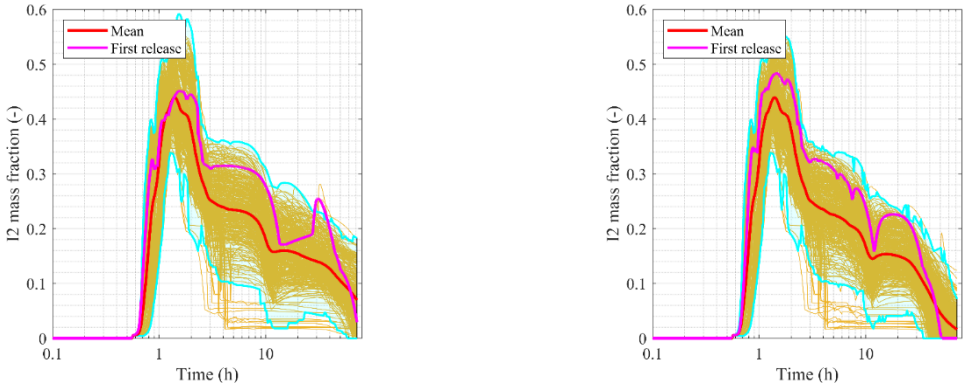

(c) SBO-IDEJ0 (d) SBO-IDEJ1

Figure 5-19. I2 mass fraction [-] deposited in the RPV for 4 SA scenarios.

Largely similar behaviour is seen in the case of I2 deposited fraction for these SA scenarios. Post LHF, during SBO, GAMMA is the most significant factor for I2 deposited inside the RPV.

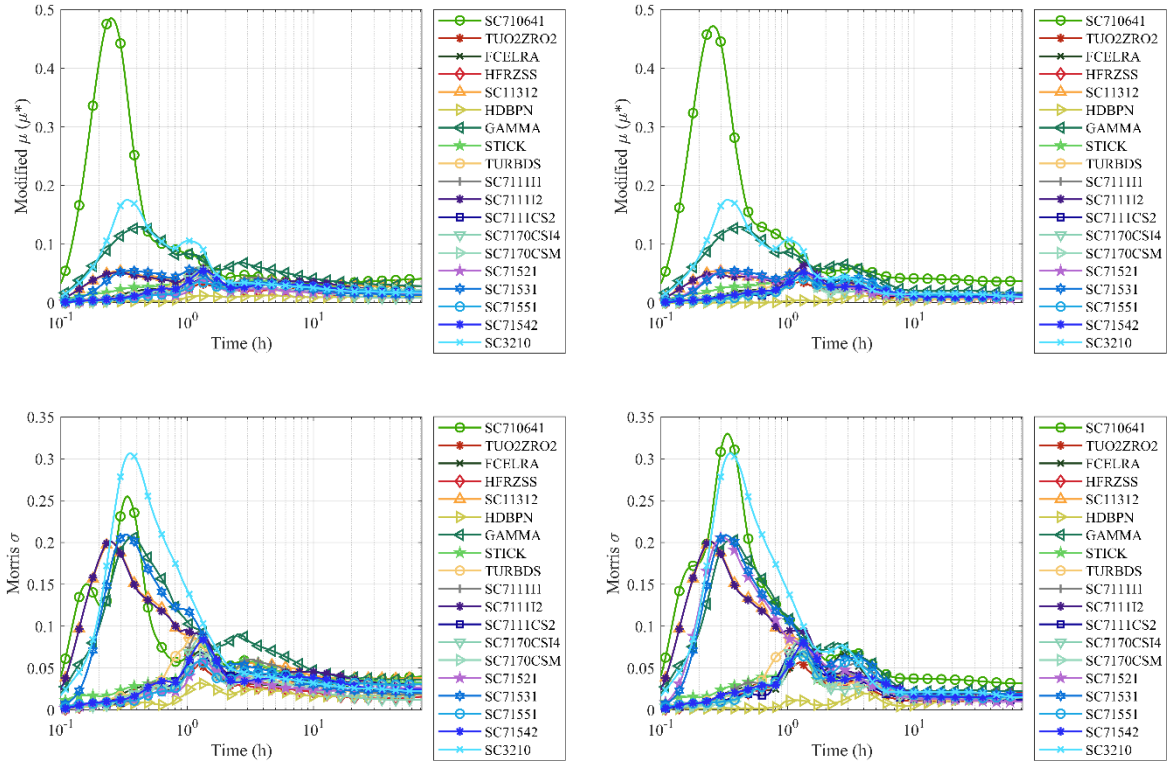

(a) LOCA-IDEJ0 (b) LOCA-IDEJ1

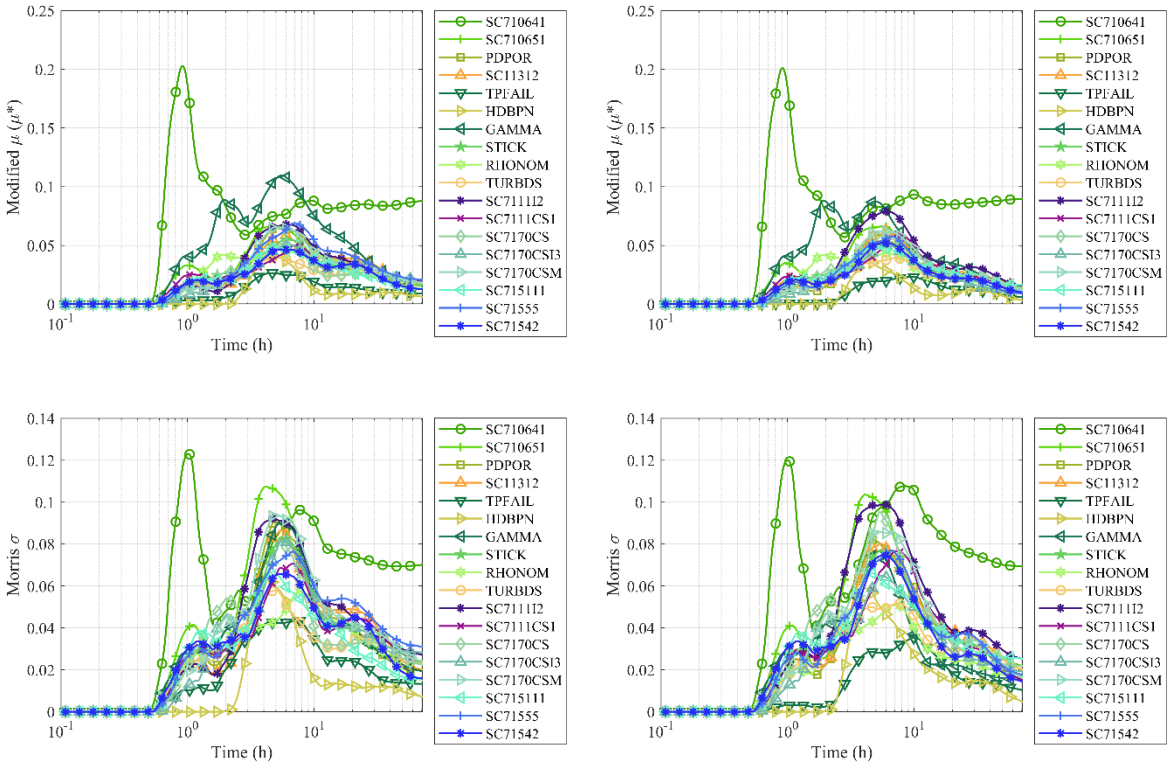

(c) SBO-IDEJ0 (d) SBO-IDEJ1

Figure 5-20. Morris sensitivity indices for deposited CS mass fraction for 4 SA scenarios.

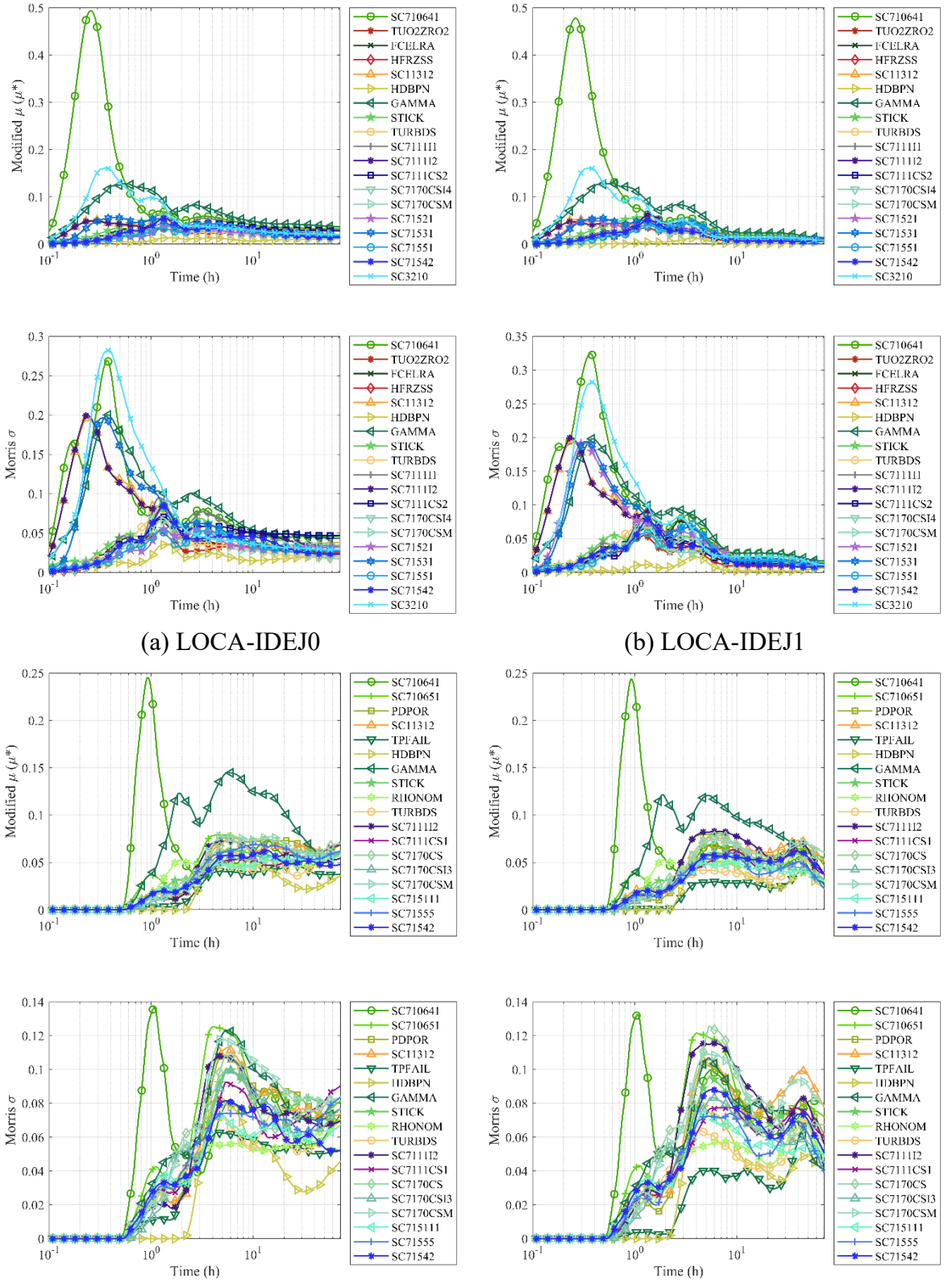

Figure 5-21. Morris sensitivity indices for deposited I2 mass fraction for 4 SA scenarios.

5.3.2. Fission Products Deposited in Containment

Figure 5-22 and Figure 5-23 shows the deposited mass fraction of CS and I2 in the containment. Here CNT includes the CVs of upper drywell (UDW), lower drywell (LDW), blowdown pipes and overflow pipes, and all associated heat structures. The general behaviour of different mass fractions, whether in the atmosphere, in the pool or deposited for the 4 SA scenarios can also be found in [74][75]. In LOCA, the delayed addition of molten melt to the cavity leads to a larger vapour temperature in the containment atmosphere. This leads to dryout of the containment structures and subsequently a decrease in the deposited fraction which may be released to the atmosphere and then to the environment, seen as a general dip in the fraction after ~8h. The effect of IDEJ is not as evident in SBO, because unlike LOCA, fission products are scrubbed inside WW pool and not deposited. In SBO, after LHF, the LDW pool that boils may transfer the FPs in the water to the air, that can be deposited. This is seen as a general increase after ~6h. A similar behaviour is observed for CS and I2 as the aerosol form of CsI that is deposited, contributes largely to this trend.

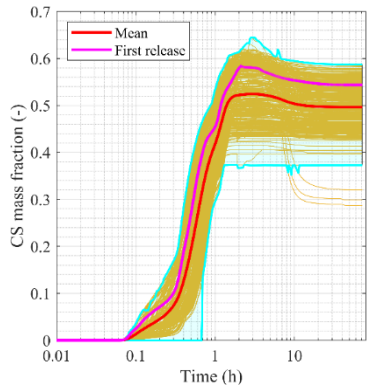

(a) LOCA-IDEJ0

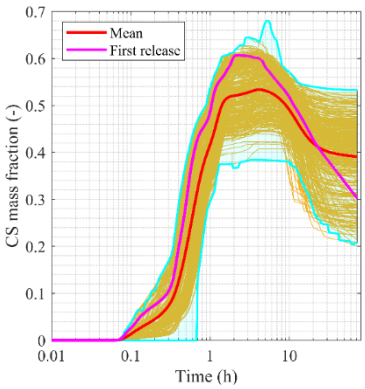

(b) LOCA-IDEJ1

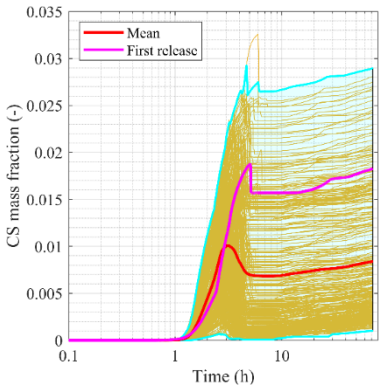

(c) SBO-IDEJ0

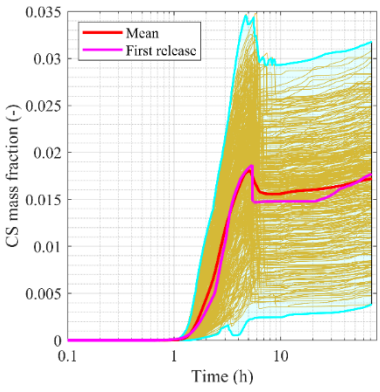

(d) SBO-IDEJ1

Figure 5-22. CS mass fraction [-] deposited in the CNT for 4 SA scenarios.

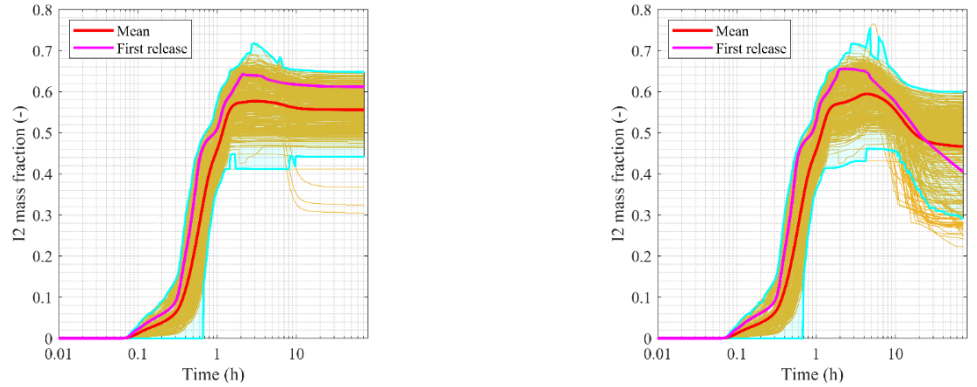

(a) LOCA-IDEJ0 (b) LOCA-IDEJ1

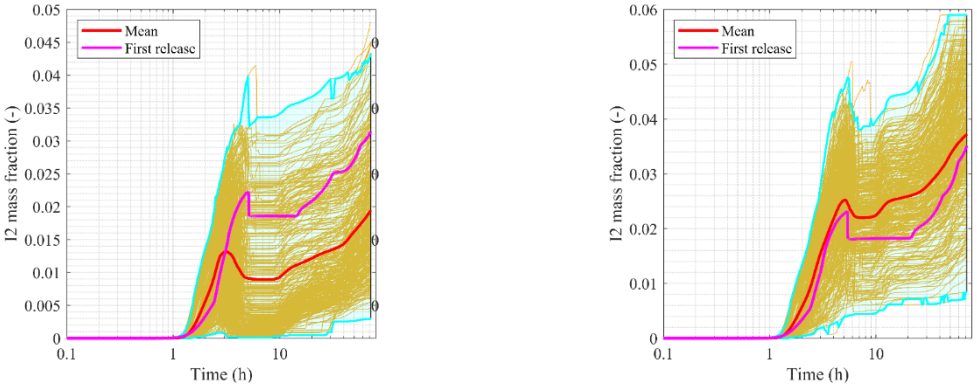

(c) SBO-IDEJ0 (d) SBO-IDEJ1

Figure 5-23. I2 mass fraction [-] deposited in the CNT for 4 SA scenarios.

Figure 5-24 and Figure 5-25 presents the time evolution of Morris sensitivity indices: modified mean μ^* and standard deviation σ for deposited CS and I2 mass fractions respectively. For CS deposited fractions in the CNT during LOCA-IDEJ0, SC710641 is the most important, and post LHF, SC3210 becomes the most important. Whilst, in LOCA-IDEJ0, until the time that solid debris remelts in the LH before being ejected (~10h), SC3210 is significant, and once large amounts of liquid melt are ejected, FCELRA (radiative exchange factors for radiation radially outward and upward from the cell boundary to the next adjacent cell) becomes the most significant. This is likely due to hot molten melt directly influencing vapour in the CNT atmosphere, that drives CS deposition. During SBO, SC710641 remains the most significant followed by SC71542 (IDEJ0, constant in the SPARC-90 bubble swarm velocity rise correlation) and GAMMA (IDEJ1). Similar behaviour is observed for I2 deposited fraction during LOCA and SBO as in CS fractions.

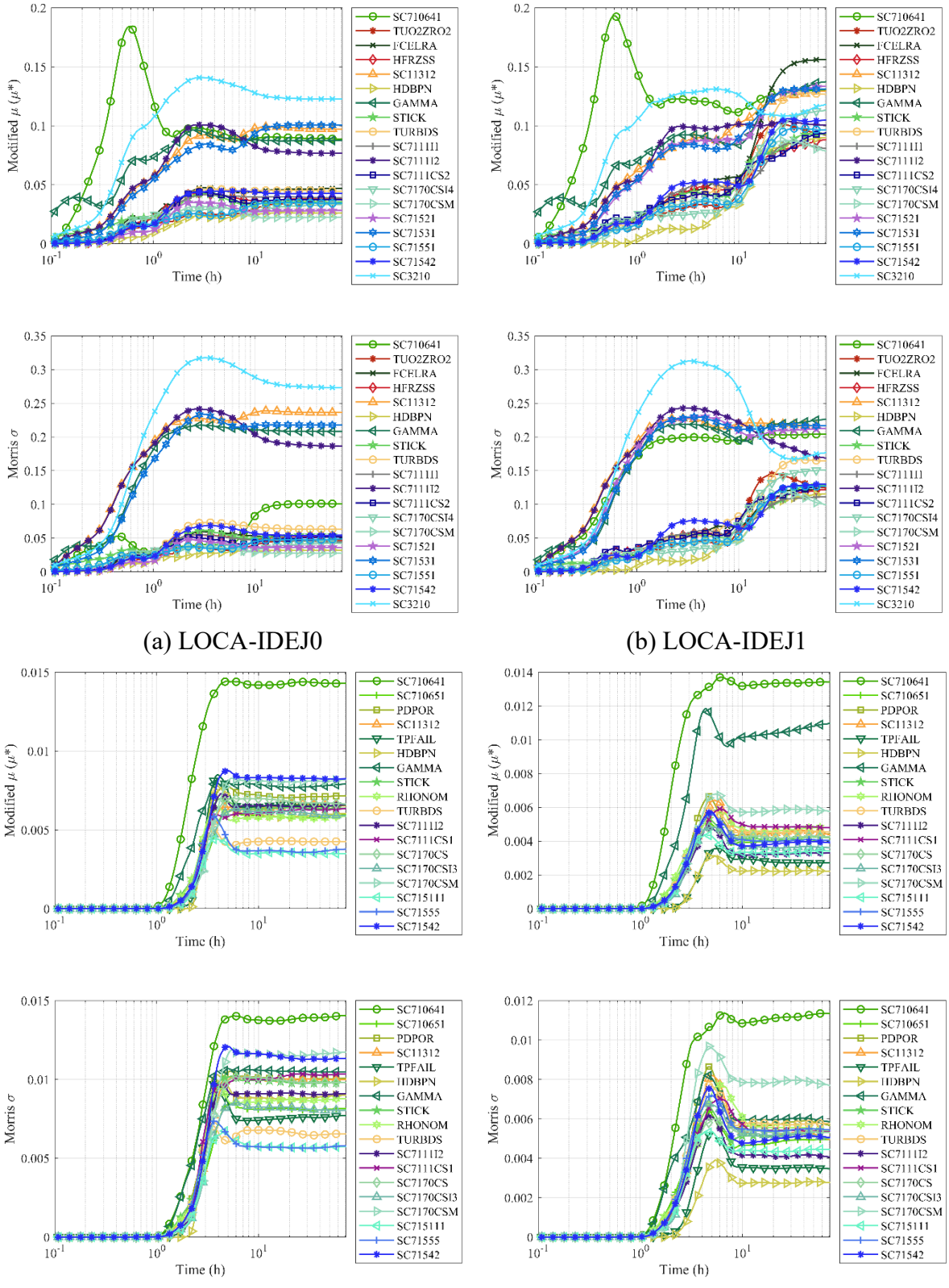

Figure 5-24. Morris sensitivity indices for deposited CS mass fraction for 4 SA scenarios.

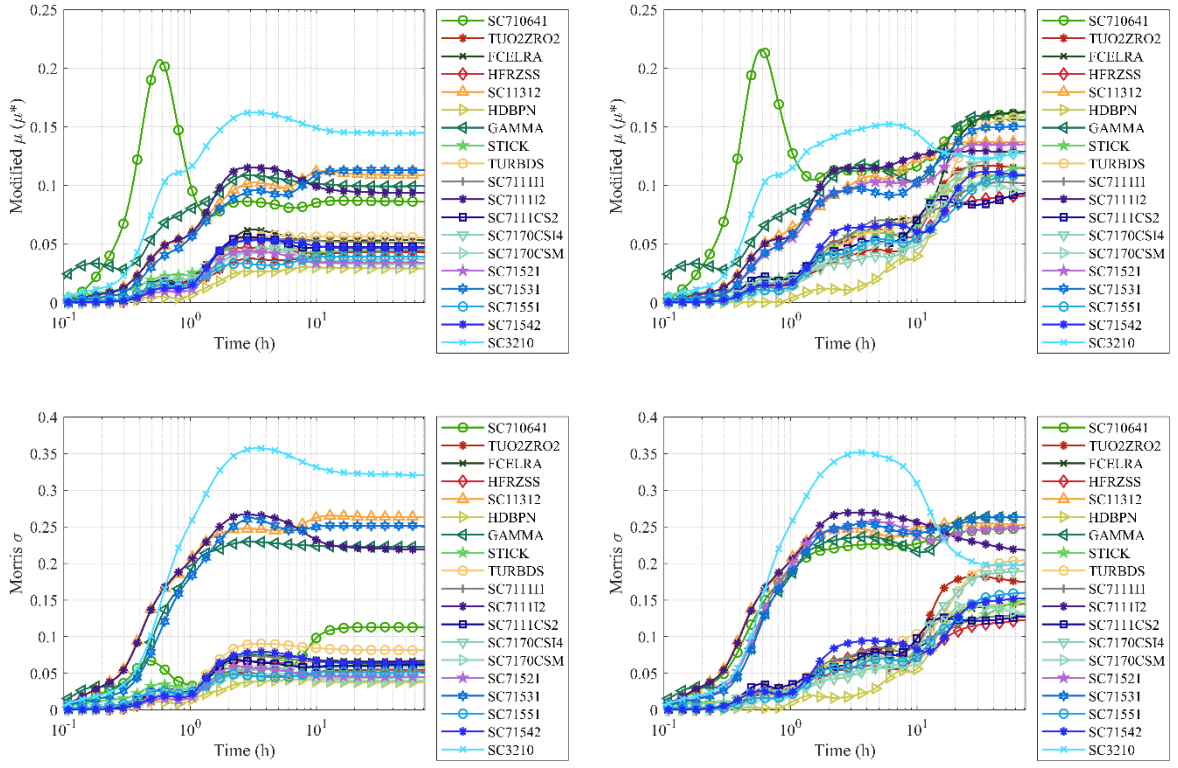

(a) LOCA-IDEJ0 (b) LOCA-IDEJ1

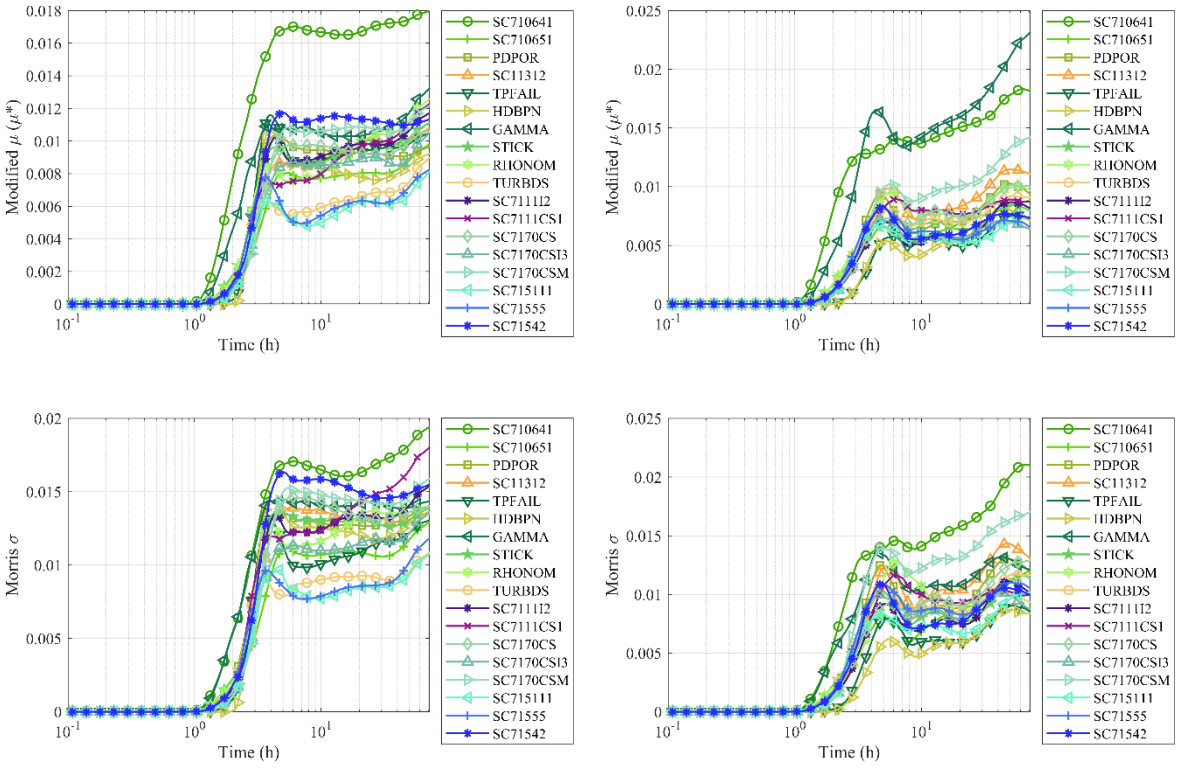

(c) SBO-IDEJ0 (d) SBO-IDEJ1

Figure 5-25. Morris sensitivity indices for deposited I2 mass fraction for 4 SA scenarios.

5.3.3. Thermal-hydraulic Parameters

Figure 5-26, Figure 5-27, Figure 5-28 and Figure 5-29 below show the evolution of key T-H parameters in the CNT for the 4 SA scenarios. The color coding is as follows: brown-FCVS is not activated, blue-FCVS is activated (as per control logic) close to LHF, that its effect is not pronounced, and green-FCVS is activated (as per control logic). FCVS is generally only activated during LOCA, where the CNT is highly pressurized before LHF (and coincidental CNT failure), unlike in SBO, where RPV is depressurized directly to the WW. However, in a very few cases FCVS is activated (when CNT pressure > 5.5bar) due to pressure spikes caused by debris ejection to cavity pool.

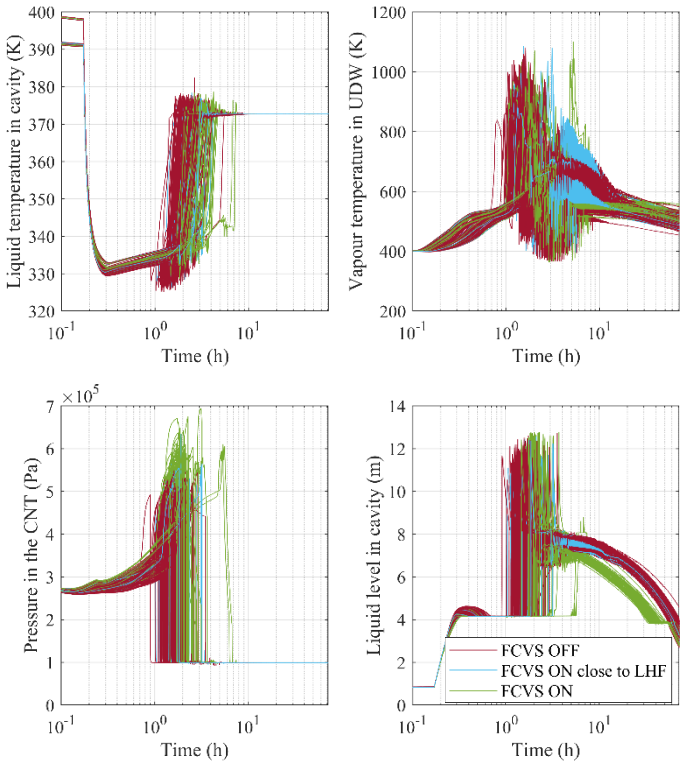

Figure 5-26. T-H parameters evolution in the CNT for LOCA-IDEJ0.

It is observed that cases leading to FCVS venting result in a rapid reduction of the LDW water pool mass. In LOCA-IDEJ0, pool boiling in the LDW begins slightly earlier than in LOCA-IDEJ1. This difference can be explained by the more protracted debris ejection from the RPV into the cavity in LOCA-IDEJ1, since the IDEJ1 modelling switch limits the amount of solid debris ejected. Consequently, this leads to significantly higher temperatures inside both the RPV and the containment, and causes revaporization of Cs and I aerosols previously deposited in these regions..

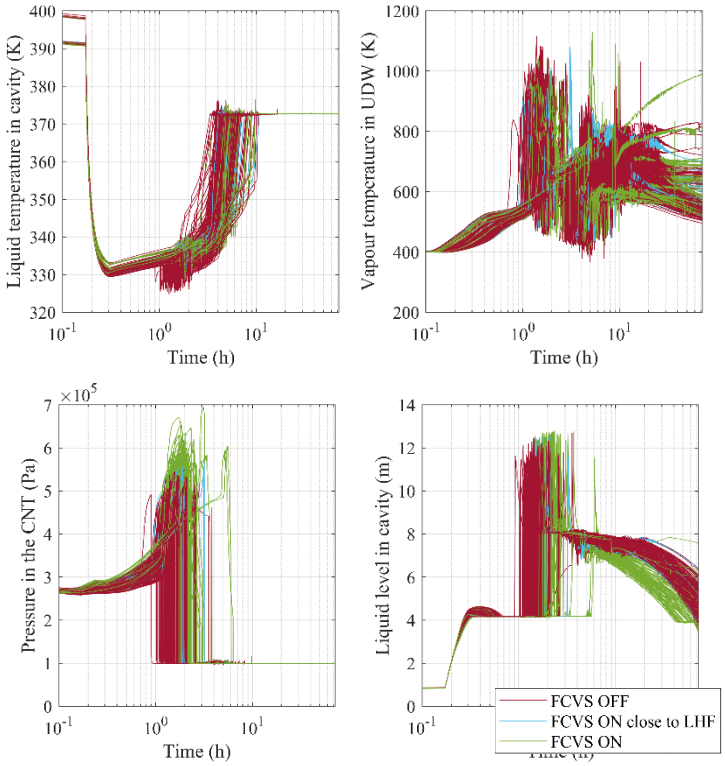

Figure 5-27. T-H parameters evolution in the CNT for LOCA-IDEJ1.

During SBO, containment atmosphere temperatures are not as high as in LOCA, and IDEJ0 leads to UDW reaching ~400-450K while IDEJ1 leads to ~400-500K in the UDW. The uncertainty in the properties is smaller than in LOCA.

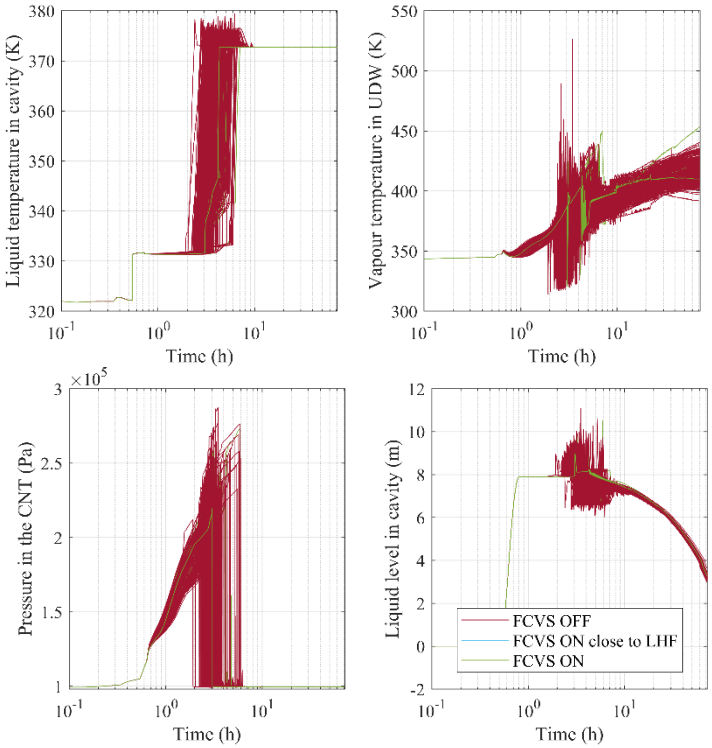

Figure 5-28. T-H parameters evolution in the CNT for SBO-IDEJ0.

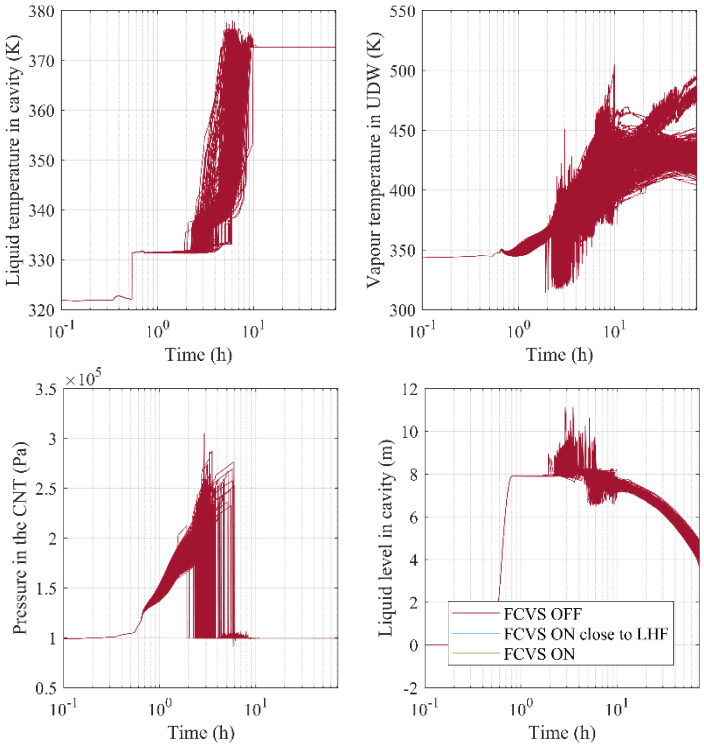

Figure 5-29. T-H parameters evolution in the CNT for SBO-IDEJ1.

5.3.4. Separate Effect Analysis

Resuspension:

In the MELCOR model of the Nordic BWR, the resuspension model is turned off for left and right boundaries of heat structures [4][6][7]. Aerosols deposited on surfaces can be vaporized (if they are volatile) but can only be resuspended if the resuspension model is enabled. If activated, the resuspension model determines if deposited aerosols are released from a given surface. For wet surfaces – includes pools and surfaces with film present – the resuspension model is automatically turned off, meaning that there is no resuspension from these surfaces. For dry surfaces, the particles remain attached to a heat structure surface until the gas flow past the surface is sufficient to aerosolize the deposit. Then all particles larger than a critical diameter are resuspended. The critical diameter can be user defined or calculated internally or defined by a control function. Here we let MELCOR determine the diameter but define the fraction of aerosols resuspended as 0.5.

Deposition models:

In the reference case, all deposition models are turned on. Here we consider cases where the following models are either turned on or off.

1. Reference – All deposition models are turned on.
2. Brown OFF – Only Brownian deposition model is turned off, while all other models are on.
3. Dif OFF – Only diffusiophoresis model is turned off.
4. Grv OFF – Only gravitational deposition model is turned off.
5. Thm OFF – Only thermophoresis model is turned off.
6. All OFF – All deposition models are turned off.

7. Brown ON – Only Brownian deposition model is turned on, while all other models are off.
8. Dif ON – Only diffusiophoresis model is turned on.
9. Grv ON – Only gravitational deposition model is turned on.
10. Thm ON – Only thermophoresis model is turned on.

Hygroscopic model:

For water soluble aerosols a solubility or hygroscopic effect is considered whereby the particles can grow by absorbing water vapor from moist, unsaturated atmospheres. An important consequence of this growth in size is an increase in the gravitational settling rate, and the subsequent depletion of airborne fission product aerosols. In reference case, this is turned on, and here we turn it off.

Figure 5-30, Figure 5-31, Figure 5-32, Figure 5-33, Figure 5-34 and Figure 5-35 below show only the deposited mass fraction of CS and I2 in the CNT for the 4 SA scenarios. CNT SIZE1 here corresponds to a case where the CNT breach size (upon LHF) is negligible (i.e. a breach diameter of 1cm, against the 1.596m breach in reference case).

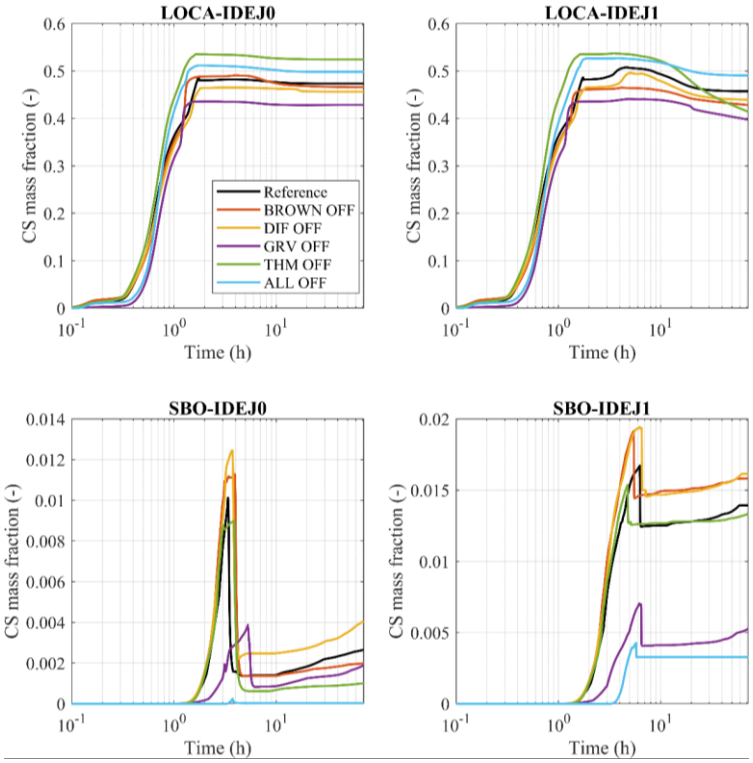

Figure 5-30. CS mass fraction [-] deposited in the CNT for 4 SA scenarios.

In these figures, the reference is the case where all deposition models are turned on. For LOCA, it is seen that turning off gravitational deposition leads to the least deposited CS fraction. For SBO, turning off all models leads to least deposited CS mass fraction in the CNT, followed by the case of gravitational model being off. During LOCA, turning off thermophoresis deposition model seems to have an effect on settling after ~10h, with rapidly decreasing deposited fraction. The effect of the deposition models appears to have a similar effect in the case of I2 mass fractions as it is in CS mass fraction.

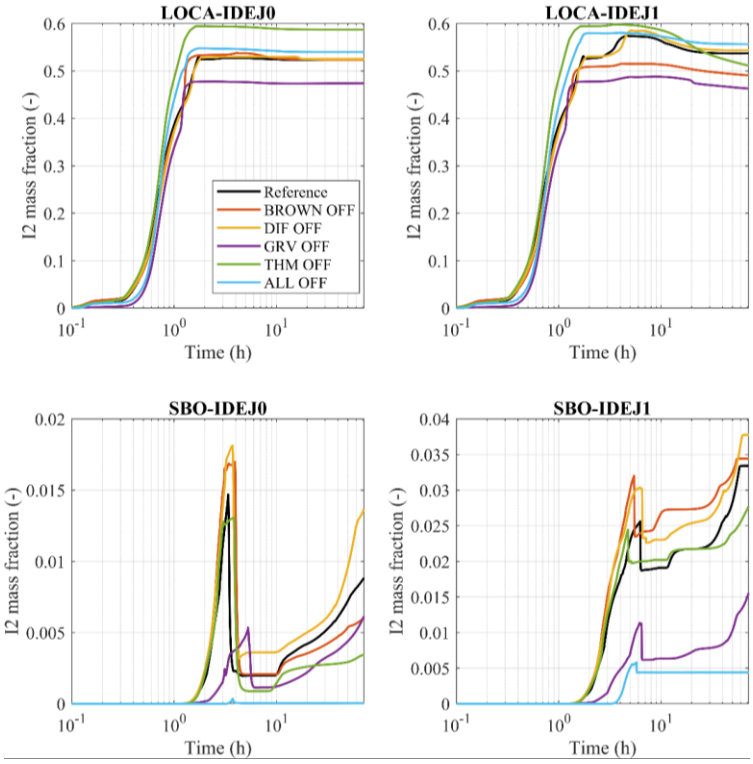

Figure 5-31. I2 mass fraction [-] deposited in the CNT for 4 SA scenarios.

Consequently, when only thermophoresis model is turned on, it is seen that MELCOR calculates the least deposition in the CNT during LOCA, and the most when Brownian or gravitational model is turned on. During SBO, it is seen that gravitational deposition has the largest effect on CS deposition in CNT.

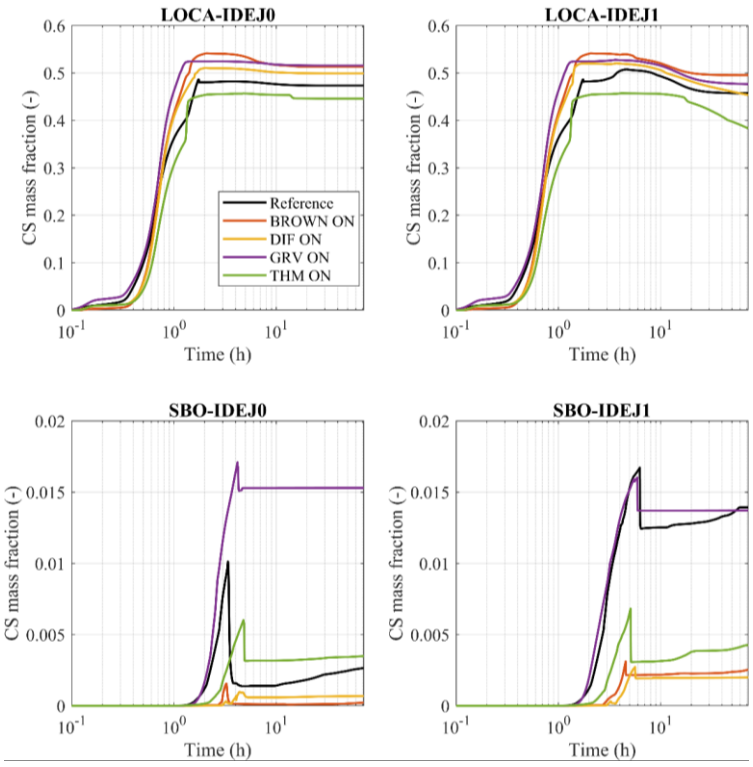

Figure 5-32. CS mass fraction [-] deposited in the CNT for 4 SA scenarios.

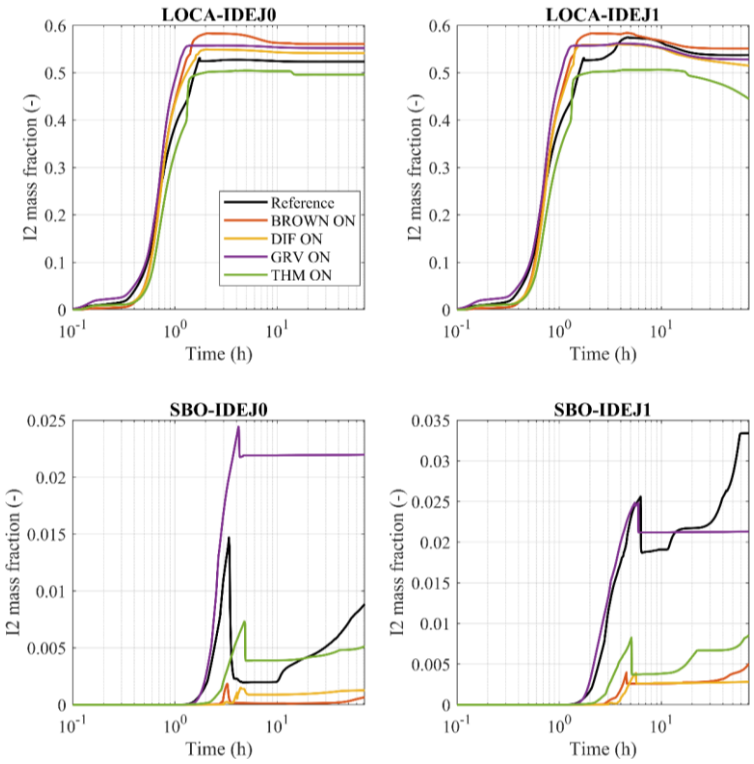

Figure 5-33. I2 mass fraction [-] deposited in the CNT for 4 SA scenarios.

In the setup where the reference case is compared with resuspension model is turned on during LOCA, there are different masses deposited of CS and I2 in the CNT. It is seen that resuspension does not affect deposition mass as much during LOCA as in SBO. The least mass of CS and I2 deposited is when the CNT breach size is the least.

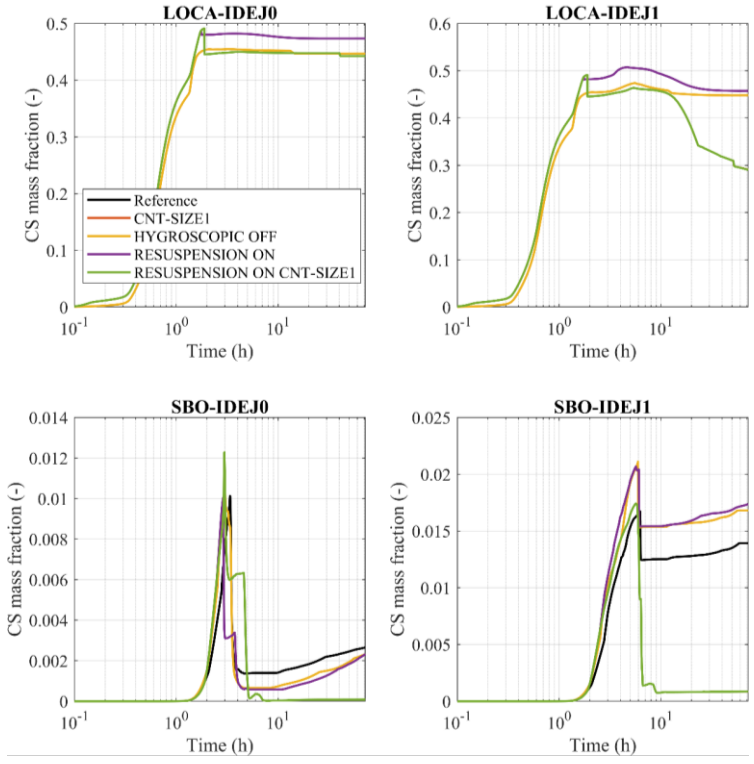

Figure 5-34. CS mass fraction [-] deposited in the CNT for 4 SA scenarios.

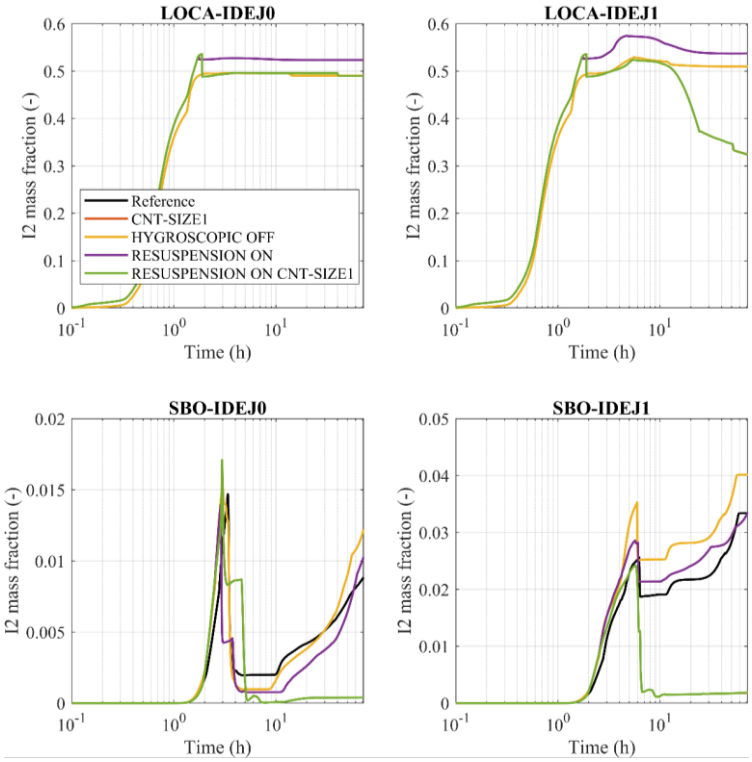

Figure 5-35. I2 mass fraction [-] deposited in the CNT for 4 SA scenarios.

5.4. Analysis of the Effect Manual Containment Depressurization via MVSS on Fission Products Behavior in NBWR

For the evaluation of mitigative actions, KTH considered the effect of early depressurization of the CNT by activation of MVSS in RC4A and RC4B scenarios. The rupture disk in the pipe to the MVSS bursts at a pressure of 5.5bar. The MVSS is then vented to ambient air. During the EOP stage it can be opened manually to limit the pressure inside the containment. When transitioning into SAMGs, the system is closed to limit the release of noble gases (no filtering), and the system is activated via the rupture disk. Since LOCA leads to LHF at 6246s and SBO at 9841s, for early opening, 11 instances of operator delay are added in the period [0, 6246s] and [0, 9841s] respectively, as shown in Table 5-9 below. In all these cases it is assumed that CNT does not fail when RPV fails, and therefore the system parameters is unaffected by loss of CNT integrity.

Table 5-9. Time of early manual MVSS activation [s].

	1	2	3	4	5	6	7	8	9	10	11
LOCA	568	1136	1700	2271	2839	3407	3975	4543	5110	5678	6246
SBO	895	1789	2684	3579	4473	5368	6263	7157	8052	8946	9841

5.4.1. Thermal-Hydraulic Parameters

Figure 5-36, Figure 5-37, Figure 5-38 and Figure 5-39 below show the evolution of the T-H parameters for the 4 SA scenarios. The colours in the plot represent these 11 instances, blue is early activation and red is late activation. As a consequence of early MVSS activation during

LOCA-IDEJ0, the cavity pool temperature increases more slowly, than with late MVSS activation. Manual MVSS activation also effects accumulation of hydrogen in the WW airspace.

During LOCA-IDEJ1, it is seen that atmosphere temperature can reach >900K with early MVSS activation. In the only case where the temperature reduces post LHF (green line in Figure 5-37), it is caused by the reduction of solid debris in the LH, that undergoes melting and heating up the UDW atmosphere.

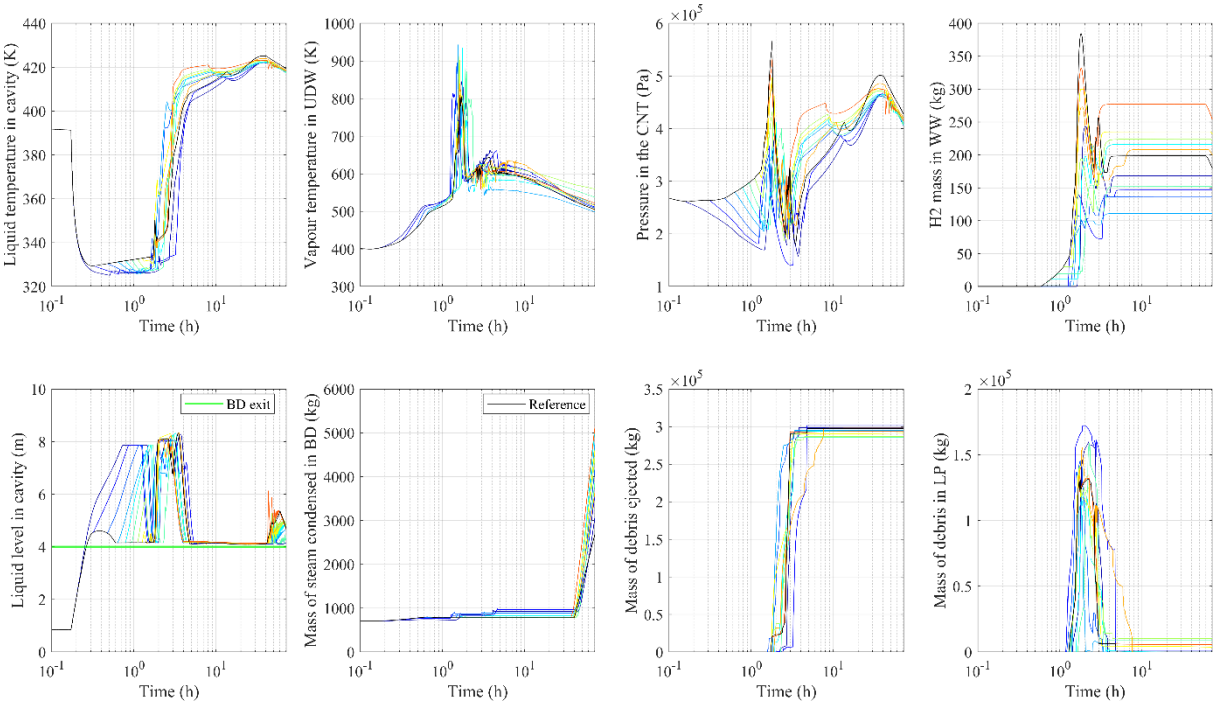

Figure 5-36. T-H parameters evolution during LOCA-IDEJ0 (blue is early activation and red is late activation).

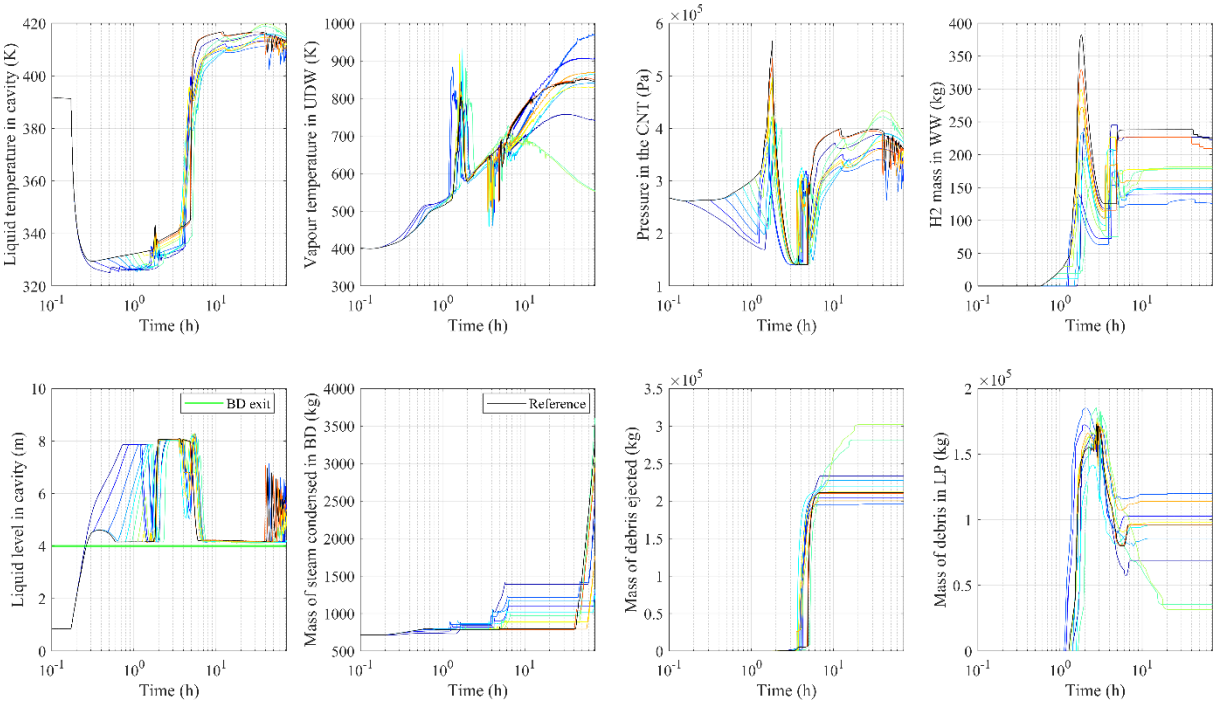

Figure 5-37. T-H parameters evolution during LOCA-IDEJ1 (blue is early activation and red is late activation).

During SBO, the effect of manual MVSS activation is less pronounced than in LOCA. One difference that can be observed with LOCA is the loss of hydrogen mass in the WW at after 40h, that is caused due to boiling of the WW pool and the transfer of gases through vacuum breakers to the containment UDW.

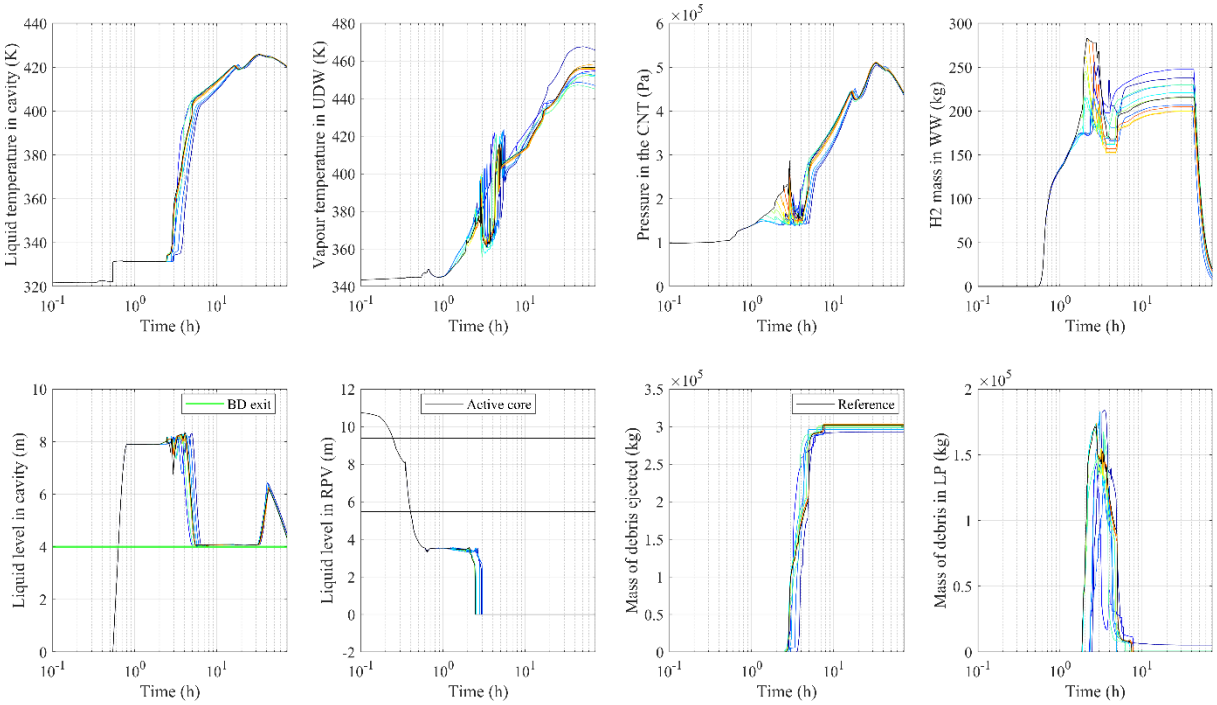

Figure 5-38. T-H parameters evolution during SBO-IDEJ0 (blue is early activation and red is late activation).

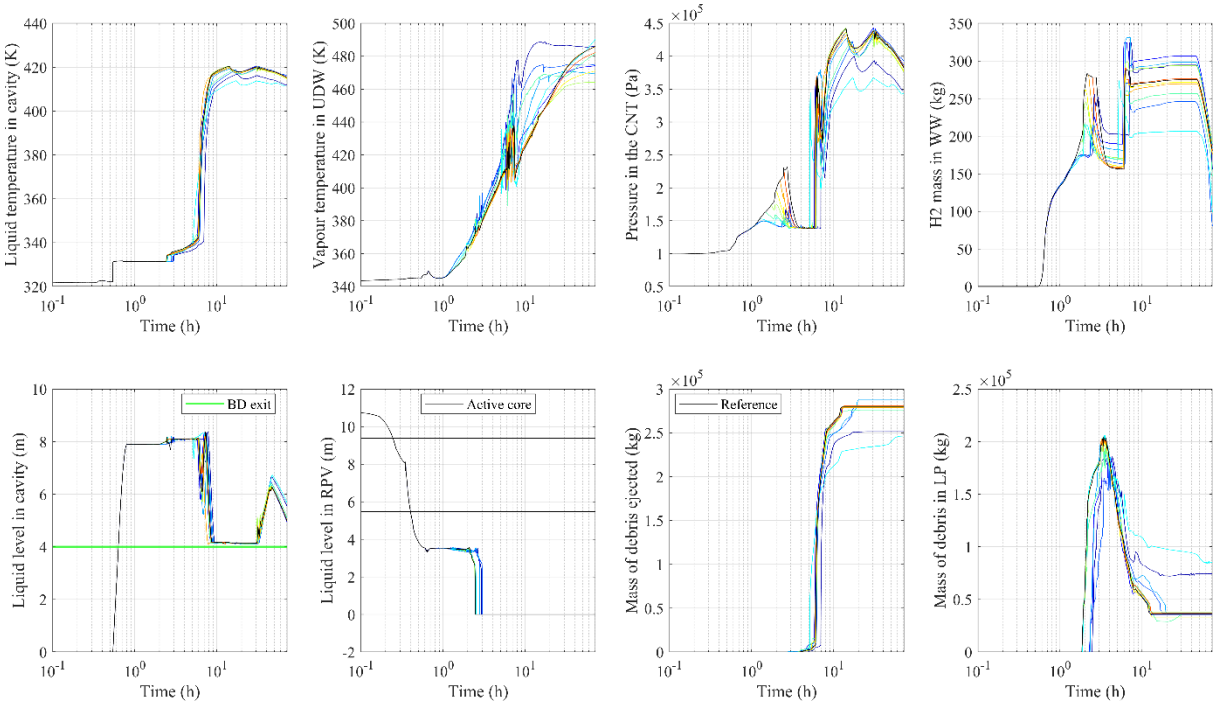

Figure 5-39. T-H parameters evolution during SBO-IDEJ1 (blue is early activation and red is late activation).

5.4.2. Fission Product and Source Term

Figure 5-40, Figure 5-41, Figure 5-42 and Figure 5-43 show the CS and I2 mass fraction deposited in the CNT and the total hydrogen generated in the core due to oxidation of the cladding. As observed earlier, LOCA-IDEJ1 leads to drop in deposited mass of CS and I2 after LHF, while the cases with green line remain so (UDW temperature does not peak). The amount of hydrogen produced can vary anywhere from +/-600kg from the reference case during LOCA-IDEJ0 and roughly +/-500kg during LOCA-IDEJ1.

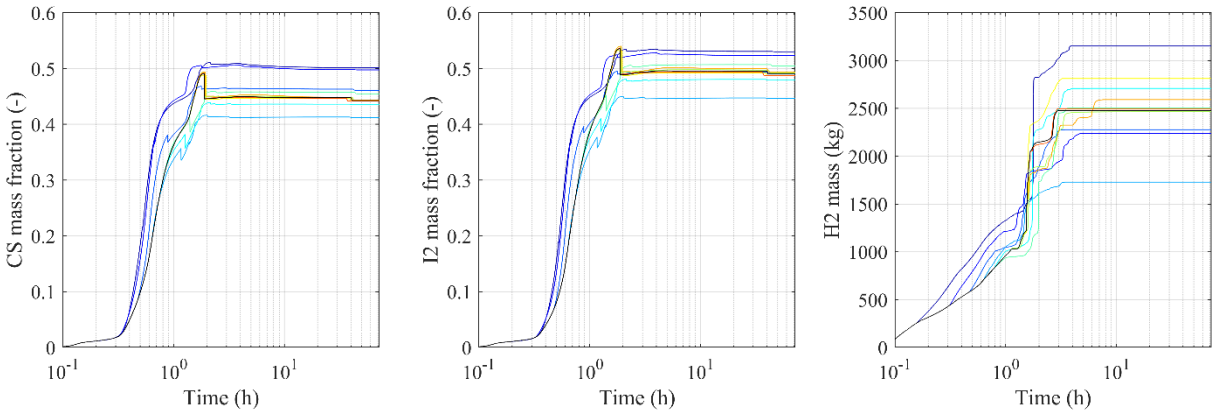

Figure 5-40. FP deposited mass fractions in CNT and H2 generation in core during LOCA-IDEJ0 (reference is in black).

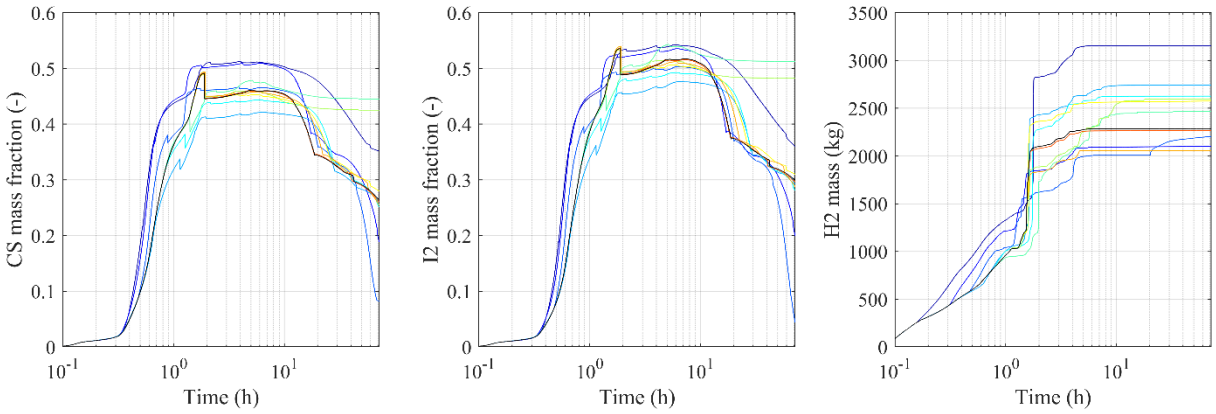

Figure 5-41. FP deposited mass fractions in CNT and H2 generation in core during LOCA-IDEJ1 (reference is in black).

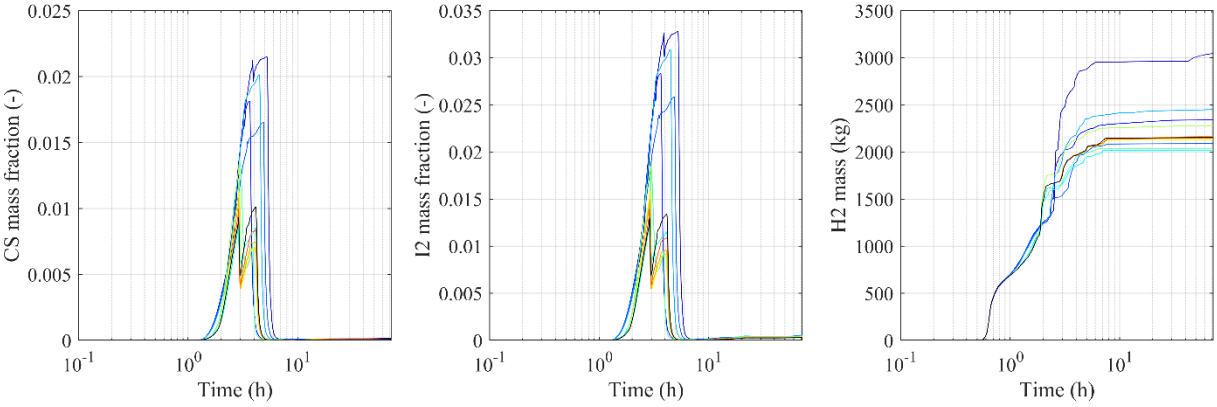

Figure 5-42. FP deposited mass fractions in CNT and H2 generation in core during SBO-IDEJ0 (reference is in black).

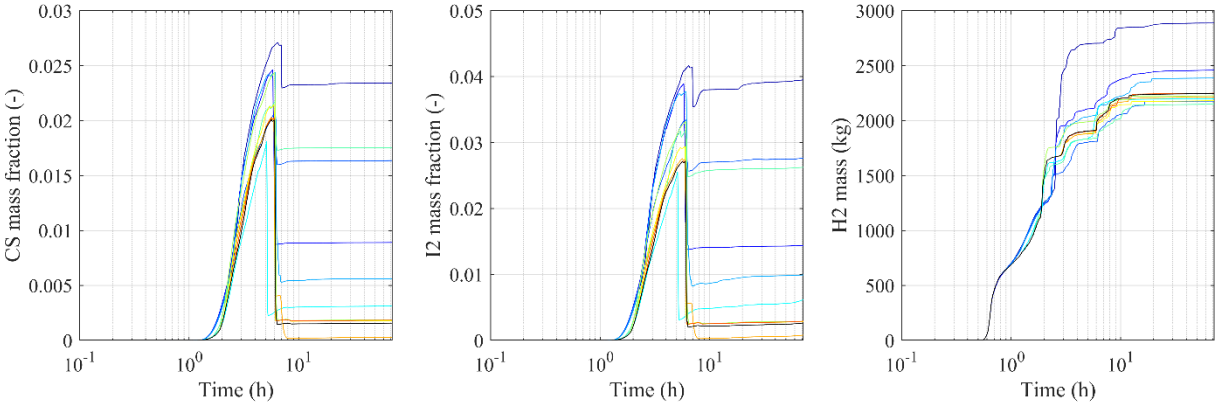

Figure 5-43. FP deposited mass fractions in CNT and H2 generation in core during SBO-IDEJ1 (reference is in black).

5.4.3. Timing of Events

Figure 5-44 below shows the timing of certain events in the containment during the accident progression.

Table 5-10. Timing of events activation.

Abbreviation	Description
ADS	Time of activation of ADS
FUNC	Time of full core uncovery
WWB	Time of commencement of WW boiling
SSF	Time of failure of supporting plate in RPV
LHF	Time of failure of LH
FCVS	Time of (manual) activation of FCVS
LDWB	Time of commencement of LDW boiling
MVSSB	Time of commencement of MVSS boiling
MVSSEMP	Time of complete evaporation of water in MVSS

While LHF occurs between 1h and 2h in LOCA, during SBO it occurs between 2h and 3h. LDW pool boiling and MVSS pool boiling follows closely in LOCA. Whereas in SBO, firstly LDW starts to boil, and then MVSS scrubber. In LOCA-IDEJ1, it is also observed that the MVSS scrubber is completely dry after ~40h when early MVSS activation occurs. It can also be seen that in SBO-IDEJ0, the WW starts to boil after ~35h.

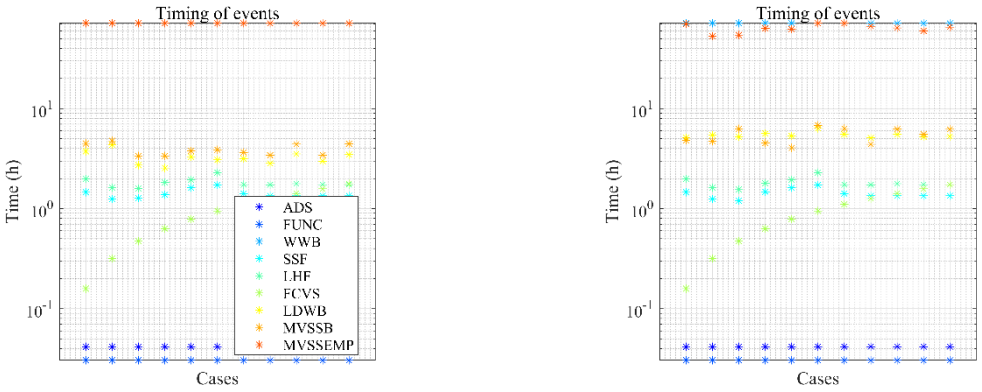

(a) LOCA-IDEJ0 (b) LOCA-IDEJ1

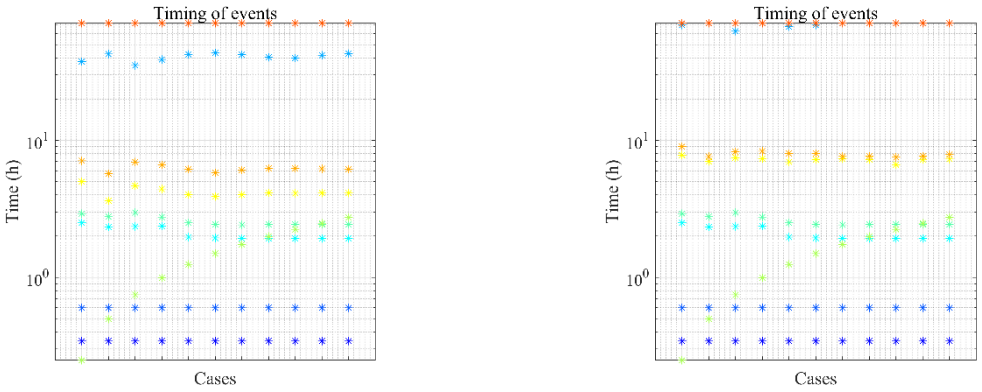

(c) SBO-IDEJ0 (d) SBO-IDEJ1

Figure 5-44. Timing of events for 4 SA scenarios. Cases here implies the 11 instances (in increasing order of delay) of manual activation of MVSS.

5.4.4. Debris Ejection Rate

Figure 5-45 and Figure 5-46 below show the mass-averaged mass flow rate of debris (either solid and liquid or only liquid) for the 4 SA scenarios. The mass-averaged mass flow rate is calculated as,

$$\bar{\dot{M}}_i = \left(\frac{1}{\Delta M_i}\right)\sum_{j=1}^{N}\frac{\Delta m_j^2}{\Delta t_i} \tag{5-1}$$

where, ΔM_i is the mass ejected in a coarse time step (5s or 100s), Δm_j is the mass ejected during N fine time steps Δt_i (1ms). The figures show those 5s or 100s instances where mass flow rate of the debris from the RPV exceeded 50kg/s (filtered).

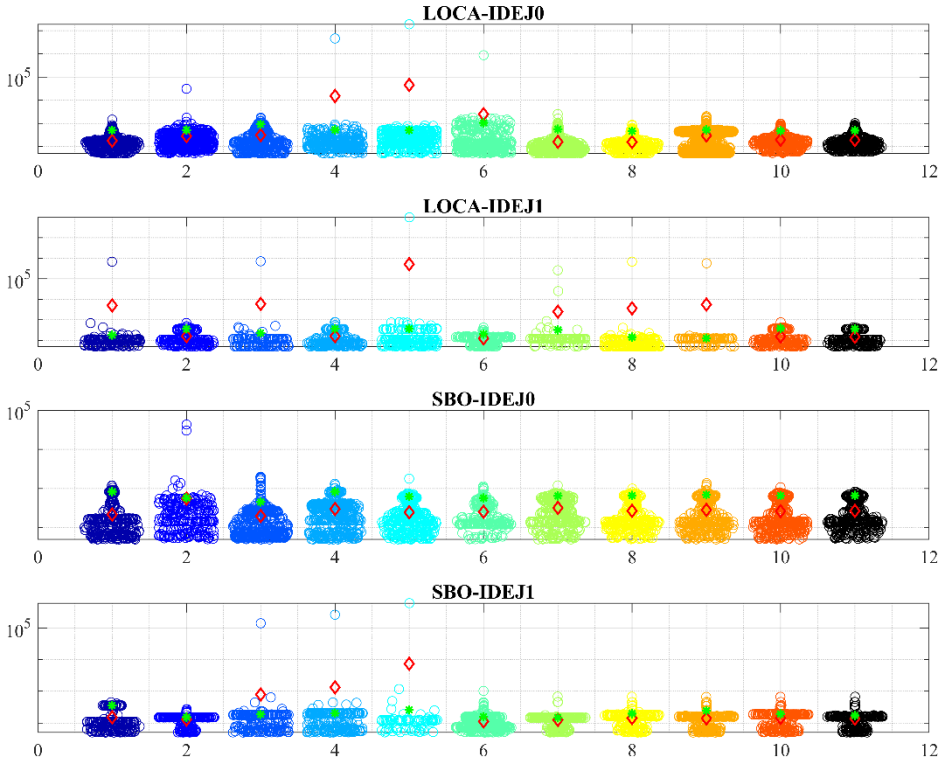

Figure 5-45. Mass-averaged mass flow rate [kg/s] of ejection (5s period).

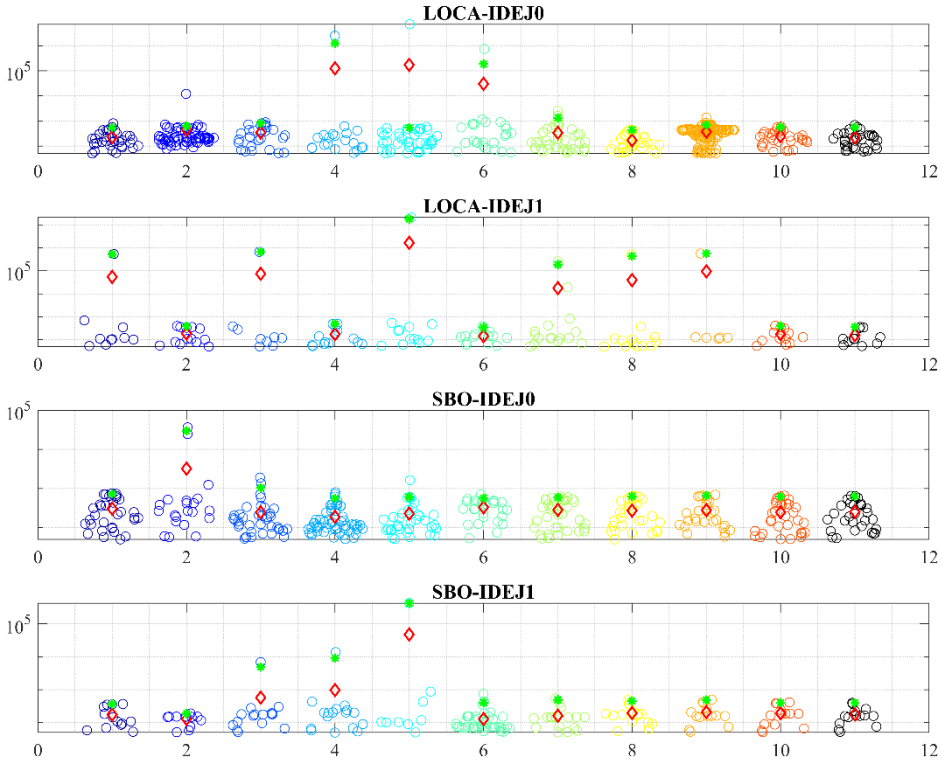

Figure 5-46. Mass-averaged mass flow rate [kg/s] of ejection (100s period).

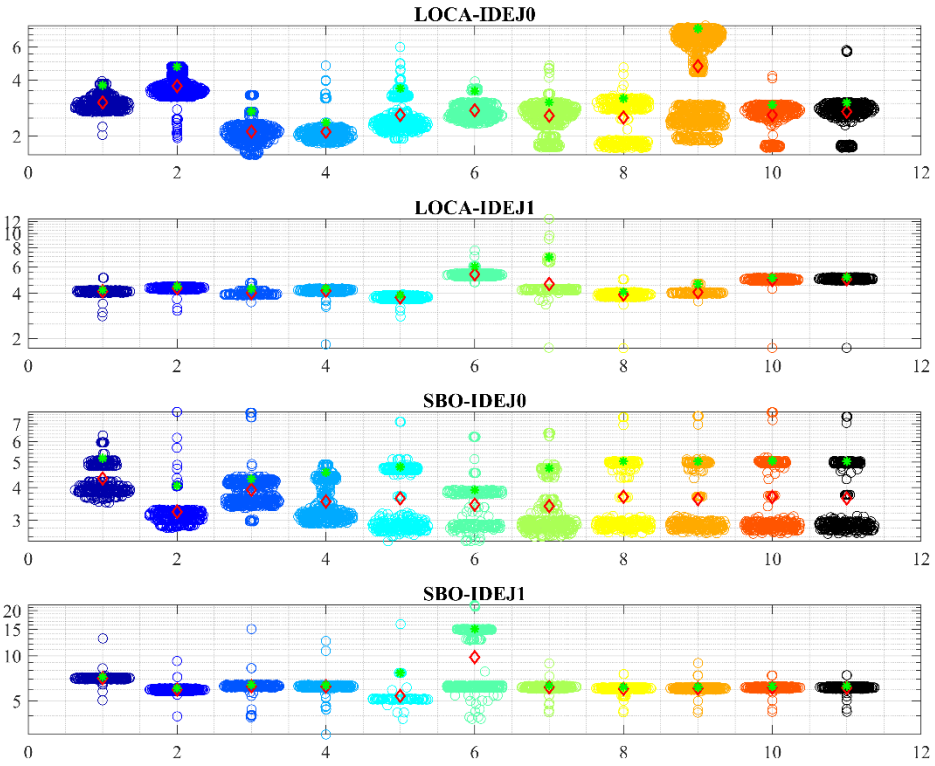

Figure 5-47. Time [h] when >50kg/s flow rate of ejection is observed (5s period).

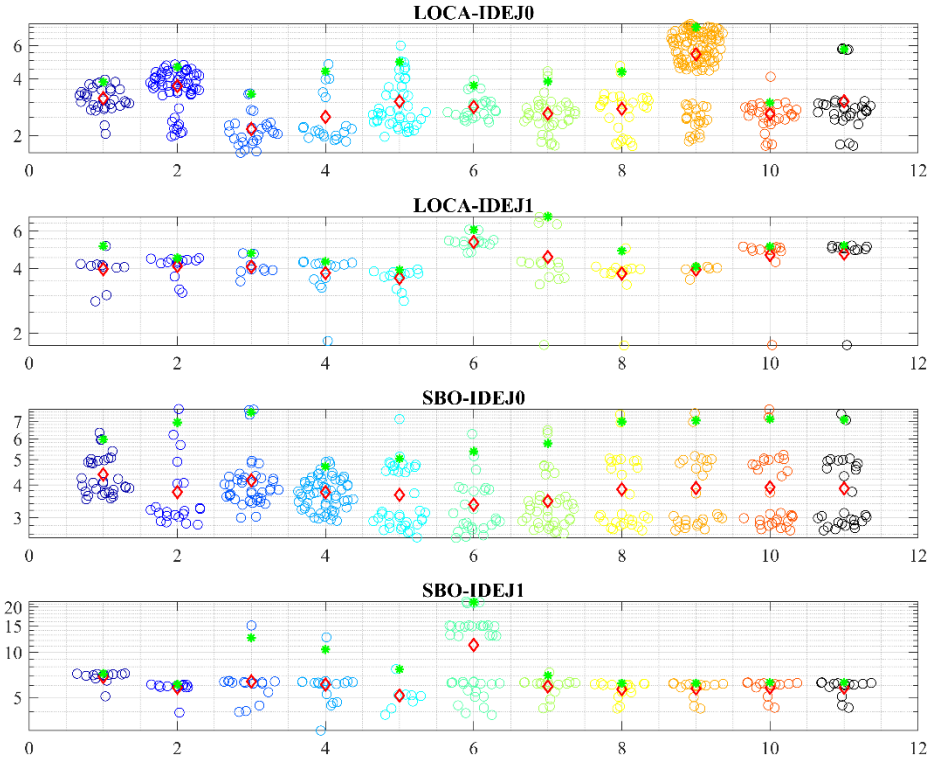

Figure 5-48. Time [h] when >50kg/s flow rate of ejection is observed (100s period).

5.5. Evaluation of the Effect of the Mode of RPV Failure and Debris Ejection of the Steam Explosion Loads on the Containment and the Source Term

For this task, KTH used the accident conditions in the reference case where there is no failure of CNT upon RPV failure, to get details of debris ejection conditions, pool and CNT conditions. As in previous task, mass-averaged mass flow rates were computed and filtered, shown in figure below. After synthesizing parameters from MELCOR calculations, shown in Table 5-11 below, steam explosion calculations were performed using TEXAS-V code [59].

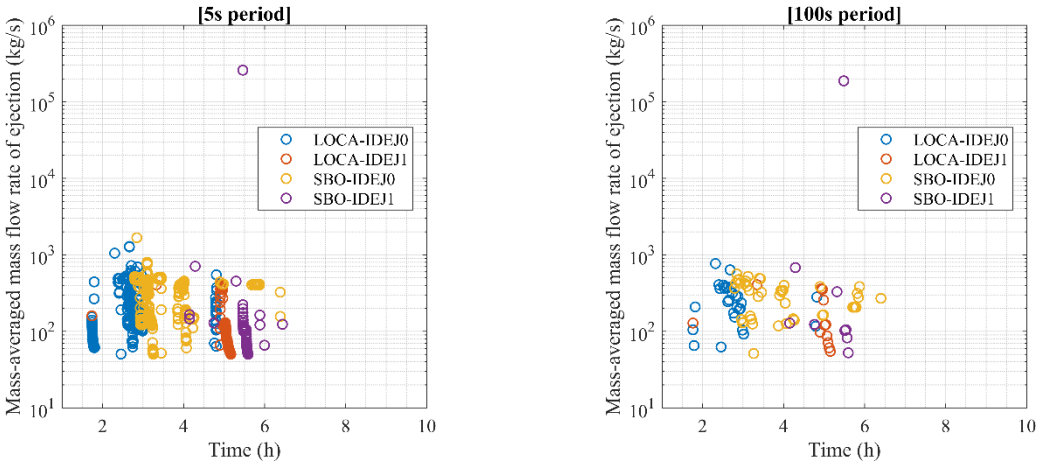

(a) 5s period (b) 100s period

Figure 5-49. Mass-avergaed mass flow rate of debris ejected (filtered for >50kg/s) for every 5s or 100s period.

Table 5-11 MELCOR variable extracted during melt debris ejection from the vessel.

MELCOR variable	Definition	Unit
EXEC-TIME	Absolute time in MELCOR simulation	s
EXEC-DT	Time step value	s
CAV-RHO(CAVITY, HMX)	Density of melt layer in cavity	$kg.m^{-3}$
COR-ABRCH	Vessel breach area	m^2
COR-MEJEC-TOT	Cumulative mass of melt ejected to cavity	kg
COR-T-LP(OXI, CH)	Temperature of oxidic pool in lower plenum	K
COR-T-LP(MET, CH)	Temperature of metallic pool in lower plenum	K
CVH-CLIQLEV('LDW')	Collapsed liquid level of water in cavity	m
CVH-P('LDW')	Pressure in the cavity	Pa
CVH-VOID('LDW', POOL)	Void fraction of the water phase in the cavity	-
CVH-TVAP('LDW')	Temperature of the vapour phase in the cavity	K
CVH-TLIQ('LDW')	Temperature of the water phase in the cavity	K

One of the issues for development of a well posed full model is the high sensitivity of the explosion impulse to the triggering time [77]. In [78] premixing was calculated starting from melt release till the jet front arrival to the bottom of the domain and instantaneous premixing configurations were saved with 1ms time step; steam explosion calculations were carried out for every saved premixing configuration. The results in the Figure 5-50 indicate that small variations in the triggering time may lead to large changes in the explosion energetics. For

example, between 1.9s and 2.01s, i.e. within 110ms time window, the explosion impulse changes almost 50 times from 377kPa·s to 8kPa·s. From the risk perspective, the choice of the triggering time can change prediction of containment failure from physically unreasonable (at ~8kPa·s) to unavoidable (at ~377kPa·s).

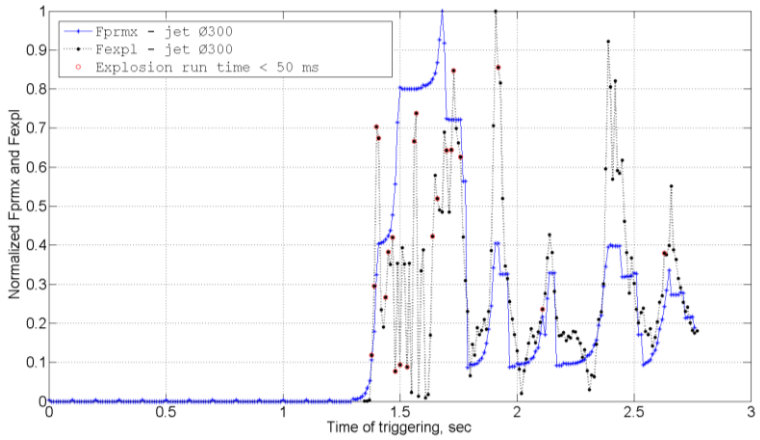

Figure 5-50. The dependence of normalized premixing function F_{prmx} and explosion impulse F_{expl} on the triggering time (release of oxidic corium melt with jet Ø300 mm into a 7m deep water pool).

Chaotic behavior of the steam explosion impulse with respect to the timing of the trigger makes the problem ill-posed. Ill-posedness is one of the main reasons for the large spread of (i) predictions with different FCI codes, and (ii) predictions with the same FCI code obtained by different users (see also discussion in [76]). In order to make model output well-posed and independent from the choice of the triggering time, steam explosion calculation is carried out for each possible triggering time of the melt jet in its instantaneous premixing conditions with a 1ms time step for triggering. Thus, the ill-posedness is addressed by considering statistical distributions of the impulses obtained at the same conditions except for the triggering time. For example, evolution of the explosion impulse can be characterized by a cumulative density function (CDF) of the predicted impulses as shown in Figure 5-51.

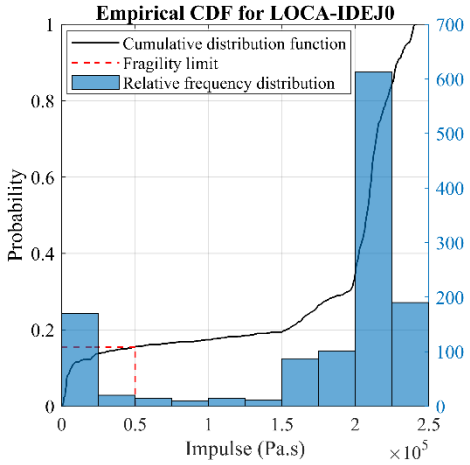

Figure 5-51. Empirical CDF of explosion impulses for all possible triggering times of one LOCA-IDEJ0 premixing case.

Following this statistical approach significantly increases the computational time required to analyse each premixing condition. In some cases, depending on jet velocity, size, and pool conditions, it may take more than 4 seconds for the jet to reach the bottom of the domain, resulting in approximately 4000 explosion cases for a single premixing condition.

The explosion impulse CDFs, along with the established method for calculating the failure probabilities of the containment wall hatch door (both non-reinforced and reinforced) and the

containment base based on their fragility limits, are depicted through the empirical CDF (eCDFs) and normalized failure probability distributions.

As mentioned before, the fragility limits considered in this study for the failure of the,

1. non-reinforced hatch door is 6kPa·s,
2. reinforced hatch door/containment wall is 50kPa·s,
3. containment base is 80kPa·s.

Table 5-12 gives the number of instances considered in mass flow calculations and time steps after filtering. A thorough analysis in the coupling of MELCOR and TEXAS-V would mean running all the 1,122 cases for all 5s instances of potential occurrence of SE. In order to demonstrate the methodology, the 100s period with a total of 92 MELCOR runs was deemed sufficient in this study. Time-averaged (TA) filtering may miss potential peaks in the mass flow rate which the mass-averaged (MA) filtering captures, hence the set is larger. One can be assured that all flow rates in TA set are a subset of MA set.

Table 5-12 Number of time steps for mass flow calculations.

Period	LOCA-IDEJ0	LOCA-IDEJ1	SBO-IDEJ0	SBO-IDEJ1	Total
Unfiltered					
5s	18,709	18,709	18,029	17,885	73,332
100s	939	939	903	903	3,684
Filtered (MA)					
5s	358	194	465	105	1,122
100s	28	12	43	9	92

The scenario and modelling parameter information are provided to TEXAS-V to perform SE calculations for the 4 scenarios, 92 cases in total. These scenario parameters; containment pressure, water and atmosphere temperatures, water level, are vital for the prediction of impulse loads due to SE calculation in TEXAS-V. In a way they carry historical information of the presence of melt and debris in the pool of water. While historical information, for instance:

1. presence of fragmented particles of melt from previous pre-mixing calculations cannot be modelled in later calculations;
2. TEXAS-V calculation domain is small, and earlier calculations may lead to completely dry cavity, which in reality may be replenished.

cannot directly be fed to TEXAS-V, transient thermodynamic properties of materials in the cavity can give a better representation of this.

5.5.1. Source Term Releases

Figure 5-52, Figure 5-53, Figure 5-54 and Figure 5-55 below present the CS and I2 mass fraction released to the ENV considering opening of CNT-ENV flow (CNT failure due to SE) at those instances where >50kg/s debris was ejected. Generally, later CNT failure (due to potential SE) leads to lesser release of CS and I2 mass fraction to the environment in all the accident scenarios.

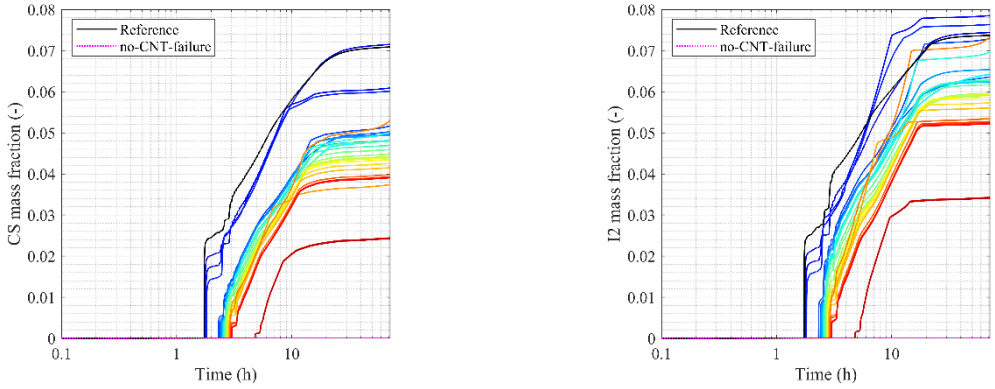

(a) (b)

Figure 5-52. Mass fraction in the environment of (a) CS; (b) I2 for all instances of SE in LOCA-IDEJ0.

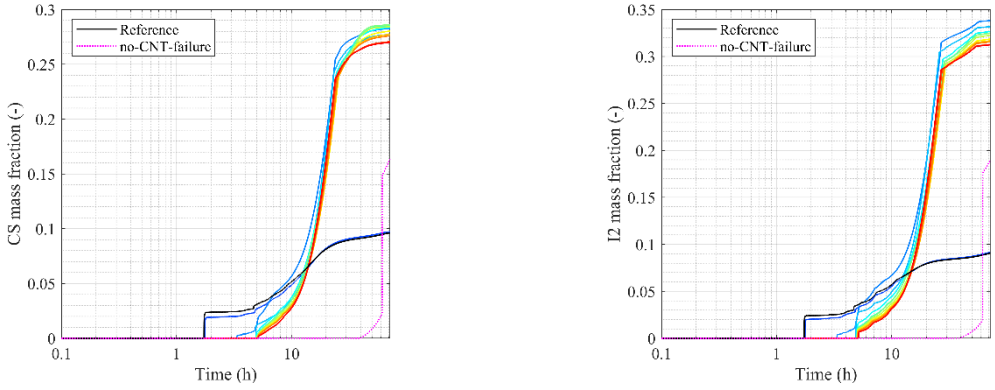

(a) (b)

Figure 5-53. Mass fraction in the environment of (a) CS; (b) I2 for all instances of SE in LOCA-IDEJ1.

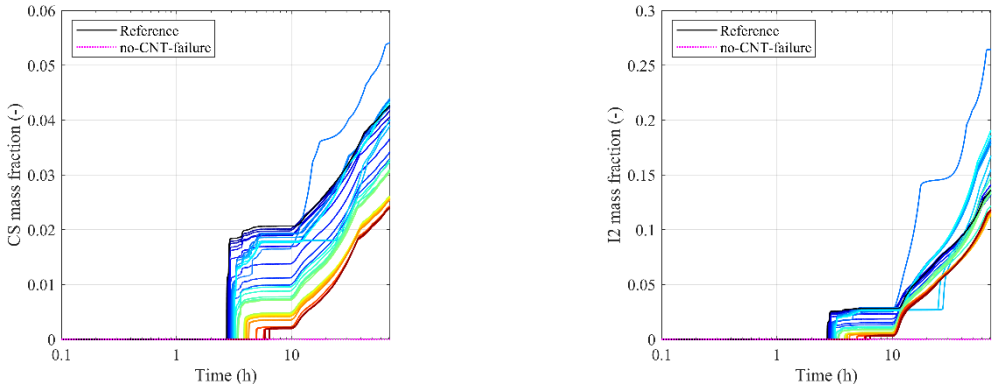

(a) (b)

Figure 5-54. Mass fraction in the environment of (a) CS; (b) I2 for all instances of SE in SBO-IDEJ0.

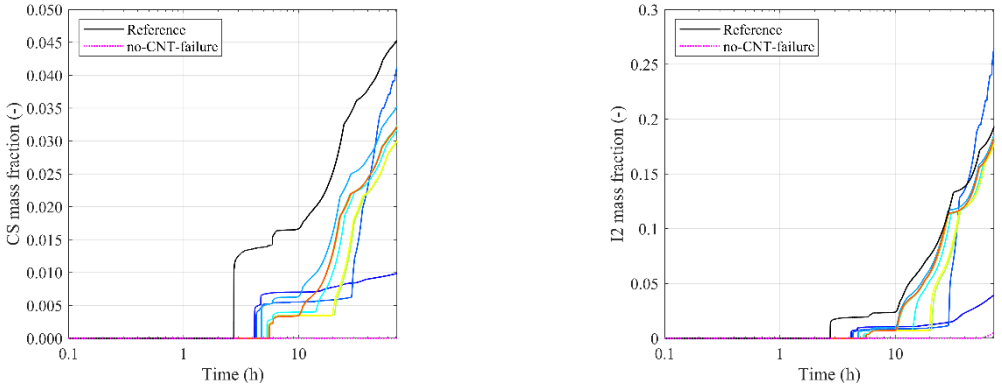

(a) (b)

Figure 5-55. Mass fraction in the environment of (a) CS; (b) I2 for all instances of SE in SBO-IDEJ1.

5.5.2. Steam Explosion Impact Loads

By applying the criterion of only considering premixing cases where the mass flow rate exceeds 50kg/s and excluding any failed explosion case, the number of premixing cases and the total explosion cases for each MELCOR scenario are summarized in Table 5-13.

Table 5-13 MELCOR scenarios premixing and explosion cases numbers.

Scenario	Number of Premix Cases	Number of Explosion Cases
LOCA-IDEJ0	28	17,295
LOCA-IDEJ1	12	7,429
SBO-IDEJ0	43	23,851
SBO-IDEJ1	9	5,096

The results for all premixing cases, represented by eCDFs, for the hatch door, is shown in Figure 5-56. As before, cases from early CNT failure to late CNT failure are coloured from blue to red.

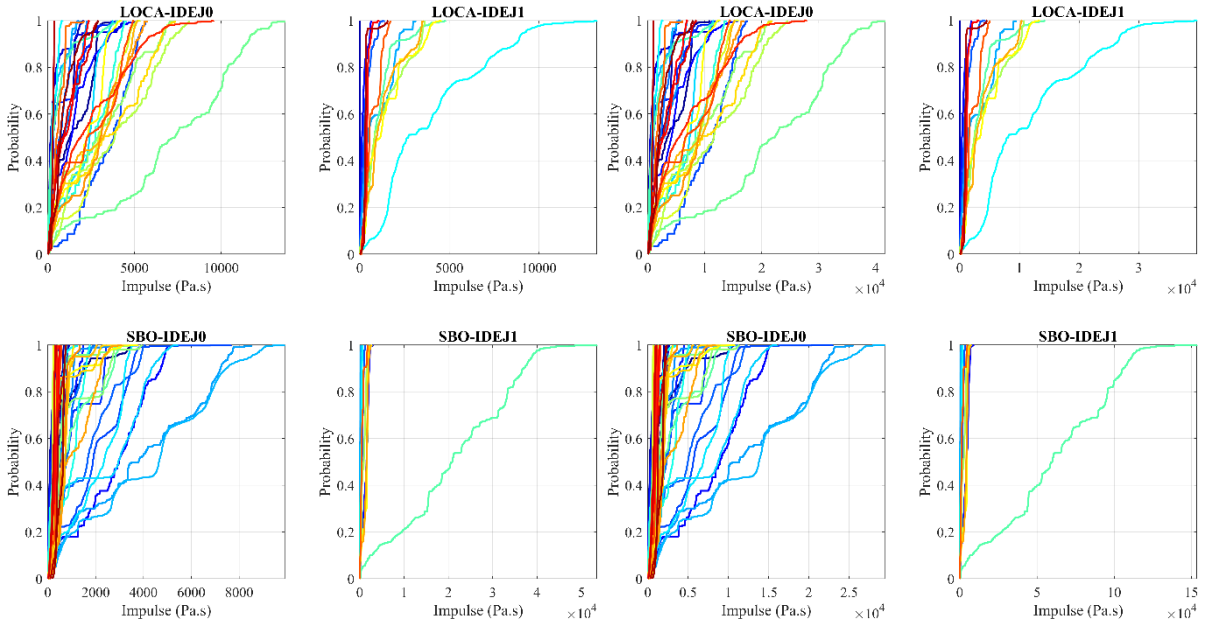

(a) Minimum impulse (SE far). (b) Maximum impulse (SE near).

Figure 5-56. eCDFs of impulses at the hatch door for all premixing cases.

One can observe similar ranges of impulses for LOCA-IDEJ0 and IDEJ1, and for SBO-IDEJ0 and IDEJ1. In the case of SBO-IDEJ1, there is an instance where a large amount of melt is ejected, due to gross failure of the LH walls, leading to a massive jet ejection, causing a huge SE impulse, ~50kPa·s (minimum) -150kPa·s (maximum). Nevertheless, it is clear that the fragility limit of 6kPa·s is exceeded among these scenarios for the non-reinforced hatch door, and thus probability of failure can be estimated by these eCDFs.

Empirical CDFs of probabilities of failure for the non-reinforced hatch door is presented in Figure 5-57. It is evident that the failure probability is highest for the non-reinforced hatch door, which is consistent with its low fragility limit of 6kPa·s. Here, the 95th percentile failure probability for the maximum impulse approaches 0.8, 0.6, 0.65 and 0.9 respectively for these scenarios, indicating that steam explosions lead to hatch door failure in the majority of cases.

In general, LOCA-IDEJ0 exhibits a higher probability of failure, with most probabilities concentrated at the higher end. If the SE were to occur at the farthest end from the target, the 95th percentile of failure probabilities for the non-reinforced hatch door are 0.25, 0.25, 0.3 and 0.85 respectively for the 4 scenarios, and for the containment base are 0 for all scenarios. This indicates that a steam explosion, regardless of its onset, whether it occurs immediately upon pressure vessel failure or is delayed, will still likely result in the failure of the hatch door, and in the case of the containment base, there is a limiting height from the base wherein a SE can cause its failure.

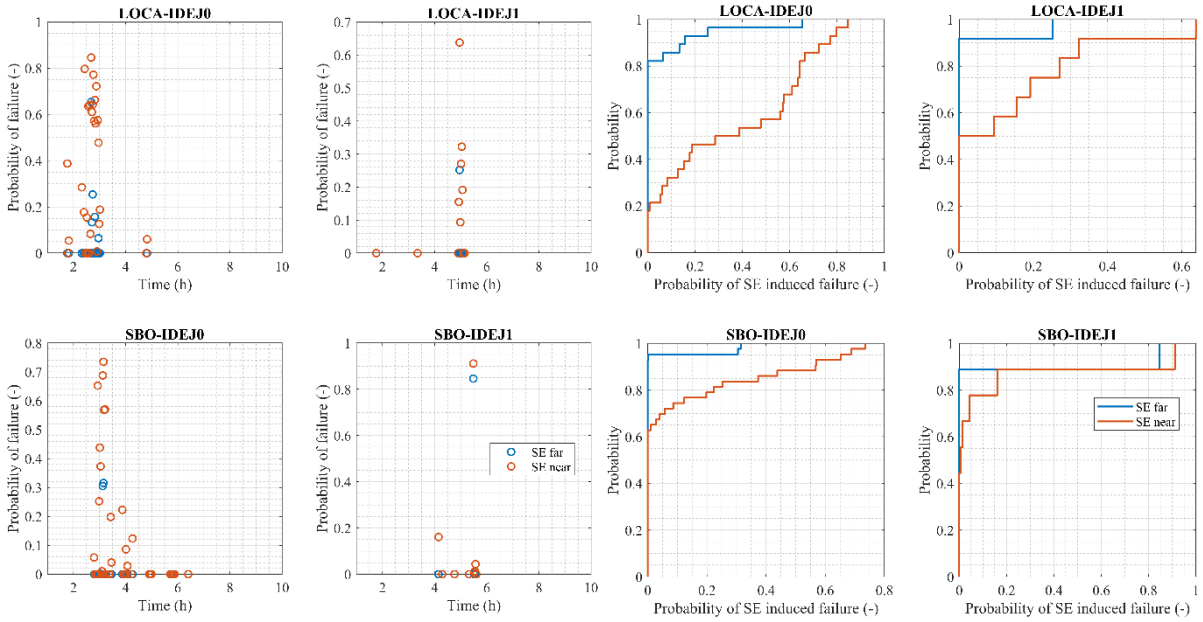

(a) Absolute probabilities. (b) eCDF of failure probabilities.

Figure 5-57. Failure probability for non-reinforced hatch door for 4 SA scenarios.

5.5.3. Updated Source Term Empirical CDFs

Figure 5-58 and Figure 5-59 show the updated eCDFs for the CS and I2 release fractions in the environment for all scenarios considered in this study. In the case of LOCA-IDEJ0, the updated CDF is different from the original CDF, with 95th percentile of CS release is between 0.046 and 0.052 which is little lesser than original 0.06, and I2 release is between 0.06 and 0.073, lesser than the original 0.076. For LOCA-IDEJ1 95th percentile for CS release is 0.285 which is the same as the original release and for I2 is 0.326, slightly lesser than original 0.33. CS and I2 mass fractions in SBO-IDEJ0 are significantly different than the original owing to spread of the

individual probabilities. 95th percentiles for CS fraction is between 0.04 and 0.054 with the original at 0.043 falling in between the updated bounds, and the original I2 fraction at 0.19 is between the updated bounds of 0.17 and 0.26. And lastly, in the case of SBO-IDEJ1 95th percentile for CS release originally at 0.041 is larger than the updated release fraction of 0.0323 and the original I2 release at 0.265 is larger than the updated release fraction of 0.186. As can be seen in the updated figures, there are large jumps in the CDFs for LOCA-IDEJ1, and SBO. Further analysis with reduced mass flow limit (so that more instances of SE pass the filtering criteria) could improve these results.

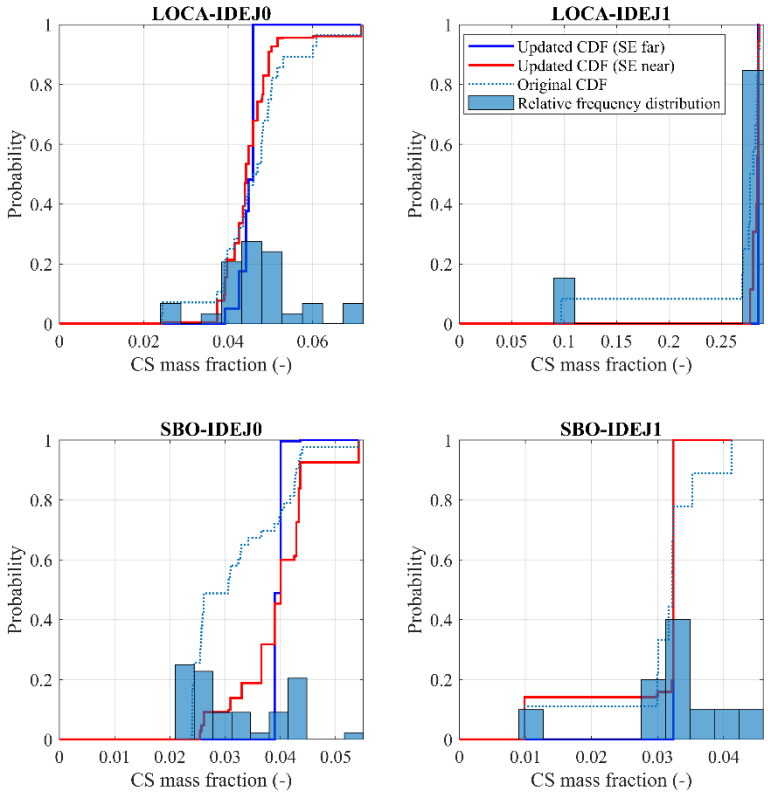

Figure 5-58. Updated empirical CDF for mass fraction in the environment of CS considering probabilities of failure of non-reinforced hatch door for 4 SA scenarios.

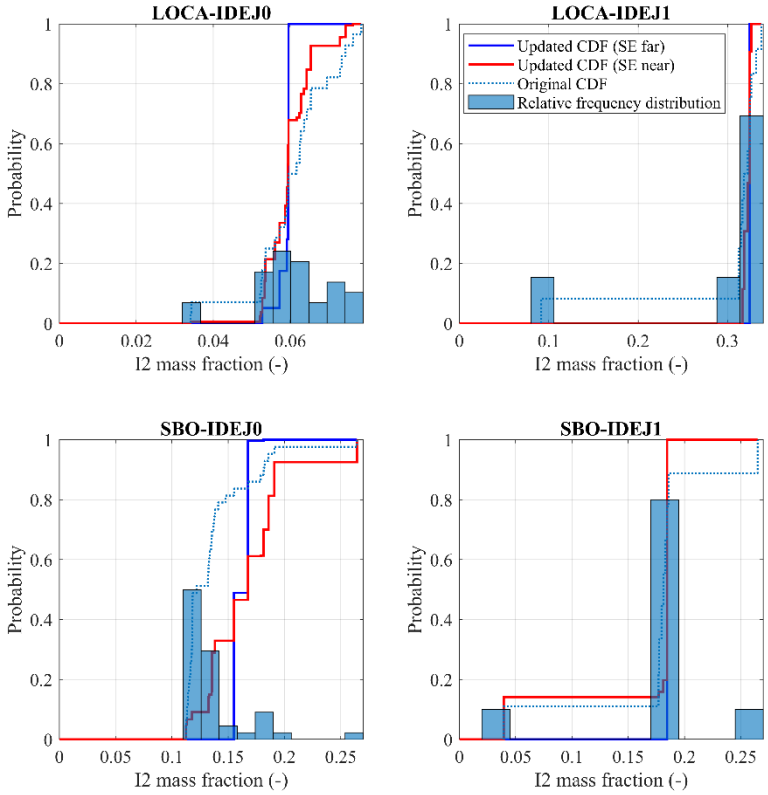

Figure 5-59. Updated empirical CDF for mass fraction in the environment of I2 considering probabilities of failure of non-reinforced hatch door for 4 SA scenarios.

5.6. Probabilistic Evaluation of the Source Term Uncertainty in Filtered Containment Venting Scenarios in Nordic BWR

Accident scenarios initiated by a LOCA that lead to a filtered containment venting, based on the NKS-STATUS phase 2 and 3 results, may exceed the acceptable release threshold (in terms of the fraction of the core inventory of Cs released to the environment) depending on the MELCOR code uncertain parameters combinations and selected modelling options. This can affect the release categories classification within the L2 PSA.

Thus, the goal of this work is to evaluate the effect of the MELCOR analysis results on unacceptable release frequency in the Level 2 PSA for Nordic BWR.

Section 5.6.1 provides a general introduction to a common approach for modelling of severe accident progression sequences in Probabilistic Safety Assessment (PSA) developed in [65,66]. Section 5.6.2 discusses possible methodological enhancements of PSA modelling to account for phenomenological uncertainties in PSA Level 2.

5.6.1. Sequence modelling in PSA Level 2

In a standard PSA, the output of PSA Level 1 is typically core damage (possibly separated in a few sub-categories). These sequences are further divided into subcategories based on key factors influencing Level 2 progression.

The interface between PSA Level 1 and Level 2 is defined by Plant Damage States (PDS), which describe not only the core damage state but also the conditions of the primary system and containment. Typically, 20 to 40 PDSs are defined at this interface.

For the generic Nordic BWR PSA model analyzed in this study, 27 PDSs have been identified for power operation and low-power operating modes. The attributes considered relevant for modeling accident progression include:

- Core damage state (failure of shutdown, core cooling or residual heat removal).
- Initiating event (transient or LOCA).
- Time of core melt (early, late).
- Reactor pressure (low, high).
- Containment atmosphere (inert, air).
- Containment spray system status.
- Containment pressure relief status (activated, not activated).
- Filtered containment venting status (activated, not yet activated, failed).
- Bypass of containment (bypass, intact).
- Suppression pool temperature (warm if pool cooling fails, else cool).

PSA Level 2 considers events that may influence the retention of radioactive releases within the reactor pressure vessel (RPV) or containment. Any variation in RPV coolability across different scenarios is critical information, as are the sequences affecting key accident phenomena. For each PDS, a Containment Event Tree (CET) is developed to model the progression of the accident.

Accident progression is influenced by various physical phenomena, which are typically accounted for in PSA analysis:

- Re-criticality (in the core, in lower plenum, in containment).
- Hydrogen burn (deflagration and detonation).
- In-vessel steam explosion.
- Ex-vessel steam explosion.
- Direct containment heating.
- Rocket mode.
- Melt concrete interaction (basemat penetration).
- Steam generator tube rupture (only for PWR).

These phenomena can affect the containment function and result in different release modes to the environment:

- Containment rupture.
- Different types of containment bypass.
- Activation of filtered containment venting.

Furthermore, accident progression phenomena – such as in-vessel debris interaction with the vessel's lower head and internal structures, debris ejection into the cavity, and its interaction with the coolant in the cavity – can significantly impact the effectiveness of various consequence mitigation measures, including the filtering efficiency of the Multi Venturi Scrubbing System (MVSS) in filtered containment venting scenarios.

The effect most focused on in the following is the scrubbing efficiency of the filtered containment venting system in various scenarios, as the results presented in the previous phases of the NKS-STATUS project [50,67] indicate that there is significant uncertainty in

the source term released to the environment in the accident scenarios initiated by a LOCA that leads to core melt and fission products release through the filtered containment venting system (MVSS).

In general, the sequences in the CET end at the release categories (RC) and there are normally around 15-40 of such. The RCs can be defined in different ways, for example by release size or type of sequence. The normal approach is to use the sequence type, because then only a limited amount of verifying deterministic calculations are considered to be required. For the sequence type approach, the characterization is for example based on:

- Release path (containment bypass, containment rupture, filtered release, leakage).
- Timing of release (early, late).
- Initiator (pipe rupture, transient).
- Sprinkling of containment established (yes/no).

Since only a limited number of deterministic verification calculations are performed to assess accident sequences and determine their consequences (consequence mapping in PSA Level 2), these analyses do not account for the effects of phenomenological uncertainties on fission product behavior inside the containment, the effectiveness of accident mitigation systems, or the source term released to the environment. The results from previous phases of the NKS-STATUS project [50,67] indicate that, in accident sequences initiated by a LOCA leading to core melt and filtered containment venting, the acceptable release threshold may be exceeded for certain combinations of uncertain MELCOR code parameters.

The current modelling is based on the generic PSA model for Nordic BWR [65,66], which serves as the reference case in this report. The MVSS system is modelled as a functional event that accounts for active components within the system. Its primary safety function is to preserve containment integrity by relieving excess pressure through the scrubber, thereby filtering fission products and maintaining containment integrity.

Point estimate analyses of these accident sequences, performed using integral plant response codes, indicate that the release of fission products in these scenarios remains within the acceptable release threshold.

In the following chapters, both the reference PSA model and an enhanced model, incorporating information from uncertainty analysis using the MELCOR code, are presented. The enhanced model accounts for epistemic uncertainties associated with fission products behavior inside the containment and the source term released to the environment.

Table 5-14. Summary of release categories for the Nordic BWR [23].

Release Category	Description
RC1	Severe accident initiated by a transient. Containment sprays. Early containment failure.
RC2	Containment bypass due to IS-LOCA.
RC3	Containment bypass due to unisolated RPV (failure to close main steam or main feedwater isolation valves).
RC4	Severe accident initiated by a transient or LOCA. Containment failure due to a containment phenomenon.
RC5	Severe accident initiated by a LOCA. Early containment failure. No containment sprays.

Release Category	Description
RC6	Severe accident initiated by a transient. Early containment failure. No containment sprays.
RC7	Intact containment. Release through FCV (MVSS)
RC8	Diffuse leakage.
RC9	Containment melt-through.

5.6.2. Uncertainties in PSA Level 2 and Improved Sequence Modelling

Figure 5-60 outlines the simplified accident progression and release categories for accident scenarios initiated by a LOCA in Level 2 PSA.

In this analysis, it is assumed that the successful recovery of the Low-Pressure Safety Injection (LPSI) or High-Pressure Safety Injection (HPSI), and Residual Heat Removal (RHR) after the onset of core damage would prevent failure of the RPV and would lead to diffuse leakage from the intact containment (RC8 release category in Figure 5-60).

However, failure to restore cooling of the degraded core would results in failure of the vessel lower head failure and debris ejection into the cavity. Further, based on the LDW flooding system logic, if core damage is imminent, water from the condensation pool is used to flood the lower drywell (LDW Flooding in Figure 5-60) to fragment and cool ejected debris and molten material from the reactor pressure vessel (RPV) and prevent failure of cable penetrations located in the pedestal floor (see Section 3.1 for further details on the safety design and severe accident management in the Nordic BWR)). If water is not supplied to the cavity, basemat melt-through occurs as a consequence (RC9 – release category [23]).

If cavity flooding is successful, there remains a risk of ex-vessel steam explosions (No STEX in Figure 5-60), due to the interaction of molten debris with water in the cavity, potentially damaging the containment (RC4 – release category [23]). Additionally, depending on the properties of the melt and debris, there is a risk of forming a non-coolable debris configuration (DECO in Figure 5-60). This can lead to hot-spots formation, debris reheating, localized remelting, and melt attack on the cable penetrations in the pedestal floor, ultimately resulting in the basemat melt-through (RC9 – release category [23]).

Further details on the effects and modeling of ex-vessel steam explosions, ex-vessel debris coolability, and associated risk analysis can be found in [65,67,68,69,70].

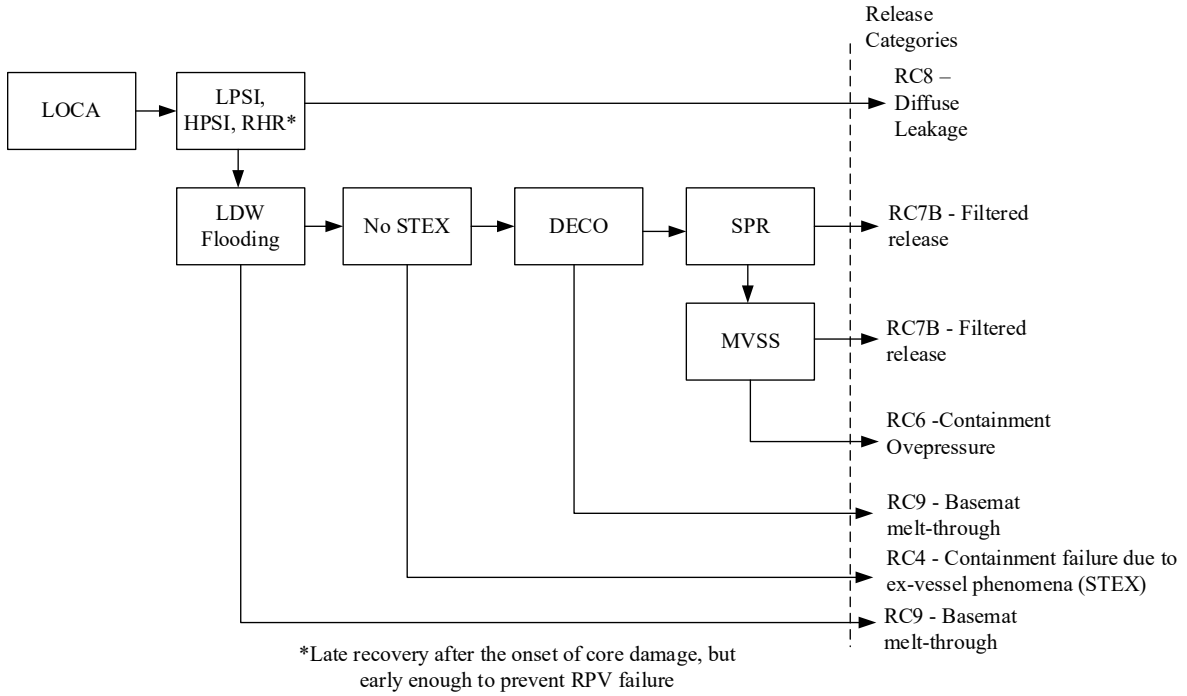

Figure 5-60. Reference case. Modelling of filtered containment venting scenarios in accident sequences initiated by a LOCA.

Further accident progression is influenced by the delayed activation of the containment spray system. Successful operation of this system condenses steam within the containment and scrubs radioactive materials suspended in the containment atmosphere. In the current implementation of PSA Level 2 for the Nordic BWR, it is assumed that reactor pressure vessel melt-through results in a pressure spike due to interactions between molten core material and water in the cavity. This spike activates the MVSS, leading to filtered venting of the containment atmosphere to the environment, classified as release category RC7B with active spray (grouped under the same acceptable release category) [23].

However, this assumption regarding the pressure spike does not apply to the sequences that explicitly credit MVSS activation (i.e., no positive credit of failed components). In this case, failure to activate the containment spray system leads to a gradual pressure increase, eventually resulting in filtered venting of the containment atmosphere through the MVSS. This scenario also corresponds to release category RC7B [23].

If the MVSS fails, the containment would rupture due to overpressure, leading to a large unfiltered release to the environment(RC6 – release category [23]).

In the case of successful MVSS activation, the release category depends on the filtering efficiency of the scrubber, which is subject to both, uncertainties related to the filtering efficiency of the scrubber, and phenomenological uncertainties related to the severe accident progression, fission product release and behavior inside the containment, and transport to the scrubber.

The evaluation of these uncertainties, regarding both the source term release to the environment and the scrubber efficiency, has been carried out during the second and third phases of the NKS-STATUS project. The results of these analyses are presented in [50,67] and summarized in Section 5.6.2.1.

5.6.2.1. Uncertainty analysis of filtered containment venting scenarios in Nordic BWR

The uncertainty analysis performed within the second and the third phases of the NKS-STATUS project [50,67] showed that the magnitude of the source term released to the environment in unmitigated filtered containment venting scenarios initiated by a LB-LOCA may lead to exceedance of the acceptable release threshold for some MELCOR modelling parameters combinations, such as the mode of debris ejection from the vessel (IDEJ) and decontamination factor for radioactive vapors (MVSSDFV), for further details refer to [23,49,50,67,73].

The analyses performed in [50,67] were performed using the MELCOR code. Table 5-15 summarize MELCOR code uncertain modelling parameters considered in uncertainty analysis of filtered containment venting scenarios.

Table 5-15. MELCOR code modelling parameters considered in uncertainty analysis.

Parameter ID	Parameter description and proposed distribution	Accident scenario
STICK [-]	Particle sticking probability. Scaled beta (2.5, 1.0), scaled on [0.5, 1.0] [31]	All
FCELRA [-]	Radiative exchange factors. Truncated normal (0.1, 0.035) truncated on [0.020, 0.30] [27]	All
SC71521 [m]	Initial bubble diameter correlation coefficient in SPARC-90 model. Triangular M = 7.E-3, range [5.E-3, 8.E-3] [EJ]2	LOCA-IDEJ0 LOCA-IDEJ0-SPR
SC1020 [-]	Multiplication factor for time constant for radial solid and molten debris relocation. Scaled beta (1.33, 1.67) scaled on range [1.0, 4.0] [29]	LOCA-IDEJ0 LOCA-IDEJ0-SPR
CORNSBLD [K]	NS failure temperature threshold. Uniform [1520-1700] [30]	All
VFALL [m/s]	Velocity of falling debris. Scaled beta (0.85, 1.14), scaled on range [0.01, 1.0] [29]	All
TZRSSINC [K]	Solidus temperatures for ZR/SS and ZR/INC eutectic pairs. Scaled beta (2.0, 1.0), scaled on range [1210, 1700] [EJ]	All
SC715010 [-]	Scaling factor for SPARC-90 model vent exit condensation decontamination factor. Triangular M = 2, range [1.0, 3.0] [EJ]	All
CHI [-]	Aerosol dynamic shape factor. Scaled beta (1.0, 1.5) scaled on [1.0, 5.0] [31]	All
MVSSDFV [-]	MVSS decontamination factor for radioactive vapors. Lognormal (4.6, 0.916) truncated on [10,1000], 0.99 – correlation with MVSSDFA [EJ]	All
SC71568[-]	Multiplicative constant in a temperature correction correlation in the SPARC-90 model. Triangular M = -0.00232, [-2.6691e-03, -1.9728e-03] [EJ]	All
TPFAIL [K]	Penetration failure temperature. Scaled beta (2.0, 2.0) scaled on [1273, 1600] [EJ]	All

[2] EJ – expert judgement.

Parameter ID	Parameter description and proposed distribution	Accident scenario
HFRZZR [W/m2K]	Refreezing heat transfer coefficient for Zr. Lognormal (8.9227, 0.55962) truncate on [2000, 22000] [27]	All
SC7170CSM [kg/kgH2O]	Saturation solubility at high and low temperature reference for CsM. Triangular M = 0.67, range [0.5695, 0.7705] [EJ]	LOCA-IDEJ0 LOCA-IDEJ0-SPR
SC71555 [-]	SPARC-90 model multiplication constants in the DF factor correlations for and large Stokes numbers. Triangular M = 1.13893, range [0.9681, 1.3098] [EJ]	All
RHONOM [kg/m3]	Aerosol density. Triangular M = 2000, range [870,4500] [26]	All
SC7111CS2 [K]	Characteristic energy of interaction between the molecules divided by the Boltzmann constant for CsI/CsM. Triangular M = 97, range [82.450,111.550] [EJ]	LOCA-IDEJ0 LOCA-IDEJ0-SPR
SC7170CS [kg/kgH2O]	Saturation solubility at low/high temperature reference for Cs. Triangular M = 3.95, range [3.3575, 4.5425] [EJ]	LOCA-IDEJ1 LOCA-IDEJ1-SPR
SC7111CS1 [Å]	Characteristic diameter of the molecule for Cs. Triangular M = 3.617, range [3.0745,4.1595] [EJ]	LOCA-IDEJ1 LOCA-IDEJ1-SPR
TURBDS m2/s3]	Turbulence dissipation rate. Uniform [7.5E-4, 1.25E-3] [28][EJ]	LOCA-IDEJ1 LOCA-IDEJ1-SPR
SC7111I1 [Å]	Characteristic diameter of the molecule for I. Triangular M = 4.982, range [4.2347, 5.7293] [EJ]	LOCA-IDEJ1 LOCA-IDEJ1-SPR
GAMMA [-]	Aerosol agglomeration shape factor. Scaled beta (1.0,1.5) scaled on range [1.0, 5.0] [31]	All
MVSSDFA [-]	MVSS decontamination factor for radioactive aerosols. Truncated normal (500, 250) truncated on [100,1000], 0.99 – correlation with MVSSDFV [EJ][54]	All
PDPor [-]	Particulate debris porosity. Truncated normal (0.38, 0.1) truncated on [0.25, 0.50] [27][EJ]	All
HFRZSS [W/m2K]	Refreezing heat transfer coefficient for SS. Lognormal (7.824, 0.40547), truncated on [1000, 5000] [27]	All
DIAMO [m]	Initial spray droplet diameter. Triangular M = 1.E-3, range [1.E-4, 2.E-3].	LOCA-IDEJ0-SPR LOCA-IDEJ1-SPR

Furthermore, the MELCOR code has two options for core debris ejection from the vessel, determined by a solid debris ejection switch (IDEJ). In the default option (ON, IDEJ = 0), the masses of each material available for ejection are the total debris and molten pool material masses, regardless of whether or how much they are molten [6,7]. In the second option (OFF, IDEJ = 1), the masses of steel, Zircaloy, and UO2 available for ejection are simply the masses of these materials that are molten; the masses of steel oxide and control poison materials available for ejection are the masses of each of these materials multiplied by the steel melt fraction, based on an assumption of proportional mixing; the mass of ZrO_2 available for ejection is the ZrO_2 mass multiplied by the Zircaloy melt fraction. Additionally, the mass of solid UO_2 available for ejection is the Zircaloy melt fraction times the mass of UO_2 that could be relocated with the Zircaloy as calculated in the candling model using the secondary

material transport model [6,7]. Furthermore, the MELCOR code puts additional constraints on the mass that can be ejected at vessel failure: (i) to initiate melt ejection, the mass of molten materials should be greater than SC1610(2) (5000 kg – default value), or a melt fraction should be larger than SC1610(1) (0.1 – default value). Here, the values of sensitivity coefficients SC1610(1,2) were set to zero, so any amount of melt available for ejection would be ejected. In the event of a gross failure of the vessel lower head (e.g. due to creep-rupture), it is assumed that all debris in the bottom axial level of the corresponding ring, regardless its state, is discharged linearly over a 1-second time step without taking into account the failure opening diameter [6,7].

The results of the sensitivity and uncertainty analyses performed in [24,25,49,50] showed that the mode of debris ejection from the vessel (IDEJ) has a dominant effect on the code predictions of the debris ejection from the vessel and magnitude of the Cs and I2 source terms released to the environment in case of an accident initiated by a LOCA. As it is not feasible to treat this parameter probabilistically due to a lack of knowledge, it was be considered as a phenomenological splinter[3]. Consequently, the uncertainty analyses was conducted for the accident scenarios considered in the analysis and two IDEJ parameter combinations, resulting in 2 sets of calculations per single accident scenario.

As a result, for every accident scenario, the MELCOR code simulations were performed for two options of the mode of debris ejection from the vessel – IDEJ0 and IDEJ1. In total 4 sets of calculations were considered in the analysis:

- LOCA-IDEJ0 – Accident initiated by a LOCA that leads to filtered containment venting via MVSS with IDEJ0.
- LOCA-IDEJ1 – Accident initiated by a LOCA that leads to filtered containment venting via MVSS with IDEJ1.
- LOCA-IDEJ0-SPR – Accident initiated by a LOCA that leads to filtered containment venting via MVSS with IDEJ0, and activation of the independent spray system.
- LOCA-IDEJ1-SPR – Accident initiated by a LOCA that leads to filtered containment venting via MVSS with IDEJ1, and activation of the independent spray system.

[3]In ROAAM formulation a splinter scenario is a phenomenological scenario where relevant epistemic uncertainties are *beyond the reach of any reasonably verifiable quantification*.

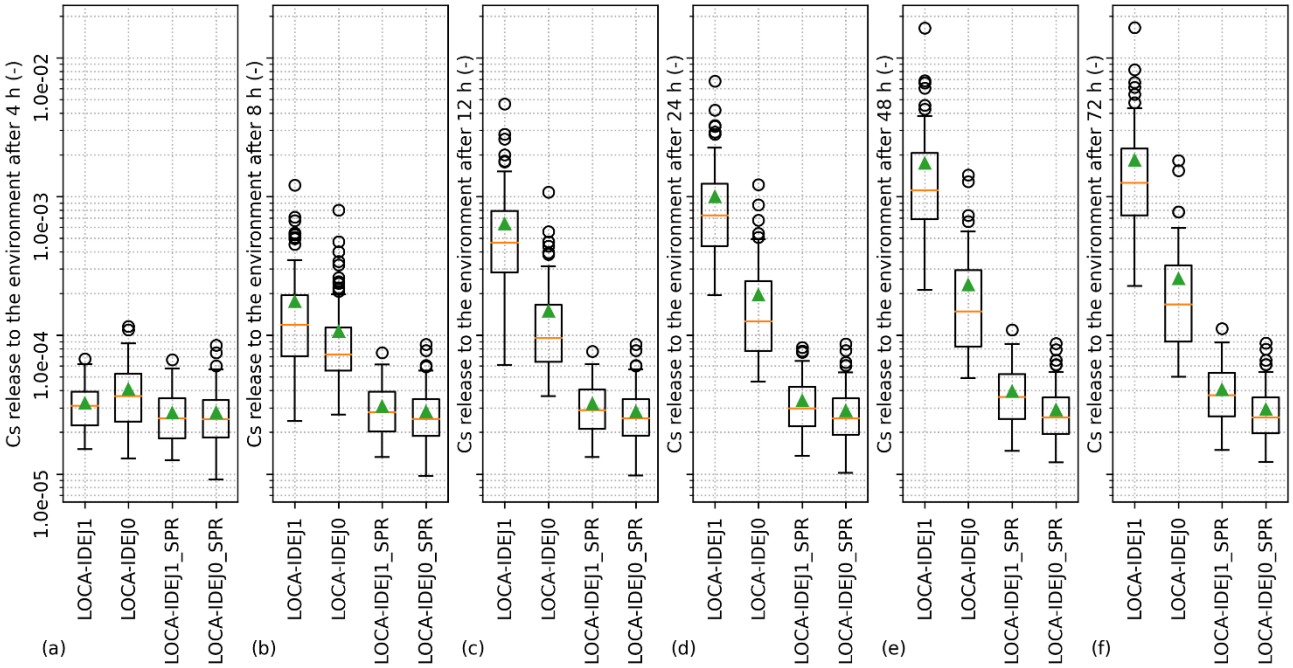

Figure 5-61. Fraction of the core inventory of Cs [-] released to the environment after (a) 4 hours; (b) 8 hours; (c) 12 hours; (d) 24 hours; (e) 48 hours; (f) 72 hours after initiating event [67].

The resulting fraction of the core inventory of Cs released to the environment after 4 h, 8 h, 12 h, 24 h, 46 h and 72 h after the initiating event, illustrated in Figure 5-61a-f, show that in the case of LOCA-IDEJ1 the acceptable release threshold is exceeded already after 8 hours in a few cases and12 hours after initiating event in over 50% of simulated cases. After 72 hours, the fraction of Cs released to the environment increases to 90% of simulated cases in the LOCA-IDEJ1 scenario and 16% in the LOCA-IDEJ0 scenario.

The results of the analyses for the LOCA-IDEJ0 and LOCA-IDEJ1 scenarios were incorporated into the PSA model of the Nordic BWR as an additional function event within the accident progression event tree structure for scenarios initiated by LOCA events that lead to filtered containment venting (Figure 5-62). The new function event, "MVSS UA", was implemented as a basic event, with branching probabilities representing the likelihood of exceeding the acceptable release threshold: (i) 16% for LOCA-IDEJ0 ($P_{MVSS_{UA-IDEJ0}} = 0.16$), and (ii) 90% for LOCA-IDEJ1 ($P_{MVSS_{UA-IDEJ1}} = 0.9$).

Success of the MVSS UA function event results in a filtered release that falls within the acceptable release category (RC7B release category [23]), while failure leads to a filtered release classified as unacceptable, denoted as “Filtered release–UR” Figure 5-62, defined as a new RC7B-UR release category.

Note that the modelling switch IDEJ, which represents the mode of debris ejection from the reactor pressure vessel into the cavity in the MELCOR code, is considered a phenomenological splinter, i.e., a phenomenological scenario where the relevant epistemic uncertainties are beyond the scope of any reasonably verifiable quantification. In the PSA analysis, these splinters are treated in the same manner as in the uncertainty analysis. Specifically, two sets of evaluations are carried out for LOCA scenarios leading to filtered containment venting. The underlying deterministic analyses and evaluation of branching probabilities in the “MVSS UA” function event are performed using: (i) IDEJ = 0 (solid debris ejection – ON), and (ii) IDEJ = 1 (solid debris ejection – OFF).

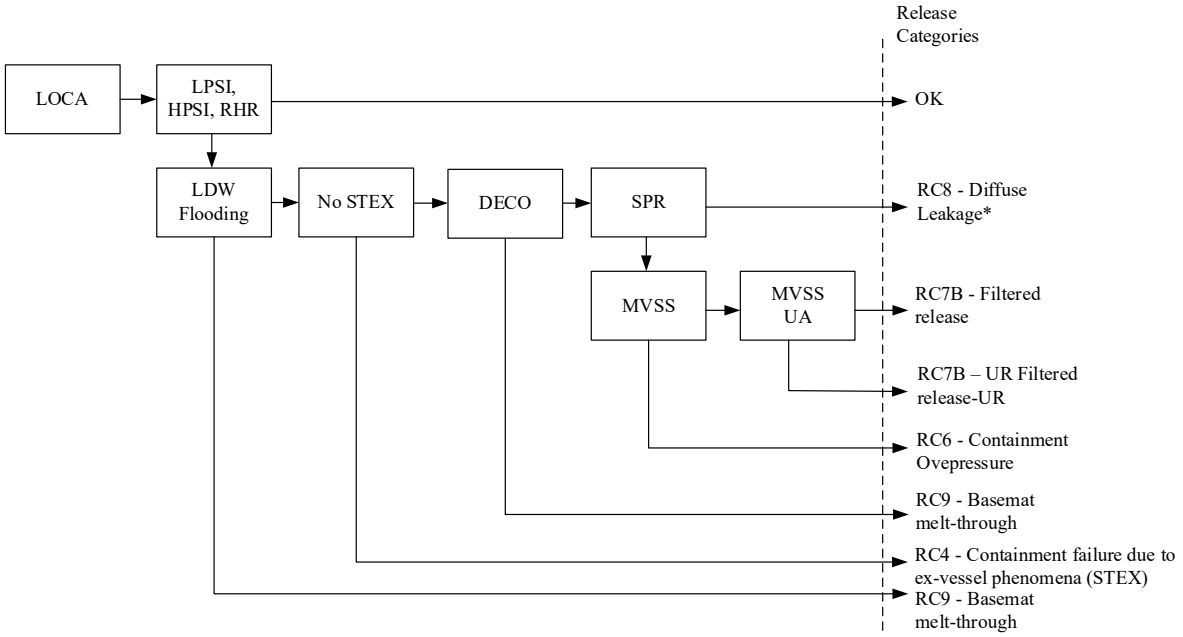

Figure 5-62. Enhanced case. Modelling of filtered containment venting scenarios in accident sequences initiated by a LOCA.

Note that the treatment of filtered containment venting scenarios, as presented in Figure 5-62, was applied for all LOCA sizes considered in the model. This effectively means that the influence of uncertain modelling parameters in the MELCOR code (as listed in Table 5-15), as well as the assumed mode of debris ejection from the vessel, was considered identical for all pipe breaks in the RCSPB inside the containment. These pipe breaks are thus assumed to result in release characteristics similar to those analyzed in [50] and summarized in Section 5.6.2.1.

Another crucial aspect that was identified in the study performed in the third phase of the project, but was not considered in the present analysis is the long-term behavior of the scrubber. This involves consideration the effects of scrubber water temperature and level, as well as the impact of decay heat from fission products deposited in the filter pool on the scrubbing efficiency of the MVSS. This may necessitate modelling of additional operator actions, such as scrubber inventory makeup, which are currently not considered in either the MELCOR model of Nordic BWR or in the PSA L2 for Nordic BWR.

5.6.3. Results

The results of PSA evaluation of the accident sequences initiated by LOCA events that lead to the filtered containment venting are summarized in Table 5-16.

The resulting frequencies were normalized against the value obtained using the reference model [65,66] for the RC7B release category.

Table 5-16.Normalized release frequencies for various release categories (RC) for the accident sequences initiated by LOCA.

Release categories in LOCA initiated accident sequences	Reference model	IDEJ0*	IDEJ1*
Unacceptable release RC3B, RC4B, RC5 (incl. RC7B-UR*)	1.27E-01	1.27E-01	1.29E-01
RC7B (acceptable release)	1.00E+00	1.00E+00	1.00E+00
RC7B-UR (% of total unacceptable release)*	-	0.33%	1.84%

* RC7B-UR is only calculated using the enhanced model for LOCA-IDEJ0 and LOCA-IDEJ1 scenarios.

The results show that the frequency of unacceptable releases in severe accident scenarios initiated by LOCA events is almost eight times lower than the frequency of filtered releases in similar scenarios. Additionally, the RC7B-UR release category contributes 0.33% (LOCA-IDEJ0) and 1.84% (LOCA-IDEJ1) to the total frequency of unacceptable release for LOCA-initiated accident scenarios.

Overall, severe accident scenarios initiated by LOCAs contribute approximately 2% to the total frequency of unacceptable release across all initiating event groups. Similarly, their contribution to the total frequency of filtered release to the environment, via the MVSS, is approximately 3%. The contribution of RC7B-UR to the total frequency of unacceptable release from all initiating events is only 0.007% for LOCA-IDEJ0 and 0.038% for LOCA-IDEJ1.

These results indicate that, although the phenomenological uncertainties in these particular scenarios (RC7B-LOCA-IDEJ1 and RC7B-LOCA-IDEJ0) are relatively large, their overall impact on the total frequency of unacceptable release is minimal. As discussed in [23], the dominant contributors to unacceptable release frequency remain the containment bypass sequences and interfacing system LOCA events.

6. Discussion and conclusions

Within the study of fission product remobilization in SBO scenarios that lead to filtered containment venting in Finnish BWRs, the focus heavily being on cesium. Sensitivity and uncertainty analyses based on the second phase of STATUS project were run and the results were analyzed in order to find out whether cesium remobilization occurs within 30 hours and what would be the most probable sources for the remobilization. Additionally, sensitivity studies were performed to find out the most influential model parameters, and separate effect tests were performed by disabling the solid debris ejection model (IDEJ).

In the SBO scenario leading filtered containment venting, remobilization from wetwell and lower dry well pools was not observed during the 30 hours of simulation, even though they had a quite significant amount of cesium retained. When studying the deposited masses of radioactive species and cesium, it was found out that most of the changes in the deposit masses occurred on the heat structures of the inner walls of the RPV. These changes were traced to originate from Cesium disappearing from the heat structures, which was assumed to be indicating resuspension of cesium. When comparing the Cs release between 10 and 30 hours it was observed that the possible resuspension of cesium contributes quite little (around one tenth) to the total Cs release.

Sensitivity studies showed that regarding the total Cs release, the most influential parameters in SBO-IDEJ0 case were GAMMA (aerosol agglomeration shape factor) and CHI (aerosol dynamic shape factor), and in SBO-IDEJ1 case GAMMA, CHI, RHONOM (aerosol density) and SC71521 (Initial bubble diameter correlation coefficient in SPARC-90 model). In post analysis sensitivity studies, the parameters that seemed to affect most the FP (mainly cesium) resuspension were TPFAIL (lower head penetration failure temperature), SC71568 (multiplicative constant in a temperature correction correlation in the SPARC-90 model), FTHERM (thermal accommodation coefficient) and TURBDS (turbulence dissipation ratio) for SBO-IDEJ0 case and CHI and FTHERM for SBO-IDEJ1 case.

Additionally, the effect of an independent containment spray system on FP remobilization has been investigated in SBO-IDEJ0. Sensitivity and uncertainty studies along with further analyses based on the third NKS-STATUS phase results were performed in order to find the effect of the sprays, the most influential parameters and whether remobilization occurs or not. No separate effect test was done in this task, and only SBO-IDEJ0 case was considered.

The results were quite similar with the ones from unmitigated SBO scenarios. Overall, the sprays seemed to decrease the Cs release to the environment, although this might not have anything to do with the FP remobilization but rather the initial release occurring right after the opening of the FCV. Sensitivity studies indicated that the most influential parameters here were again GAMMA and CHI, with some elevated influence on SPRDELAY (time delay for spray activation) and FTHERM. In additional sensitivity studies the effect of the input parameters on the FP and Cs resuspension was studied, and the study suggested that the most influential parameters would in that case be TPFAIL and SC71568.

The influence of the SPRDELAY (delay in the start of the spray systems after the vessel breach) on Cs release or remobilization was quite small in all cases. It might indicate that the sprays do not actually do much after the initial release has passed, since the amount of aerosols in the containment atmosphere was very low.

Furthermore, valuable insights have been gained into the behavior of fission products (Cs and I_2) during RC4A (SBO) and RC4B (LOCA) scenarios, which involve containment failure due to ex-vessel phenomena in Nordic BWRs, with particular focus on deposition, remobilization, and release to the environment. Key findings include: CS and I_2 deposition in the RPV and

containment (CNT) is influenced by thermal-hydraulic conditions, with significant remobilization observed due to the heat up of the heat structures, the RPV and containment atmosphere due to in-vessel debris. The Morris sensitivity analysis identified SC710641 (activation energy in diffusion correlation) and SC3210 (decay heat multiplier) as dominant parameters affecting deposition, highlighting the importance of fuel matrix release models.

The analysis of vessel lower head failure modes and debris ejection into the cavity indicated that the debris ejection conditions (e.g., mass flow rates >50 kg/s) significantly influence the probability of containment failure due to steam explosions. The statistical approach using TEXAS-V demonstrated that non-reinforced hatch doors are highly vulnerable, with failure probabilities exceeding 80% in some scenarios. Updated empirical CDFs for CS and I2 releases show variability depending on containment failure timing. For instance, later failures generally result in lower releases due to increased deposition and scrubbing.

Lastly, the probabilistic evaluation of uncertainty analysis results for fission product release in filtered containment venting scenarios initiated by a LOCA (RC7B release category) indicates that these scenarios contribute minimally to the overall risk of unacceptable release. LOCA-initiated sequences account for approximately 2% of the total frequency of unacceptable releases and about 3% of filtered releases. The contribution of accident sequence reclassification due to source term uncertainty in scenarios included in the RC7B release category is very low, 0.007% for IDEJ0 and 0.038% for IDEJ1. Despite significant phenomenological uncertainties, the overall impact on the unacceptable release frequency remains limited, with containment bypass and ISLOCA scenarios continuing to dominate the risk profile.

7. Outlook

The findings presented in this report, together with those from previous phases of the project [25,50,67] have highlighted several areas for further research and development.

Key areas for future improvement include reducing excessive conservatism in source term estimates for release categories involving containment bypass (RC3) and containment failure (RC4).

There is also a need to enhance confidence in the results for filtered containment venting sequences (RC7). Uncertainty analyses conducted during the second, third, and fourth phases of the project have shown that, depending on the specific accident conditions and modeling assumptions in MELCOR, the threshold for acceptable releases may be exceeded.

Another important area for future research is the long-term behavior of the MVSS scrubber. This includes evaluating the impact of scrubber water temperature and water level on scrubbing efficiency, as well as the effect of decay heat from deposited fission products on water level, boil-off rate, and overall system performance. Analyses indicate that some remobilization of fission products initially deposited on surfaces inside the RPV and containment may occur several hours after the initiating event. When combined with reduced scrubbing efficiency caused by high water temperatures and declining water levels, this could further increase the source term released to the environment, an effect not yet fully accounted for in current analyses, potentially resulting in underestimation of the release.

All of these factors underline the importance of continued efforts to improve modeling fidelity of the Multi-Venturi Scrubbing System and reduce uncertainties in severe accident analysis.

Additionally, further research efforts are needed to better understand and quantify the impact of containment phenomena, particularly ex-vessel debris coolability and steam explosions, on the containment performance, release paths from the containment and, ultimately, the source term. The coolability of relocated corium in the reactor cavity directly affects the likelihood and timing of basemat melt-through and containment pressurization rate, while ex-vessel steam explosions can lead to early damage of the containment, significantly affecting possible release paths and release dynamics. These phenomena are currently subject to high uncertainty and merit focused investigation.

Acknowledgements

NKS conveys its gratitude to all organizations and persons who by means of financial support or contributions in kind have made the work presented in this report possible.

The work performed by VG was performed with additional support from the Swedish Radiation Protection Authority (SSM).

Disclaimer

The views expressed in this document remain the responsibility of the author(s) and do not necessarily reflect those of NKS. In particular, neither NKS nor any other organization or body supporting NKS activities can be held responsible for the material presented in this report.

References

[1] Preparedness and Response for a Nuclear or Radiological Emergency, INTERNATIONAL ATOMIC ENERGY AGENCY, 2015

[2] Actions to Protect the Public in an Emergency due to Severe Conditions at a Light Water Reactor, INTERNATIONAL ATOMIC ENERGY AGENCY, 2013

[3] Störningshandboken – BWR, SKI Rapport 03:02, 2003

[4] Nilsson L., Development of an Input Model to MELCOR 1.8.5 for Oskarshamn 3 BWR, SKI Report 2007:05, May 2006.

[5] Strandberg, M., Hydrogen Fire Risk in BWR Simulations with MELCOR. Research Report VTT-R-00669-17, 2017.

[6] L.L. Humphries, B.A. Beeny, F. Gelbard, T. Haskin, D.L. Louie, J. Phillips, R.C. Schmidt, MELCOR Computer Code Manuals Vol. 2: Reference Manual Version 2.2.18019, SAND2021-0241 O, 2021.

[7] L.L. Humphries, B.A. Beeny, F. Gelbard, D.L. Louie, J. Phillips, MELCOR Computer Code Manuals Vol. 1: Primer and Users' Guide Version 2.2.19018, SAND2021-0252 O, 2021.

[8] A. Saltelli, S. Tarantola, F. Campolongo and M. Ratto, "Sensitivity Analysis in Practice. A Guide to assessing scientific models". John Wiley & Sons Ltd, The Atrium, Southern Gate, Chichester, West Sussex PO19 8SQ, England. 2004.

[9] F. Campolongo, J. Cariboni, A. Saltelli, An effective screening design for sensitivity analysis of large models, Environmental Modelling & Software, Volume 22, Issue 10, 2007, Pages 1509-1518, ISSN 1364-8152. 2007.

[10] Adams, B.M., et al., Dakota, A Multilevel Parallel Object-Oriented Framework for Design Optimization, Parameter Estimation, Uncertainty Quantification, and Sensitivity Analysis: Version 6.0 Reference Manual. 2014, Sandia National Laboratories. (2014).

[11] Troy C. Haskin, The MELCOR Plot File Format, SAND2018-9566, 2018.

[12] Bertrand Ioos, Paul Lemaitre, A review on global sensitivity analysis methods.

[13] S. Galushin, D. Grishchenko, P. Kudinov, "Implementation of Framework for Assessment of Severe Accident Management Effectiveness in Nordic BWR", Reliability Engineering & System Safety, Vol 203, Article 107049, https://doi.org/10.1016/j.ress.2020.107049, November 2020

[14] Jon C. Helton, Jay D. Johnson , William L. Oberkampf & Cédric J. Sallaberry Representation of analysis results involving aleatory and epistemic uncertainty, International Journal of General Systems, 39:6, 605-646, (2010)

[15] Grishchenko D., Basso S., Kudinov P., "Development of a surrogate model for analysis of ex-vessel steam explosion in Nordic type BWRs," Nuclear Engineering and Design, Volume 310, Pages 311-327, 2016

[16] Dmitry Grishchenko, Sergey Galushin, Pavel Kudinov, “Failure Domain Analysis and Uncertainty Quantification using Surrogate Models for Steam Explosion in a Nordic type BWR”, Nuclear Engineering and Design, Volume 343, Pages 63-75, 2019.

[17] Galushin and P. Kudinov “Uncertainty Analysis of Vessel Failure Mode and Melt Release in Station Blackout Scenario in Nordic BWR Using MELCOR Code.” 18th International Topical Meeting on Nuclear Reactor Thermal Hydraulics (NURETH-18), no. Portland, OR, USA, August 18-22, (2019).

[18] S. Galushin S., Kudinov P., “Sensitivity Analysis of the Vessel Lower Head Failure in Nordic BWR using MELCOR Code”, Probabilistic Safety Assessment and Management PSAM 14, September 2018, Los Angeles, CA. (2018).

[19] N. W. Porter, Wilks' Formula Applied to Computational Tools: A Practical Discussion and Verification, SAND2019-1901J

[20] T. G. Theofanous, “On Proper Formulation of Safety Goals and Assessment of Safety Margins for Rare and High-Consequence Hazards,” Reliability Engineering and System Safety, 54, pp.243-257, (1996).

[21] SARNET Technical Report, In-Vessel Core Degradation in Water-Cooled Reactor Severe Accidents, State-of-the-Art Report Update, (CoreSOAR), 1996-2018, SARNET Report No. SARNET-CoreSOAR-D3, 2018.

[22] Galushin, S., and P. Kudinov. “Sensitivity and Uncertainty Analysis of the Vessel Lower Head Failure Mode and Melt Release Conditions in Nordic BWR Using MELCOR Code.” Annals of Nuclear Energy, Volume 135, 2020, ISSN 0306-4549.

[23] Sergey Galushin, Anders Riber Marklund, Dmitry Grishchenko, Pavel Kudinov, Tuomo Sevón, Sara Ojalehto, Ilona Lindholm, Patrick Isaksson, Elisabeth Tengborn, Naeem Ul-Syed, Source Term And Timing Uncertainty in Severe Accidents (NKS-STATUS), NKS-461, 978-87-7893-554-0, 01 Jul 2022.

[24] S. Galushin, P Kudinov “Uncertainty Analysis of Vessel Failure Mode and Melt Release in Station Blackout Scenario in Nordic BWR Using MELCOR Code.” 18th International Topical Meeting on Nuclear Reactor Thermal Hydraulics (NURETH-18), Portland, OR, USA, August 18-22, (2019).

[25] Sergey Galushin, Pavel Kudinov, Sensitivity and uncertainty analysis of the vessel lower head failure mode and melt release conditions in Nordic BWR using MELCOR code, Annals of Nuclear Energy, Volume 135, 2020

[26] Rafael Bocanegra, Luis E. Herranz, CIEMAT’s outcomes from the PHEBUS-FPT1 uncertainty analysis in the framework of the EU-MUSA project, The 10th European Review Meeting on Severe Accident Research (ERMSAR2022), Karlsruhe, Germany, May 16-19, 2022

[27] Darnowski, P.; Mazgaj, P.; Włostowski, M. Uncertainty and Sensitivity Analysis of the In-Vessel Hydrogen Generation for Gen-III PWR and Phebus FPT-1 with MELCOR 2.2. Energies 2021, 14, 4884

[28] Rafael Bocanegra, Luis Enrique Herranz, The importance of characterizing input uncertainties in severe accident analyses. The effect on pool scrubbing modeling in a Fukushima Unit 1 sequence, Sociedad Nuclear Española, Reunion Virtual, 2020.

[29] Fukushima Daiichi Unit 1 Accident Progression Uncertainty Analysis and Implications for Decommissioning of Fukushima Reactors – Volume I, SAND2016-0232,Sandia National Laboratories

[30] Lucas I. Albright, Nathan Andrews, Larry L. Humphries, David L. Luxat, Tatjana Jevremovic, Material Interactions in Severe Accidents – Benchmarking the MELCOR V2.2 Eutectics Model for a BWR-3 Mark-I Station, Nuclear Engineering and Design Volume 383, November 2021, 111398 Blackout: Part II – Uncertainty Analysis.

[31] F. Mascari, M. Massone, G. Agnello, M. Angelucci, S. Paci, M. D'Onorio, F. Giannetti, Comparison of PHEBUS FPT1 uncertainty applications using MELCOR 2.2 with three different methodologies The 13th Meeting of the "European MELCOR and MACCS User Group" 27th –29th April 2022

[32] T.K.S. Liang, L,Y, Chou, Z. Zhang, H.Y. Hsueh, and M. Lee. "Development and application of a deterministic-realistic hybrid methodology for LOCA licensing analysis," Nuclear Engineering and Design, 241 (5), pp. 1857-1863, (2011).

[33] I.M. Chakravarti, R.G. Laha, and J. Roy. "Handbook of Methods of Applied Statistics, Volume I," John Wiley and Sons, pp. 392-394, (1967).

[34] T.W. Anderson, and D.A. Darling. "Asymptotic theory of certain "goodness-of-fit" criteria based on stochastic processes," Annals of Mathematical Statistics, 23 (2), pp. 193-212, (1952).

[35] A. Buse. "The Likelihood Ratio, Wald, and Lagrange Multiplier Tests: An Expository Note," The American Statistician, 36 (3-1), pp. 153-157, (1982).

[36] B. Efron, and R.J. Tibshirani. An Introduction to the Bootstrap. Chapman and Hall/CRC, (1994).

[37] Applied Programming Technology, Inc., "Symbolic Nuclear Analysis Package (SNAP): User's Manual, Version 3.1.9," Bloomsburg, 2021.

[38] B. M. Adams, W. J. Bohnhoff, K. R. Dalbey and Et.al., "Dakota, A Multilevel Parallel Object-Oriented Framework for Design Optimization, Parameter Estimation, Uncertainty Quantification, and Sensitivity Analysis: Version 6.16 User's Manual," Sandia National Laboratories, Albuquerque,, 2022

[39] A. Saltelli and P. Annoni, "How to avoid a perfunctory sensitivity analysis," *Environmental Modelling & Software,* vol. 25, no. 12, pp. 1508-1517, 2010,

[40] Pavel Kudinov, Sergey Galushin, Dmitry Grishchenko, Sergey Yakush, Yvonne Adolfsson, Lisa Ranlöf, Ola Bäckström, Anders Enerholm, Scenarios and Phenomena Affecting Risk of Containment Failure and Release Characteristics, NKS-395, ISBN 978-87-7893-483-3, 2017.

[41] Weimin Ma, Walter Villanueva, Sevostian Bechta, Qiang Guo, Andrei Komlev, Mohsen Hoseyni, Peng Yu, Anna Korpinen, Veikko Taivassalo, Tero Tyrväinen, Ilkka Karanta, Anders Riber Marklund, Sergey Galushin, Ola Bäckström, Scenarios and Phenomena Affecting Risk of Containment Failure and Release Characteristics, NKS-428, ISBN 978-87-7893-518-2, 2019.

[42] Sergey Galushin, Anders Riber Marklund, Dmitry Grishchenko, Pavel Kudinov, Tuomo Sevón, Sara Ojalehto, Ilona Lindholm, Patrick Isaksson, Elisabeth Tengborn, Naeem Ul-Syed, Source Term And Timing Uncertainty in Severe Accidents, NKS-461, 2022.

[43] Sergey Galushin, Anders Riber Marklund, Anders Olsson, Ola Bäckström, Dmitry Grishchenko, Pavel Kudinov, Treatment of Phenomenological Uncertainties in Level 2 PSA for Nordic BWR Using Risk Oriented Accident Analysis Methodology, Probabilistic Safety Assessment and Management PSAM 16, Honolulu, Hawaii, June 26-July 1, 2022.

[44] John N. Ridgely, Assessment of BWR Main Steam Line Release Consequences, PRAB-02-01, NRC, 2002.

[45] Browns Ferry Nuclear Plant (BFN), Units 1, 2, and 3 - Supplement to Proposed Technical Specification Change to Revise the Leakage Rate Through MSIVs (TS-485), Enclosure 1 TS-485 S1, Alternative Leakage Treatment (ALT) Pathway – U.S. NRC.

[46] Artur Szymański Sławomir Dykas, Evaluation Of Leakage Through Labyrinth Seals With Analytical Models, Scientific Bulletin of the Centre of Informatics - Tricity Academic Supercomputer & network, Volume 23, Issue 1, 2019

[47] Mark Anderson, Advanced Supercritical Carbon Dioxide Brayton Cycle Development, FINAL REPORT Advanced Supercritical Carbon Dioxide Brayton Cycle Development (NEUP project 12-3318)

[48] J-E. Holmberg, M. Knochenhauer, Probabilistic Safety Goals, Phase 1 – Status and Experiences in Sweden and Finland, NKS-153, ISBN 978-87-7893-216-7, (2007)

[49] Sergey Galushin, Govatsa Acharya, Dmitry Grishchenko, Pavel Kudinov, Source Term Uncertainty Analysis of Filtered Containment Venting Scenarios in Nordic BWR, The 11th European Review Meeting on Severe Accident Research (ERMSAR2024), Stockholm, Sweden, May 13-16, (2024)

[50] Sergey Galushin, Govatsa Acharya, Dmitry Grishchenko, Pavel Kudinov, Sara Ojalehto, Tuomo Sevón, Ilona Lindholm, Patrick Isaksson, Elisabeth Tengborn, Naeem Ul-Syed, Source Term and Timing Uncertainty in Severe accidents NKS-STATUS Phase 2 report, NKS-475, July (2023)

[51] C. Berna, A. Escrivá, J.L. Muñoz-Cobo, L.E. Herranz, Enhancement of the SPARC90 code to pool scrubbing events under jet injection regime, Nuclear Engineering and Design, Volume 300, (2016)

[52] Luis E. Herranz, Claudia Lopez, Jaime Penalva, Investigation on jet scrubbing in nuclear reactor accidents: From experimental data to an empirical correlation, Progress in Nuclear Energy, Volume 107, (2018)

[53] Taizo Kanai, Masahiro Furuya, Takahiro Arai, Yoshihisa Nishi, Development of an aerosol decontamination factor evaluation method using an aerosol spectrometer, Nuclear Engineering and Design, Volume 303, (2016)

[54] S. Johst, T. Steinrötter, Optimization of the MELCOR Input Deck of Oskarshamn-3 NPP for Source Term Analyses with MELCOR 2.2, GRS – V – SSM2019 – BWR (2019)

[55] Taizo Kanai, Masahiro Furuya, Takahiro Arai, Yoshihisa Nishi, Development of an aerosol decontamination factor evaluation method using an aerosol spectrometer, Nuclear Engineering and Design, Volume 303, (2016)

[56] C. Berna, A. Escrivá, J.L. Muñoz-Cobo, L.E. Herranz, Enhancement of the SPARC90 code to pool scrubbing events under jet injection regime, Nuclear Engineering and Design, Volume 300, (2016)

[57] Luis E. Herranz, Claudia Lopez, Jaime Penalva, Investigation on jet scrubbing in nuclear reactor accidents: From experimental data to an empirical correlation, Progress in Nuclear Energy, Volume 107, (2018)

[58] A. Saltelli and P. Annoni, "How to avoid a perfunctory sensitivity analysis," *Environmental Modelling & Software,* vol. 25, no. 12, pp. 1508-1517, 2010. DOI: https://doi.org/10.1016/j.envsoft.2010.04.012.

[59] Corradini, M.L., et al., Users' manual for Texas-V: One dimensional transient fluid model for fuel-coolant interaction analysis. 2002, University of Wisconsin-Madison: Madison WI 53706.

[60] T. Okkonen, T. N. Dinh, V. A. Bui, and B. R. Sehgal. Quantification of the Ex-vessel Severe Accident Risks for the Swedish Boiling Water Reactors. Scoping Study Performed for the APRI Project, SKI Report 95:76, July 1995.

[61] Aniello Amendola. Advanced Seminar on Common Cause Failure Analysis in Probabilistic Safety Assessment. Proceedings of the ISPRA Course held at the Joint Research Centre, Ispra, Italy, 16–19 November 1987. https://doi.org/10.1007/978-94-017-0629-2

[62] F. Mascari et al., "PHEBUS FPT1 Uncertainty Application With The MELCOR 2.2 Code," The 19th International Topical Meeting on Nuclear Reactor Thermal Hydraulics (NURETH-19), Brussels, Belgium, March 6 - 11, 2022.

[63] R. O. Gauntt, T. Radel, D. A. Kalinich, and M. Salay, "Analysis of Main Steam Isolation Valve Leakage in Design Basis Accidents Using MELCOR 1.8.6 and RADTRAD, SAND2008-6601," 2008.

[64] R. Bocanegra and L. E. Herranz, "CIEMAT's outcomes from the PHEBUS-FPT1 uncertainty analysis in the framework of the EU-MUSA project," *The 10th European Review Meeting on Severe Accident Research (ERMSAR2022) Log Number: 324 Akademiehotel, Karlsruhe, Germany, May 16-19*, 2022.

[65] P. Kudinov, S. Galushin, D. Grishchenko, S. Yakush, A. R. Marklund, O. Bäckström, “Scenarios and Phenomena Affecting Risk of Containment Failure and Release Characteristics”, NKS-410, ISBN 978-87-7893-499-4, 2018.

[66] W. Ma, W. Villanueva, S. Bechta, Q. Guo, A. Komlev, M. Hoseyni, P. Yu, A. Korpinen, V. Taivassalo, T. Tyrväinen, I. Karanta, A. R. Marklund, S. Galushin, O. Bäckström, “Scenarios and Phenomena Affecting Risk of Containment Failure and Release Characteristics”, NKS-428, ISBN 978-87-7893-518-2, 2019.

[67] S. Galushin, G. Acharya, D. Grishchenko, P. Kudinov, S. Ojalehto, T. Sevón, I. Lindholm, P. Isaksson, N. Ul-Syed, Source Term and Timing Uncertainty in Severe accidents NKS-STATUS Phase 3 report, NKS-487, ISBN: 978-87-7893-583-0, 27 June 2024.

[68] S. Galushin, D. Grishchenko and P. Kudinov, "Analysis of the Effect of Vessel Failure and Melt Release on Risk of Containment Failure Due to Ex-Vessel Steam Explosion in Nordic BWR Using ROAAM+ Framework." ASME, ASME Journal of Nuclear Engineering and Radiation Science. https://doi.org/10.1115/1.4047552, June 17, 2020.

[69] S. Galushin, D. Grishchenko, P. Kudinov, “Implementation of Framework for Assessment of Severe Accident Management Effectiveness in Nordic BWR”, Reliability Engineering & System Safety, Vol 203, Article 107049, https://doi.org/10.1016/j.ress.2020.107049, November 2020.

[70] P. Kudinov, S. Galushin, D. Grishchenko, S. Yakush, “Development of Risk Oriented Accident Analysis Methodology (ROAAM+) for Assessment of Ex-Vessel Severe Accident Management Effectiveness, 18th International Topical Meeting on Nuclear Reactor Thermal Hydraulics (NURETH-18), no. Portland, OR, USA, August 18-22, (2019).

[71] Galushin S., Ranlöf L., Bäckström O., Adolfsson Y., Grishchenko D., Kudinov P., Marklund A., “Joint Application of Risk Oriented Accident Analysis Methodology and PSA Level 2 to Severe Accident Issues in Nordic BWR”, Probabilistic Safety Assessment and Management PSAM 14, September 2018, Los Angeles, CA. (2018)

[72] S. Galushin, A.R. Marklund, A. Olsson, O. Bäckström, D. Grishchenko, P. Kudinov, “Treatment of Phenomenological Uncertainties in Level 2 PSA for Nordic BWR Using Risk Oriented Accident Analysis Methodology”, Probabilistic Safety Assessment and Management PSAM 16, June 26th to July 1st, Honolulu, USA (2022).

[73] S. Galushin, G. Acharya, D. Grishchenko, P. Kudinov, “Source term uncertainty analysis of filtered containment venting scenarios in Nordic BWR”, Annals of Nuclear Energy, Volume 218, https://doi.org/10.1016/j.anucene.2025.111406 , August 2025.

[74] G. Acharya, et al., “Effect of Debris Ejection Mode on the Accident Progression and Source Term in Nordic BWRs”, ICONE 32, June 22-26, Shandong, China, 2025.

[75] G. Acharya, et al., “MELCOR Analysis of the NORDIC BWR Pressure Suppression Pool during LOCA”, ICAPP 2025, September 17-19, Antibes, France, 2025.

[76] Kudinov P., Grishchenko D., Galushin S., Yakush S., Konovalenko A., Basso S., Davydov M., Thakre S., Villanueva W., Ma W., Yu P., Manickam L., “Integrated

ROAAM+ Development and Analysis Results for Nordic BWRs". Accident Phenomena of Risk Importance (APRI-9) Report, January 2017.

[77] Grishchenko, D., et al., KROTOS KS-4 test data report 2011, CEA: France, Cadarache.

[78] Grishchenko, D., Basso, S., Galushin, S., Kudinov P., "Development of TEXAS-V Code Surrogate Model for Assessment of Steam Explosion Impact in Nordic BWR," The 16th International Topical Meeting on Nuclear Reactor Thermal Hydraulics (NURETH-16), Chicago, IL, USA, August 30-September 4, paper 13937, 2015.

Bibliographic Data Sheet **NKS-503**

Title	Source Term and Timing Uncertainty in Severe accidents NKS-STATUS Phase 3 report
Author(s)	Sergey Galushin[1], Govatsa Acharya[2], Dmitry Grischenko[2], Pavel Kudinov[2] Sara Ojalehto[3], Tuomo Sevón[3], Ilona Lindholm[3] Patrick Isaksson[4] Naeem Ul-Syed[5]
Affiliation(s)	[1] Vysus Sweden AB [2] KTH Royal Institute of Technology [3] VTT Technical Research Centre of Finland Ltd [4] SSM Swedish Radiation Safety Authority [5] DSA Norwegian Radiation and Nuclear Safety Authority
ISBN	978-87-7893-601-1
Date	September 2025
Project	NKS-R / STATUS - NKS-R(24)133/1
No. of pages	91
No. of tables	18
No. of illustrations	69
No. of references	78
Abstract max. 2000 characters	The overall goal of the NKS-STATUS project is to advance knowledge on the uncertainty in the magnitude of fission product release during potential severe accidents in Nordic Boiling Water Reactors (BWRs). The work aims to provide insights into the effect of various types of uncertainty on the source term predictions. This 4th phase of the NKS-STATUS project builds on previous work by focusing on fission product behavior inside the containment, with particular attention to remobilization, mitigative actions, and probabilistic evaluation of uncertainty. Results obtained for the SBO scenario leading to filtered containment venting showed a limited contribution of cesium remobilization to total release, with dominant sensitivity to aerosol shape factors (GAMMA, CHI). The role of independent containment spray systems was also assessed in this scenario. Sprays slightly reduced cesium release to the environment, primarily affecting the initial release phases, but had minimal influence on remobilization. In LOCA scenarios, significant remobilization of Cs and I_2 deposited in the reactor pressure vessel and containment was

observed, with the mode of debris ejection (IDEJ) identified as the main driver of uncertainty. The project further examined vessel lower head failure and debris ejection, identifying conditions under which steam explosion loads increase containment failure probabilities. Debris ejection conditions were shown to significantly influence the probability of containment failure due to ex-vessel steam explosions. A statistical approach using TEXAS-V demonstrated that non-reinforced hatch doors are highly vulnerable, with failure probabilities exceeding 80% in some scenarios. Updated empirical CDFs for Cs and I_2 releases show variability depending on containment failure timing; later failures generally result in lower releases due to increased deposition and scrubbing.
Probabilistic evaluation of uncertainty analysis results for fission product release in filtered containment venting scenarios initiated by LOCA (RC7B) indicates that despite significant phenomenological uncertainties, the overall impact on unacceptable release frequency remains limited, with containment bypass sequences and Interfacing System LOCAs (IS-LOCAs) scenarios continuing to dominate the risk profile.

Key words: Severe accident, uncertainty quantification, MELCOR, Nordic BWR, fission products, source term

---

Available on request from the NKS Secretariat, P.O.Box 49, DK-4000 Roskilde, Denmark.
Phone (+45) 4677 4041, e-mail nks@nks.org, www.nks.org